STUDIES OF VACANCIES IN METALS BY MODULATION METHODS

ADRIAN H. SEVILLE

Thesis submitted for the Degree of
Doctor of Philosophy

UNIVERSITY OF EDINBURGH

1972

The work described in this thesis was carried out under the supervision of Professor A. F. Brown in the Department of Natural Philosophy of the University of Edinburgh, and latterly in the Department of Applied Physics of the City University, London.

ABSTRACT OF THESIS

The investigation of vacancies in metals is discussed with particular reference to methods using sinusoidal temperature modulation about an elevated mean temperature; the theory of these methods is given for the case of thermal vacancies near equilibrium.

A first experiment is described briefly, in which the phase of the temperature modulation of a specimen is compared with that of the associated resistance modulation. The temperature modulation of a gold wire (diameter $\sim$ 50 μm) was observed using the variation in the light emitted; a carrier-frequency bridge was used to observe the resistance modulation. The modulation frequency was $\sim$ 20 Hz, and the mean temperature 1000 K - 1200 K. The phase comparison accuracy ($\pm$ about 5^{o}) was not adequate to reveal any vacancy relaxation effects, and null results were obtained.

A second modulation experiment is described in which the specific heat of a platinum wire specimen (diameter $\sim$ 50 μm) was measured. The amplitude of temperature modulation was determined from the variation in light emitted from the specimen. Results are given for modulation frequencies in the range 100 Hz - 1 kHz and mean temperatures 1200 K - 1900 K. Above 1500 K, the measured specific heat exceeds the values extrapolated from the low-temperature results. Such effects have been commonly interpreted in terms of large vacancy concentrations ($\sim$ 1% at the melting point). Reasons are given for preferring an explanation based on lower vacancy concentrations, and taking into account anharmonic and vacancy relaxation effects.

Contents

Page

Index of Symbols

The following list is intended as a guide only to those more important symbols which recur from section to section, and are generally defined only at their first appearance. The basic symbols may be appropriately modified by suffixes and superfixes as follows:-

Suffixes:

D	Debye
d	associated with detector of emitted radiation
du	dummy
el	electronic
eq	equilibrium value
h	hemispherical (emittance)
ice	value at $0^{\circ}C$
L	lattice
lin	linearised theory
m	melting-point value
max	value at maximum
n	normal (emittance)
r	at radial distance r
s	self-diffusion
sp	specimen
sp-du	effective specimen
t	total (emittance)
th	thermal
v	vacancy (except that the traditional symbol c_v is retained for specific heat at constant volume)
λ	spectral (emittance)
0	steady component
1	fundamental component
2 (or 3)	component at twice (or thrice) fundamental frequency

Superfixes:

F	formation
M	motion

Symbols:

a	radius of cylinder or lattice parameter, as defined in section
B	$(1/R)(dR/dT)$
C	vacancy concentration as atom fraction
c_k	apparent specific heat (as measured by Kraftmakher and co-workers)
c_p	specific heat at constant pressure
c_v	specific heat at constant volume
D	diffusion coefficient
E	"activation energy" (i.e. enthalpy) of vacancy process
f	vacancy specific heat as fraction of quasi-static value
i	current
j	current density
j	$(-1)^{\frac{1}{2}}$
J	Bessel function
k	Boltzmann constant
K	$(1/W)(dW/dT)$
m	mass
n_o	number of jumps made by vacancy in reaching sink
Q	activation energy for self-diffusion
r	radial distance (but n.b. the following)
r_e	electrical resistivity ratio $R(T)/R(0^oC)$
R	electrical resistance
S	entropy
t	time
T	absolute temperature
V	potential difference
W	radiated power
x	vacancy relaxation parameter for cylindrical geometry; $a(\omega/D_v)^{\frac{1}{2}}$
X_A, X_K	c_p/α as measured respectively by this work and by Kraftmakher et al.
z	co-ordination number
α	temperature coefficient of resistivity dr_e/dT
γ	Grüneisen constant
ε	emittance
θ	temperature interval

κ	thermal conductivity
λ	thermal expansion coefficient
Λ	diffusion distance $(D/\omega)^{\frac{1}{2}}$
μ	chemical potential
ν	effective atomic vibration frequency
ρ	electrical resistivity (n.b. ρ_v is the electrical resistivity due to unit vacancy function)
τ	relaxation time
ϕ	phase angle
ω	angular frequency

1. Introduction

1.1 The nature, existence and importance of vacancies in metals

The vacancy, or vacant lattice site, has been an object of interest since its prediction by Frenkel (1926): at high temperatures, approaching the melting point, the configurational entropy term associated with the formation of a vacancy begins to decrease the free energy of the crystal significantly. The defect can thus exist in equilibrium despite the energy required to create it.

Since then, the vacancy has been shown to be an important agent for change within the crystal. In particular, a vacancy mechanism underlies the phenomenon of self-diffusion in metals; the measured activation energies provide a check on the vacancy hypothesis, and rule out an interstitial mechanism. More generally, vacancies are involved in the explanation of a wide range of processes in metals - high-temperature creep, plastic deformation, radiation damage.

Apart from its practical importance, the vacancy is of interest within the field of study of point defects as the simplest such defect, and as a defect whose involvement in particular processes is well established. In a field where direct observation of the defects studied is generally not possible, the development of a reliable and complete body of knowledge concerning even one defect type is obviously of particular value.

1.2 The problem of vacancy creation and destruction

The existence of a temperature-dependent equilibrium concentration of vacancies in a metal at once poses the question of what sources and sinks operate to create or destroy vacancies as occasioned by temperature changes. It is easy to rule out the suggestion that an atom might move into an interstitial position to create a vacancy in the perfect lattice - the energy required is too large. But creation at dislocations, grain boundaries and the crystal surface would all seem to be possible energetically, as the atoms are there less closely packed than in the perfect lattice. Also, it is not clear whether there is a reciprocity between sources and sinks, nor whether their efficiency is ideal or otherwise.

The answers to these questions are important. They determine what estimates can be made of vacancy lifetime, a parameter which influences the likely effectiveness of vacancies in producing measurable metallurgical changes. This aspect provided the original impetus for the present work, dating from 1962. Claims had been made for large enhancements of diffusion rates in metals subjected to plastic deformation, these enhancements being interpreted as due to excess vacancies introduced by the deformation. The interpretation involved very long vacancy lifetimes, and the present work was conceived as an experiment to measure these lifetimes more directly. The claimed enhancements however proved to be spurious, and to be due to defects in the experimental techniques used; the subject is reviewed from this point of view by Brown (1971). The general problem of how the vacancy concentration reaches equilibrium of course remained.

The experimental programme had as its objective the study of thermal vacancy concentrations in metals at mean temperatures in the diffusion range - from the melting point T_m down to absolute temperatures around $(\frac{2}{3})T_m$ - as the temperature conditions were perturbed. The response of the vacancy concentration to these perturbations was to give information about vacancy lifetime and source/sink behaviour. The aim was not only to identify the sources and sinks involved, but also to investigate their efficiencies, with the ultimate objective of providing models in microscopic terms for the processes involved. As will be seen from what follows, these aims could not be fully realised; the problems of vacancy equilibration are by no means solved.

1.3 The 'traditional' methods of studying vacancies in metals

To set the problem in context, it is appropriate to review briefly some well-known methods of studying vacancies, and, in section 1.4, to incorporate them in a standard interpretation of vacancy behaviour.

1.3.1 Equilibrium measurements

Ignoring all complications such as vacancy aggregation, we can represent the equilibrium vacancy concentration by

$$C_{eq} = \exp(S^F/k) \exp(-E^F/kT) \quad \ldots (1.1)$$

where S^F and E^F are respectively the entropy and energy of formation of a vacancy, and C_{eq} is the vacancy fraction.

Event at the melting point, fractional vacancy concentrations are small, equilibrium values between 10^{-4}

and 10^{-3} being typical. Most of the physical properties measurable in attempting to study vacancies will therefore be determined largely by the vast majority of atoms in their regular lattice sites, the effect of vacancies being a small departure from some base-line value corresponding to an ideal vacancy-free lattice. The difficulties are thus to be found in measuring the property with sufficient accuracy, and in determining the base-line value so that, by subtraction, the effect of the vacancies may be isolated. A third difficulty is that there may be no simple way of relating the observed effects to those of a known vacancy concentration. Because of these inherent difficulties, the experimental picture is not yet complete.

The most obvious way to deal with the base-line difficulty is to extrapolate from low temperatures (below $(\frac{2}{3})T_m$) at which the vacancy concentration is so small as not to influence the selected physical property. Such methods have been used extensively for electrical resistivity and specific heat studies. The danger is that the experimental accuracy is not good enough to determine unequivocally the form of the extrapolating function, nor is there an undisputed theoretical basis for the extrapolation. Vacancy parameters determined by these extrapolation methods are therefore unreliable.

Much more reliance can be placed on a method involving the simultaneous determination of the X-ray lattice parameter and of the specimen length as functions of temperature. The elastic relaxation round vacancies distributed randomly throughout the crystal affects the

unit cell volume and overall volume equally; likewise, thermal expansion affects both volumes in the same way. The difference between the relative change of specimen length and the relative change of lattice parameter is thus directly attributable to the vacancies produced as the temperature is raised from the reference state. Values for the total vacancy concentration and vacancy formation energy are now available for a number of metals (Au, Ag, Cu, Al, Pb, Na, Cd), subject to experimental errors of 1%-10% in the concentrations.

1.3.2 Diffusion experiments

A method of avoiding the base-line difficulty completely is to select a property controlled by vacancies. Self-diffusion is the usual choice. Conventional diffusion experiments are limited to relatively long times, and are therefore of quasi-equilibrium type. Again ignoring complications the self-diffusion coefficient is

$$D_s = \alpha a^2 \nu z C_{eq} \exp(S^M/k) \exp(-E^M/kT) \quad \ldots (1.2)$$

where ν is an atomic vibration frequency,
α is a geometrical factor depending on the lattice,
a is the atomic spacing,
z the co-ordination number,
and S^M and E^M are respectively the entropy and energy of movement of a vacancy.

The diffusion coefficient thus depends both on the equilibrium concentration and on the movement of the vacancies.

1.3.3 Quenching and annealing experiments

By quenching a hot specimen containing its equilibrium vacancy concentration with sufficient rapidity, some of the vacancies are retained, appearing as a supersaturation of vacancies at the after-quench temperature. If the temperature is now raised (to perhaps 0.4 T_m), these vacancies will anneal at a rate which can be followed conveniently by measuring the electrical resistance or thermoelectric power, say, of the specimen. Comparison with the well-annealed specimen at the same temperature provides a difference attributable to the quenched-in vacancies; the annealing rate provides a measure of τ_v, the vacancy lifetime at the annealing temperature, while by varying this temperature E^M can be found. Further, if the before-quench temperature T is not too high, the loss of vacancies to sinks should be small, and the quenched-in concentration should vary as $\exp(-E^F/kT)$.

1.4 A standard interpretation and its limitations

The assumptions implicit in the previous section (1.3) constitute what has been called the "standard interpretation" (Seeger and Mehrer 1970) - monovacancies created and destroyed at some fixed source/sinks, and responsible for diffusion, the phenomena being described by the simple equations given. This simple model suggests certain tests: activation energies and entropies should be consistent from one method to another, should not vary with temperature, should be within theoretical limits, and so on. These tests are almost satisfied, but there are

discrepancies, as reviewed by Seeger and Mehrer (1970), and the situation is one in which more measurements and new techniques are still required.

We can use, with due caution, this standard interpretation to make estimates concerning our problem. The form presented here is due to Brown (1966). Assume that in an annealing experiment a vacancy makes n_o jumps before becoming trapped in one of a number of randomly spaced fully efficient traps, after a mean time τ_v. The jump rate is

$$n_o/\tau_v = \nu z \exp(S^M/k) \exp(-E^M/kT), \quad \ldots (1.3)$$

or using the expression (1.2) for the self-diffusion coefficient,

$$n_o/\tau_v = D_s/(\alpha a^2 C). \quad \ldots (1.4)$$

If we may extrapolate a value of (D_s/C) from temperatures in excess of $(\frac{2}{3})T_m$, where it can be measured, down to the annealing temperature, we can combine this with observed values of τ_v to find for noble metals n_o not more than about 10^9, corresponding to a mean distance travelled by a vacancy in its lifetime of $an_o^{\frac{1}{2}} \sim 10$ μm, strongly suggestive of the dislocation spacing in a well-annealed metal. The dominant trap in the annealing situation is thus identified as the dislocation, rather than the grain boundary or surface.

Despite the simplifying assumptions, this result is quite acceptable. It is when we attempt to extend it to high temperatures ($> (\frac{2}{3})T_m$) that difficulty occurs. To make progress, we must assume that the same traps operate in the same way despite the large change in temperature, so that n_o remains the same.

We can then use equation (1.4) above to estimate τ_v. For Cu, Ag, Au this procedure gives $\tau_v \sim 3$ ms at the melting point, rising to 300 ms at the lower end of the diffusion range. For other f.c.c. metals, lifetimes are expected to be comparable in order of magnitude at corresponding fractions of the melting point temperature, given the same value of n_o. The actual value of n_o would of course depend on the particular sinks involved.

Estimates of this kind provided the initial design parameters for the experimental investigations described below.

1.5 Outline of the phase-comparison experiment

The details of this experiment are the subject of section 3; the outline here presented is intended as an introduction and to indicate the place of the experiment in the investigation.

In 1962, when the investigation was begun, the position was that, granted the interpretation of the experiments described above, a direct check on vacancy lifetimes at high temperatures appeared both possible and, in view of the many assumptions of the theory, probably necessary and useful. Work began on an experiment using a technique put forward by Blackburn (1962) and independently by Korostoff (1962). Gold was chosen as specimen material because of its purity and because its vacancy parameters were comparatively well known.

The technique was that of temperature modulation, the theory of which is given in section 2 below. The fine-wire specimen (diameter ~ 50 μm) was heated in vacuo by superimposed A.C. and D.C. Its mean temperature was thus raised to the region of interest, between $(\frac{2}{3})T_m$ and T_m, while its temperature

oscillated about this mean. Under suitable conditions, the oscillations were small compared with the absolute mean temperature, and were nearly sinusoidal.

The qualitative effect of this temperature modulation on the vacancy concentration may be predicted using for the moment simply the concept of a vacancy lifetime τ_v, interpreted as a relaxation time in the Debye sense. If the modulation period much exceeds τ_v, the vacancy concentration will "follow" the temperature oscillations. At higher modulating frequencies, the vacancies will be unable to respond fully to the temperature oscillations; the corresponding oscillations in the vacancy concentration will be of reduced amplitude, and a phase-lag will develop. Indeed, at still higher frequencies, the vacancy concentration will be almost constant. Simultaneous observations of the oscillations of the temperature and of the vacancy concentration thus, in principle, give the desired information about the relaxation time τ_v.

The experiment was designed to compare these oscillations by means of a phase measurement. The specimen temperature was followed by using the light emitted, detecting this using a photomultiplier tube. The output from this is an approximately sinusoidal waveform in phase with the temperature modulation. The vacancy concentration was followed by monitoring the electrical resistance of the specimen. The variation in this arises in several ways. The predominant electron scattering is due to the lattice, contributing a component of resistance which varies essentially in phase with the temperature (within the lattice relaxation time for electrons, say 10^{-13} s). Impurities and other constant lattice defects will cause scattering, but any

temperature-dependent part will likewise contribute an in-phase resistance. The vacancies, if undergoing relaxation at a properly-chosen frequency, will on the other hand contribute an out-of-phase component. The resulting total resistance thus contains a small component 90^{o} out-of-phase with the temperature modulation. A carrier-frequency bridge was designed and built to monitor the resistance, and the output was compared with that from the photomultiplier system. 10 Hz and 1000 Hz were used as design-frequency limits, in the light of the estimates of section 1.4 above.

The experiment was thus comparative, in the same sense as the X-ray parameter/length comparisons of section 1.3.1, i.e. no extrapolation is needed to provide a base-line. The real difficulty in the experiment lies in the smallness of the phase differences to be measured. The maximum difference, given correct choice of modulation frequency, increases with mean temperature and mean vacancy concentration, but up to only $\sim 3^{o}$ at T_m (see section 2.3.2). The reason is that lattice scattering is of course much more important than vacancy scattering of electrons in determining the electrical resistivity. Phase differences of $\sim 1^{o}$ were measurable in the early 1960's, given relatively pure waveforms. The development of phase-sensitive detectors and lock-in techniques of measurement in the presence of noise and distortion had not reached their present level, and purpose-built phasemeters using these principles were expensive. It was therefore decided to develop the experiment to the point where rough measurements could be made using conventional techniques, after which specialist phase-measuring equipment could be obtained if the results justified it.

Even this modest aim was only partly achieved. Despite improvements to the resistance bridge and photomultiplier systems which were made up to 1968, the accuracy of the system was at best a few degrees, of the order of the predicted effects sought. In these circumstances, the null results obtained were of little interest, and it was not possible to justify the acquisition of new equipment. As described below, a more promising experiment was conceived, and work on the phase-comparison experiment ceased in 1968.

1.6 Some experiments by other workers

During the work on the phase-comparison experiment, the problems associated with vacancy equilibration had become more pressing. Other attempts to perform a phase-comparison experiment had also failed to yield positive results (Van den Sype 1965). The technique of creating vacancies by pulse heating for times shorter than τ_v, pioneered by Sizmann and Wenzl (1963) and refined by Koehler and Lund (1965) and by Balluffi and Seidmann (1965), indicated that further thought should be given to the assumption of dislocations as ideal sources at all temperatures.

In these circumstances, the work of Kraftmakher and Strelkov (1966)[b] was of particular interest. They had measured the specific heat of various metals (W, Ta, Mo, Nb, Zr, Pt, Au) using a temperature-modulation technique (see section 2.4.1). The temperature oscillations of the wire samples were measured via the consequent resistance changes using a bridge method, the thermal capacity being found knowing the electrical power input. Their results showed that the measured specific heat increased

linearly with temperature up to about $(\frac{2}{3})T_m$, but thereafter increased much more rapidly. Using a linear extrapolation from the lower-temperature values, the 'extra' specific heat was determined, and was found to be governed by activation energies close to the accepted vacancy formation energies. The calculated vacancy concentrations were however significantly higher than accepted values, by factors $\sim$ 3 to 10. These high values were of course associated with large values for the 'extra' specific heat, accounting for some 10%-20% of the total specific heat near T_m, and being well outside experimental error ($\sim$ 1%).

The interest in the these results was firstly, that the large values of vacancy concentration reported made the null results of the phase comparison more interesting. For gold, Kraftmakher gave $C(T_m) = 0.4\%$, whereas Simmons and Balluffi (1962) gave 0.07%. If genuine, this sixfold increase would have increased the maximum phase shift to between 10^o and 20^o, which would have been detected given the correct choice of frequency. Secondly, Kraftmakher's analysis made no mention of vacancy relaxation, though the modulation frequencies of $\sim$ 30 Hz would be expected to be in the relaxation range at some temperatures at least. It seemed therefore worth repeating these experiments, partly to verify the large observed extra specific heats, and partly to look for vacancy relaxation effects by varying the modulation frequency.

1.7 Outline of the specific heat experiments

The techniques developed for the phase-comparison experiment were relevant to the problem of performing a modulation experiment to measure specific heat. Since the essential point is to measure

the temperature excursions of the specimen, in principle either the resistance bridge or the radiation detector could have been used. Here however the chosen system would be called upon to make quantitative measurements of the amplitude, not required for the phase-comparison experiment. For reasons discussed in section 4.1.2, the radiation system was chosen, but using a solid-state detector in place of the photomultiplier. The experimental material was also changed, from gold to platinum (principally to allow a higher working temperature to suit the radiation detector) in which large enhancements of the specific heat had also been reported (Kraftmakher and Lanina 1965).

The specific heat experiments are the subject of section 4. In brief, a trial set-up using equipment available in the laboratory indicated that the radiation detector system could be developed to measure the temperature oscillations, and it was decided to go ahead. The accuracy of measurement was severely limited by noise, and a phase-sensitive detector system was obtained to process the radiation detector output.

The first set of experiments was designed to look for vacancy relaxation effects as manifested in a variation of specific heat with modulation frequency. These experiments gave a null result which was significant, and suggested new interpretations of the specific heat measurements. The experimental technique was further developed to enable absolute measurements of the specific heat to be made. The results of all these experiments are given in section 4 and discussed in section 5.

2. The Modulation Technique

2.1 General and historical aspects

The term 'modulation technique' refers generally to any method of deriving information about the material of a specimen, usually in wire form, by observing the temperature oscillations when it is heated by an alternating current. The technique appears to have originated in 1910, when Corbino used it as a method for measuring specific heat. In these early experiments, the temperature oscillations were measured by observing the corresponding fluctuations in the electron current emitted thermionically from the specimen. This method was later refined by Smith and Bigler (1922), by Bockstahler (1925) and by Zwicker (1928). More recently, the amplitude of temperature oscillations has been determined in other ways in specific heat experiments; the variation of electrical resistance is most commonly used, but the variation of thermoelectric voltage and of emitted radiation have also been employed. The technique has been extended to measurements of thermal expansion and of electrical conductivity. Since it is possible to use the refinements of A.C. technique, it is fairly easy to make accurate measurements using small temperature excursions; the technique has therefore been proposed for studies of vacancies under close-to-equilibrium conditions. These modern developments are dealt with in section 2.4 below.

2.2 Temperature modulation of a wire heated in vacuo

Analyses of the temperature oscillations of an A.C. heated wire have been given by Holland (1963), Holland and Smith (1966)

and Van den Sype (1965). They do not cover, however, the case of superimposed A.C. and D.C., and it is therefore worth presenting here the theory required for interpretation of the experimental results.

2.2.1 The power balance equation

Consider a wire specimen in vacuo carrying a current i made up of superimposed D.C. i_o and A.C. $i_1 \cos \omega t$; for a section sufficiently far from the end connections, we may neglect longitudinal heat flow and write for the power balance of the section

$$mc_p \frac{dT}{dt} + W = i^2 R \qquad \ldots (2.1)$$

where mc_p is the thermal capacity of the section,

R its electrical resistance at the absolute temperature T

and W is the power lost by radiation, and by residual conduction effects in the vacuum system, if any.

The absolute temperature may be written as

$$T = T_o + \theta, \qquad \ldots (2.2)$$

T_o being the time-averaged temperature, and we may similarly write:

$$R = R_o(1 + B\theta) \quad \text{and} \quad W = W_o(1 + K\theta), \qquad \ldots (2.3)$$

the suffix o denoting a value at T_o, provided the fluctuation θ is always small enough compared with T_o for

a linear approximation to the variation of R and W with temperature to be appropriate.

Now,

$$i^2 = (i_o^2 + \tfrac{1}{2}i_1^2) + 2i_o i_1 \cos \omega t + \tfrac{1}{2}i_1^2 \cos 2\omega t, \quad \ldots (2.4)$$

and it is clear that the three terms correspond respectively to an effective D.C. heating term, a driving term at the fundamental frequency ω, and a second-harmonic driving term at 2ω. The overall response of the temperature of the wire to the current i may be obtained by superposition (in this linear approximation to the power balance equation) of the effects of these three terms.

For constant terms, the power balance equation (2.1) gives, as is obvious

$$W_o = R_o(i_o^2 + \tfrac{1}{2}i_1^2). \quad \ldots (2.5)$$

For the fundamental, we write the temperature response as $\theta_1 \exp(j\omega t)$ corresponding to a driving term $2i_o i_1 \exp(j\omega t)$, obtaining

$$j\omega m c_p \theta_1 + W_o K = 2i_o i_1 R_o + i_o^2 R_o B \theta_1 \quad \ldots (2.6)$$

to first order in θ_1. Hence

$$\theta_1 = \frac{2i_o i_1 R_o}{j\omega m c_p + W_o K - i_o^2 R_o B} \quad \ldots (2.7)$$

which can be written as

$$\theta_1 = \frac{\theta_{max}}{1 + j\omega\tau_{th}} \quad \ldots (2.8)$$

where θ_{max} is the amplitude of temperature oscillations in the low-frequency limit $\omega\tau_{th} \to 0$

and τ_{th} is the thermal time constant.

Thus

$$| \theta_1 | = \frac{\theta_{max}}{\sqrt{(1 + \omega^2\tau_{th})}} , \qquad \ldots (2.9)$$

a typical relaxation result.

We note that

$$\tau_{th} = mc_p/(W_oK - i_o^2R_oB). \qquad \ldots (2.10)$$

A simple way of estimating the denominator is to vary the D.C. heating, so obtaining by experiment the relationship between i_o and T_o. From equation (2.5) we have, if i_1 is constant,

$$\frac{dW_o}{dT_o} = i_o^2 \frac{dR_o}{dT_o} + 2R_oi_o \frac{di_o}{dT_o} + \tfrac{1}{2}i_1^2 \frac{dR_o}{dT_o} ,$$

so that for small i_1 with $i_1^2 \ll i_o^2$ we have the convenient expression

$$\left(W_oK - i_o^2R_oB\right) = 2R_oi_o \frac{di_o}{dT_o} \qquad \ldots (2.11)$$

and the quantities on the right are all known. If m is known, the numerator of the expression in equation 2.10 may be found using tables of c_p to give an estimate of τ_{th} adequate for the present experiments since, as will appear below, τ_{th} appears only in a small correction term.

2.2.2 The high-frequency approximation

For wire specimens of diameter 50 μm, a typical value for τ_{th} in the temperature region of interest is ∿ 100 ms. Compared with this time, the period of the modulating frequencies generally used is short, so that $\omega\tau_{th} >> 1$. This condition constitutes the high-frequency approximation, and equation (2.9) becomes

$$| \theta_1 | = \frac{\theta_{max}}{\omega\tau_{th}} \left(1 - \tfrac{1}{2} \frac{1}{\omega^2\tau_{th}^2} + \ldots\right) \simeq \frac{\theta_{max}}{\omega\tau_{th}} . \qquad \ldots (2.12)$$

(With τ_{th} = 100 ms and a frequency of 25 Hz, $\omega\tau_{th} \simeq 15$ and the error in the approximation is only 0.2%). In this approximation,

$$\theta_1 = \frac{2i_o i_1 R_o}{j\omega mc_p} ; \qquad \ldots (2.13)$$

the temperature modulation lags the driving current by 90°, and is caused essentially by the varying rate of heat production in the wire, the radiated power remaining almost constant.

The second harmonic component of the temperature variation is easily obtained in this approximation. We write this component as $\theta_2 \exp(2j\omega t)$ corresponding to a driving term $\frac{1}{2}i_1^2 \exp 2j\omega t$, obtaining by use of the power balance equation (2.1) the result

$$\theta_2 = i_1^2 R_o / 4j\omega mc_p \qquad \ldots (2.14)$$

indicating that this component lags the cos $2\omega t$ driving term by 90°.

It is important to note that this approximation does not assume that $i_1 \ll i_o$, though it does assume $\omega\tau_{th} \gg 1$ and $|\theta_1| \ll T_o$. At high frequencies, these assumptions are satisfied, and the approximation holds for any i_o, even for $i_o = 0$, when the temperature variation is pure second harmonic as in many experiments using the modulation technique. In the present work i_1 was typically in the range $i_o/10$ to $i_o/5$; the second harmonic then appears as a distortion (1% to 2½%) of the fundamental.

Higher harmonics in the temperature variation arise only when the magnitude of the temperature oscillations becomes so large that the linear approximations for W and R defined in equations (2.3) are no longer valid. In the present work, this aspect is unimportant since the radiation detector introduces a more dramatic non-linearity, as will be discussed later. We note merely that in the expansion of W in powers of θ the term in θ^2 is of order θ/T_o times the term in θ; the corresponding effect due to R is negligible by comparison.

2.2.3 The radial temperature variation

The foregoing analysis neglects the effects of finite wire thickness, and assumes that the temperature at any instant remains constant as one moves away from the axis of the wire towards its surface. Since heat is generated in the bulk of the wire, but is lost from the surface, this assumption clearly requires justification.

The power balance equation for the axially-symmetric case is

$$\frac{1}{r}\frac{d}{dr}\left(r\frac{dT}{dr}\right) = \frac{c_p\mu}{\kappa}\frac{dT}{dt} - \frac{j^2\rho}{\kappa} \qquad \ldots (2.15)$$

where ρ the electrical resistivity,

μ the density,

and κ the thermal conductivity are taken as constants,

and j is the current density.

This equation may be solved for the time-average temperature $T_{or}(r)$ and for the fluctuation $\theta_{1r}(r)$ at radius r from the axis using the methods given by Holland and Smith (1966). For the average temperature, the familiar parabolic variation for a wire heated by D.C. is obtained:

$$T_{or}(r) = T_{or}(0) - \tfrac{1}{4}(j_o^2 + \tfrac{1}{2}j_1^2)\rho r^2/\kappa. \qquad \ldots (2.16)$$

For wires of the diameter used in the present experiments, this gives a variation between axis and surface of $\sim$ 0.01 K to 0.1 K which is negligible.

For the fluctuation $\theta_{1r}(r)$ the result is expressible as

$$\frac{\theta_{1r}(r)}{|\theta_1|} = 1 - F \qquad \ldots (2.17)$$

where θ_1 is the value obtained by the methods of preceding sections, neglecting radial effects, and F is a correction term. At the surface of the wire $r = a$ and

$$F = J_o|\xi(-j)^{\frac{1}{2}}|/(J_o\{\xi(-j)^{\frac{1}{2}}\} - \omega\tau_{th}(-j)^{\frac{1}{2}}J_1\{\xi(-j)^{\frac{1}{2}}\}) \quad \ldots (2.18)$$

where J_o, J_1 are Bessel functions,

$$\xi = a/\Lambda_{th}$$

and Λ_{th} is a frequency-dependent thermal diffusion length $(D_{th}/\omega)^{\frac{1}{2}}$, D_{th} being the thermal diffusivity.

The term F can be significantly different from zero only when Λ_{th} is comparable with, or less than, the specimen radius a. In the present experiments, even at frequencies up to 1 kHz, $a/\Lambda_{th} \sim 0.1$. Also, the experiments are conducted under conditions of poor thermal contact with the surroundings; the surface conditions do not then materially affect the fluctuation θ_1, the high-frequency condition applies, and $\omega\tau_{th}$ is $>> 1$. Under these circumstances F is negligible; and expansion of the Bessel functions in powers of ξ indicates that $|F| \ngtr 10^{-3}$ under experimental conditions with wires of diameter 50 μm. Radial effects can thus be neglected. This aspect of the thermal behaviour does however limit the maximum diameter of specimen wire for frequencies in the range used, unless corrections are to be made for the radial effects.

2.2.4

Here we consider the effect of end supports on the specimen temperature distribution. These supports act as heat sinks, and the effect on the time-average temperature T_o follows an analysis similar to the D.C. heating case as given by Jain and Krishnan (1954 a,b, 1955). The end effects for θ_1 do not follow the same analysis, however. This is essentially because the thermal diffusion length

Λ_{th} limits the range of influence of the heat sinks on the temperature fluctuations. Analytic solutions are valid only in the restricted case of linear dependence of radiant heat loss on temperature, and do not apply to the case of a specimen at high temperature with supports near room temperature. The procedure generally adopted is to make the D.C. end effects negligible in some way, such as making the specimen much longer than the distance affected by the ends, or by using fine potential leads to define an effective specimen within the central portion. If such a procedure succeeds in dealing with the D.C. end effects, it will, by the argument given above, also succeed in dealing with A.C. end effects.

2.3 The behaviour of vacancies under conditions of temperature modulation

2.3.1 Behaviour in the absence of relaxation effects

The foregoing analysis has neglected any effects due to creation or destruction of vacancies. This simple point of view is adequate as long as the vacancy concentration is at all times the equilibrium concentration corresponding to the instantaneous temperature, i.e. as long as there are no vacancy relaxation effects. Under this assumption, the energy required to create vacancies as the temperature rises will appear as an increase of the specific heat, and the analysis of the preceding section 2.2 may be applied using the appropriate value for c_p. We may write the apparent specific heat c_p per unit mass at temperature T_o as

$$c_p = c_{pL} + nE^F(dC/dT)_{T_o} \qquad \ldots (2.19)$$

where c_{pL} is the specific heat of the lattice,

C is the instantaneous vacancy concentration

and n is the number of lattice sites per unit mass.

Now, by hypothesis

$$C = C_{eq}(T) = \exp(S^F/k)\exp(-E^F/kT) \qquad \ldots (2.20)$$

so

$$c_p = c_{pL} + (n(E^F)^2/kT_o^2)\, C_{eq}(T_o). \qquad \ldots (2.21)$$

Writing Δc_p for the increase in specific heat,

$$T_o^2 \Delta c_p \propto \exp(S^F/k)\exp(-E^F/kT) \qquad \ldots (2.22)$$

so that a plot of $\ln T^2 \Delta c_p$ against $1/T$ gives E^F and S^F; thus C_o, the equilibrium vacancy concentration at T_o is calculable directly.

We may estimate the magnitude of this effect in gold by using the results of the X-ray parameter/length experiments of Simmons and Balluffi(1962). They give $C_{eq}(T_m) = 0.07\%$ with $E^F \simeq 1$ eV, so that at the melting point $\Delta c_{pm}/c_{pm} \simeq 1\frac{1}{2}\%$.

The foregoing is the point of view consistently adopted until recently by Kraftmakher (1962-1970); its tenability will be discussed in section 5, but it may be remarked here that it does assume that the vacancy concentration comes to equilibrium quickly, in a time short compared with the period of modulation (typically

$\sim$ 30 ms in Kraftmakher's experiments) even at temperatures as low as 0.8 T_m.

2.3.2 The assumption of linear kinetics

The next-simplest assumption is that the vacancy concentration obeys linear kinetics in its approach to equilibrium, so that we can define a vacancy lifetime τ_v at any particular temperature by

$$\frac{dC}{dt} = -\frac{C - C_{eq}(T)}{\tau_v} . \qquad \ldots (2.23)$$

This is a reasonable assumption for any diffusion-limited process provided the times involved are long compared with τ_v; the analysis will fail when $\omega\tau_v \gg 1$, as is discussed in the next section.

The value of τ_v depends only on the vacancy diffusion coefficient D_v and the source/sink geometry. In general, we expect $l \simeq (D_v\tau_v)^{\frac{1}{2}}$ where l is a characteristic spacing of source/sinks. Jost (1952) gives solutions for the rate of change of average concentration in a cylinder of radius a whose surface is the sink, obtaining for long times a solution described by

$$1/\tau_v = (2.405)^2 D_v/a^2, \qquad \ldots (2.2)$$

while for a sphere of radius a, or parallel plates spaced by $2a$, the corresponding numerical factors are π^2 and $\pi^2/4$ respectively.

In the modulation experiment, $T = T_o + \theta_1 \exp j\omega t$ and $C_{eq}(T) = \exp(S^F/k)\exp(-E^F/kT)$ as before so that equation

(2.23) becomes

$$C + \tau_v(dC/dt) = C_{eq}(T) = \exp(S^F/k)\exp\left[-E^F/k(T_o + \theta_1 \exp j\omega t)\right]. \quad \ldots (2.24)$$

If $\theta_1 \ll T_o$, the variation of C with time is sinusoidal to good approximation and we may write

$$C = C_{eq}(T_o) + C_1 \exp j\omega t \quad \ldots (2.25)$$

when equation (2.24) becomes, for terms in exp $j\omega t$,

$$C_1 \simeq C_{eq}(T_o)(E^F\theta_1/kT_o^2)/(1 + j\omega\tau_v) \quad \ldots (2.26)$$

which has the familiar Debye-relaxation form.

We thus have, in a modulation experiment, a modified power-balance equation

$$m(c_{pL}dT/dt + nE^F dC/dt + W) = i^2R \quad \ldots (2.27)$$

and in the high-frequency region for thermal relaxation ($\omega\tau_{th} \gg 1$) we obtain

$$j\omega m\left[c_{pL} + \left(n(E^F)^2/kT_o^2\right)C_{eq}(T_o)/(1 + j\omega\tau_v)\right]\theta_1 = 2i_o i_1 R. \quad \ldots (2.28)$$

It is clear that the quantity in square brackets represents an effective complex specific heat, so that the temperature variation θ_1 will be displaced in phase by the vacancy relaxation. Also, important for any experiment in which $|\theta_1|$ is measured, $|c_p|$ is affected. At low frequencies, $\omega\tau_v \ll 1$, the result of the previous section is of course

obtained; at intermediate frequencies, however, the phase relationships between c_{pL} and the vacancy contribution are as shown in figure 1 , and we have

$$c_p(\omega) = \left[\frac{c_p^{\,2}(0) + c_p^{\,2}(\infty)\omega^2\tau_v^{\,2}}{1 + \omega^2\tau_v^{\,2}}\right]^{\frac{1}{2}} \qquad \ldots (2.29)$$

where $c_p(0)$ is the low-frequency specific heat,

and $c_p(\infty) = c_{pL}$ is the high-frequency specific heat.

This relaxation behaviour is shown in figure 2 in which $f = \Delta c_p(\omega)/c_p(0)$ is plotted against $(\omega\tau_v)$ for the case $\Delta c_p \ll c_p(\infty)$.

We next consider the effect of the vacancy relaxation on the resistance of the specimen. If the resistivity per unit vacancy concentration is ρ_v, then the total resistivity is $\rho = \rho_L + C\rho_v$ where ρ_L, the lattice resistivity, includes contributions from other (constant) defects.

Now $\rho_L = \rho_L(T_o)\left[1 + \beta\theta_1 \exp j\omega t\right]$ ... (2.30)

with $\beta = (1/\rho_L)(\partial\rho_L/\partial T)$,

while $C\rho_v = \rho_v C_{eq}(T_o)(E^F\theta_1/kT_o^{\,2})\left(1/(1 + j\omega\tau_v)\right) \exp j\omega t$ ... (2.31)

The magnitude of resistance modulation is thus changed, and analogously to the specific heat result, we obtain an effective coefficient for the increase of resistivity with temperature

$$\alpha(\omega) = \left[\left(\alpha^2(0) + \alpha^2(\infty)\omega^2\tau_v^{\,2}\right)/\left(1 + \omega^2\tau_v^{\,2}\right)\right]^{\frac{1}{2}} \qquad \ldots (2.32)$$

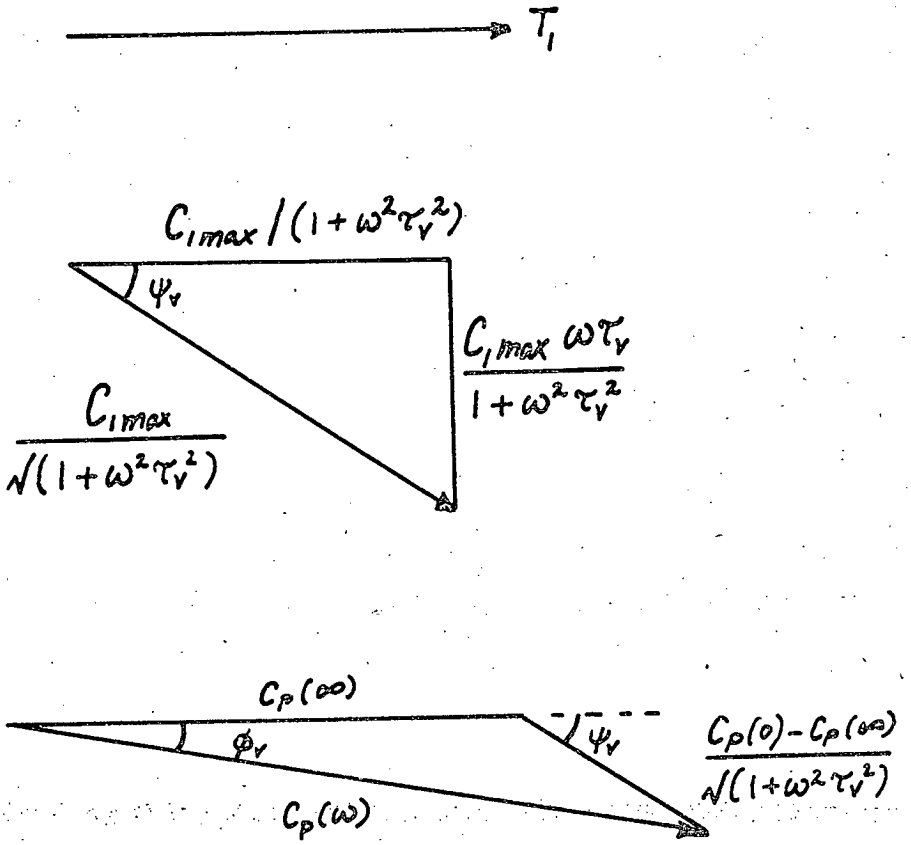

Sec.2.3.2. Fig.1 - Phase relationships assuming linear kinetics

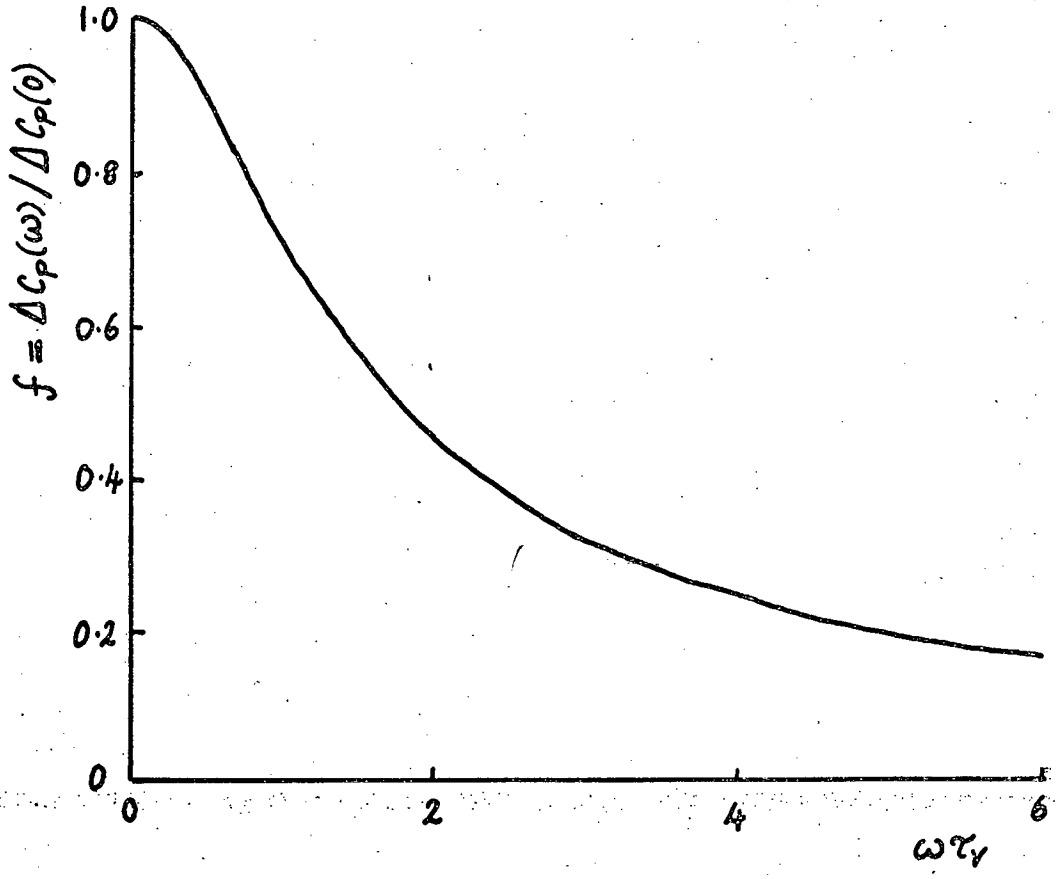

Sec.2.3.2. Fig.2 - Frequency dependence of excess specific heat assuming linear kinetics

where the coefficient α is defined by $\alpha = (1/\rho_{ice})(\partial\rho/\partial T) = \partial r_e/\partial T$, r_e being the ratio of measured resistance at temperature T to measured resistance at 0^oC.

These results for $c_p(\omega)$ and $\alpha(\omega)$ have been published by Van den Sype (1970)[a] who points out that, when resistance modulation measurements are used to determine the magnitude of temperature modulation, the value of $\alpha(\omega)$ appropriate to the frequency must be used if vacancy relaxation is important. This point will be taken up in section 5. Here we shall simply estimate typical values for

$$\big(\alpha(0) - \alpha(\infty)\big)/\alpha(0) = (\rho_v/\rho_L)C_{eq}(T_o)(E^F/\beta k T_o^2). \quad \ldots (2.33)$$

In the quenching studies of Bauerleet al. (1956), for gold at $T = T_m$ vacancies are said to account for $\sim 1\%$ of the resistivity, with $\beta \simeq 10^{-3}K^{-1}$ (Meechan and Eggleston 1954) so that at the melting point this effect is $\sim 10\%$, reducing to $\sim 1\%$ at $0.8\ T_m$.

A further effect of vacancy relaxation is to shift the phase of the resistivity modulation in relation to that of the temperature modulation. The shift ϕ is given by

$$\tan\phi = \big(\alpha(0) - \alpha(\infty)\big)\omega\tau_v/\big(\alpha(0) + \alpha(\infty)\omega^2\tau_v^2\big) \quad \ldots (2.34)$$

This tends to zero at both low and high frequencies, as expected. At intermediate frequencies it is appreciable when $\omega \sim 1/\tau_v$, and has its maximum value at $\omega_{max} = \big(1/\tau_v\big)\big(\alpha(0)/\alpha(\infty)\big)^{\frac{1}{2}}$ when

$$\tan\phi_{max} = \frac{\alpha(0) - \alpha(\infty)}{2\big(\alpha(0)\alpha(\infty)\big)^{\frac{1}{2}}}. \quad \ldots (2.35)$$

For gold at the melting point, $\phi_{max} \sim 3^{o}$.

A similar analysis has been made by Korostoff (1962) leading to comparable estimates for ϕ_{max}. All these estimates depend of course on the correctness of the interpretation of the 'extra' resistivity in gold at high temperatures as a vacancy effect.

2.3.3 Exact kinetics of diffusion-limited vacancy relaxation

We now assume that vacancies are created and destroyed at fixed source/sinks at a rate limited by vacancy diffusion rather than by the intrinsic efficiency of the source/sinks.

For low frequencies, this assumption will add nothing to the results for linear kinetics already discussed. At high frequencies however, $\omega\tau_v >> 1$, and the linear kinetics fail. We may gain some insight into this behaviour by the following simple argument: at high frequencies, only that part of the specimen within a diffusion length $\Lambda \simeq (D_v/\omega)^{\frac{1}{2}}$ of the source/sink is affected by it; the remainder of the specimen will have a constant vacancy concentration. If we assume that, in contrast, within the length Λ the vacancy concentration follows the temperature modulation exactly, an estimate of the high-frequency behaviour is obtainable for a given source/sink geometry. Thus, if the surface of the cylindrical specimen is taken as the only source/sink, of radius a, the relaxation factor $f = \Delta c_p(\omega)/\Delta c_p(0)$ will be, approximately, $f \simeq a\Lambda/a^2$. We may express this in terms of Λ_v by using $a \simeq (D_v\tau_v)^{\frac{1}{2}}$ to obtain $f \simeq 1/(\omega\tau_v)^{\frac{1}{2}}$ as an order-of-magnitude estimate for f. The high-frequency asymptotic behaviour of the linear

kinetics is $f_{lin} \simeq 1/\omega\tau_v$. As expected, the exact kinetics show that the fall-off of vacancy effects with increasing frequency is less rapid than implied by linear kinetics. This geometry has been considered by Van den Sype (1965) who obtained analytic solutions to the problem by extending the method of Carslaw and Jaeger (1959) for heat diffusion from sinusoidally-varying heat sources. The results of these calculations* as they affect the specific heat enhancement and resistance phase angle are shown in figures 1 and 2, in which the linear-kinetics curves are also shown. We note the anticipated differences in high-frequency behaviour. However, the possibility of detecting vacancy relaxation effects in an experiment is not much affected, since the differences occur only at frequencies so high that f is fairly small compared with unity. Likewise, the phase maximum is not much affected. The concept of vacancy lifetime τ_v is still a useful parameter because the linear kinetics give reasonable approximations to the exact curves, which are not, of course, describable by a single relaxation time.

The same qualitative conclusions will apply if we change the assumption regarding the dominant source/sinks and now suppose that dislocations within the bulk of the specimen are more important than the surface. The main effect will be to replace the parameter a by a distance comparable to the mean distance between dislocation lines. The dislocations can thus remain effective sources/sinks at higher frequencies than can the surface and τ_v is correspondingly reduced, because of the smaller diffusion

* See Appendix A

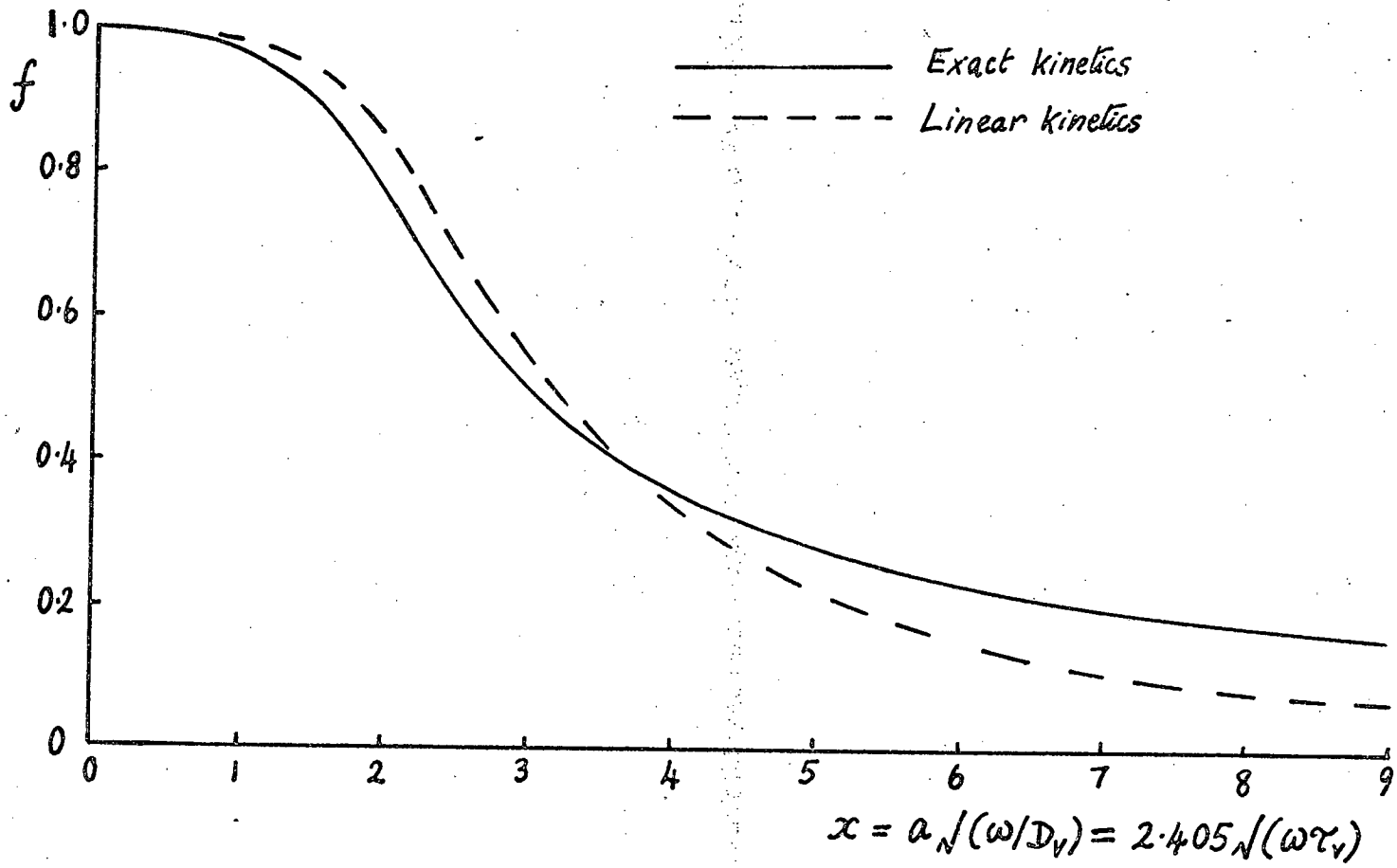

Sec.2.3.3. Fig.1 - Relaxation behaviour of excess specific heat

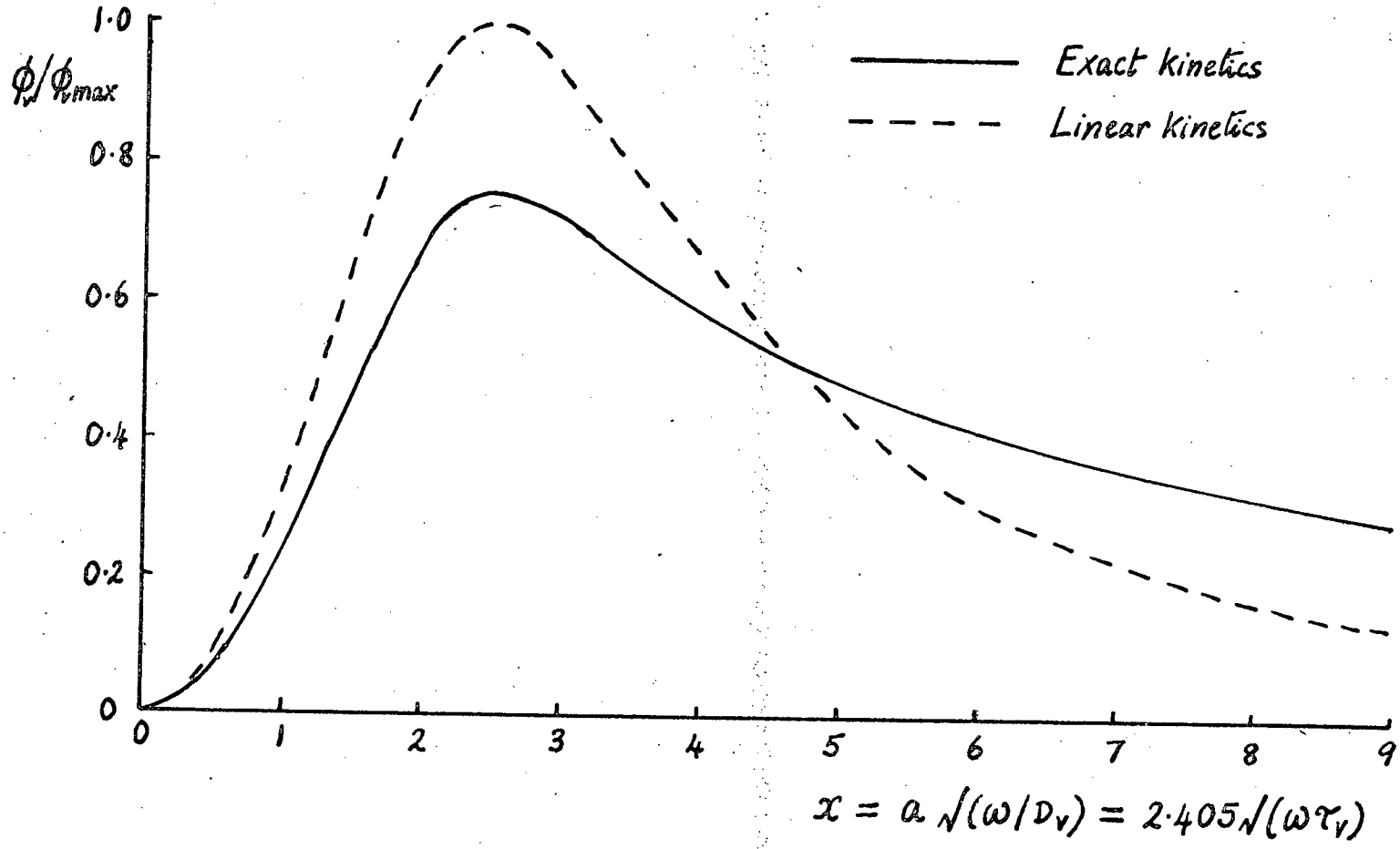

Sec.2.3.3. Fig.2 - Relaxation behaviour of vacancy phase angle
(after Van den Sype, 1965)

distances. The likelihood of the these various assumptions will be discussed in section 5.

2.4 Some modern experiments using the modulation technique

Here we review briefly some recent developments of the modulation technique, with particular reference to those which have been used for the study of vacancies in metals.

2.4.1 Specific heat measurements

In the bridge method of Kraftmakher (1962), the specimen forms one arm of a Wheatstone resistance bridge. Its temperature is modulated at about 30 Hz by passing A.C., and, because of the phase lag in its temperature variation, its electrical impedance is similar to that of a pure resistance in parallel with a small capacitance. This effective capacitance is determined by balancing the bridge using a variable capacitor across another arm. The temperature modulation amplitude is then calculated from the measured modulation of specimen resistance.

Loewenthal (1963) used a photomultiplier tube to monitor the light radiated from the specimen as a means of determining the temperature modulation amplitude. The method is similar in principle to that used in the present specific heat experiments, though the methods were developed independently. Shestopol (1965) has employed similar sample-brightness methods using a photo-conductive cell, while, in a slow-modulation method, Akimov and Kraftmakher (1970) have used thermocouples for determining the temperature fluctuations.

Holland (1963) has used for the same purpose the third-harmonic voltage generated across the specimen. The voltage across the specimen is

$$iR = (i_1 \cos\omega t)R_o\left[1 + B|\theta_2|\cos(2\omega t - \pi/2)\right] \quad \ldots (2.36)$$

for a specimen heated by A.C. alone, in the high-frequency approximation. It is clear that the voltage will contain a component at frequency 3ω from the amplitude of which $|\theta_2|$ is obtainable, knowing B.

Gerlich, Abeles and Miller (1964) used a carrier-frequency to measure the resistance modulation, thus avoiding the problem of measuring a third-harmonic voltage.

As will be discussed in section 5, these methods show large enhancements of the specific heat when used near the melting point, and these are generally attributed to vacancy effects. The only experiment showing relaxation effects is that of Smith and Holland (1966) using the third-harmonic voltage technique on germanium whiskers, though the interpretation of their results as due to vacancy effects is not beyond question.

2.4.2 Phase comparison experiments

The phase-comparison experiment outlined in section 1.5 and described in section 3 represented an attempt to exploit the lag in phase of the resistance modulation with respect to the phase of the temperature modulation discussed in section 2.3.2. Though developed independently, it will be seen to combine aspects of the techniques mentioned in the preceding section: the use of the light

output from the specimen to monitor the temperature, and the use of a carrier frequency to monitor the resistance.

The attempt by Van den Sype (1965) to detect vacancy relaxation by phase-comparison depended on comparison of the third-harmonic voltages developed across a specimen and dummy respectively. The dummy was maintained at a temperature below that at which the vacancy concentration was detectable; the third-harmonic voltage developed thus depended on thermal effects alone. The specimen was maintained at a higher temperature, when the corresponding voltage contains a component due to vacancy relaxation. A bridge method was employed to effect the comparison of these voltages.

In neither of these experiments was any effect of vacancy relaxation detectable in the material used (gold) within the limited frequency range, and limited resolution, of the apparatus used.

2.4.3 Thermal expansion coefficient measurements

Kraftmakher and Cheremisina (1965) have developed a modulation method for determining the thermal expansion coefficient at high temperatures. Specimens are in wire form of length about 100 mm and 0.05 mm diameter. The amplitude of the temperature variations is determined from the specific heat as determined by the modulation method; the amplitude of variations in length of the specimen is monitored photometrically as the mean temperature is varied, and compared with that of a similar specimen maintained at a fixed mean temperature. The absolute values of the coefficient of thermal expansion are then found from

the total elongation over the temperature range.

This method has been used by Kraftmakher (1967) to study the expansion of platinum; he interprets the results in terms of the formation of vacancies.

3. The Phase-Comparison Experiment

3.1 General considerations

An outline of this experiment has already been given in section 1.5. The experiment involves a phase comparison between two signals: one, representing the temperature modulation of the wire specimen, derived from the light output of the hot wire using a photomultiplier tube; the other, representing the resistance modulation, derived from a carrier frequency measuring current passing through the specimen. A block diagram is shown in Fig. 1.

The development of the electronic equipment for the carrier-frequency measurements was part of a general programme in the laboratory to develop a system capable of measuring small, fast changes in resistance. This programme, under the supervision of A. F. Brown, had been initiated by D. A. Blackburn; it was carried out by the author in conjunction with J. M. Anderson, and with the technical assistance of D. Anderson. The results of this development work have been published elsewhere (Anderson, Anderson and Seville 1967), and its application to studies of jump deformation in zinc has been the subject of a paper by Anderson and Brown (1965).

3.2 Apparatus used in the first experiments

3.2.1 The specimen chamber and specimen

The specimen chamber is shown in Fig. 1. It consisted

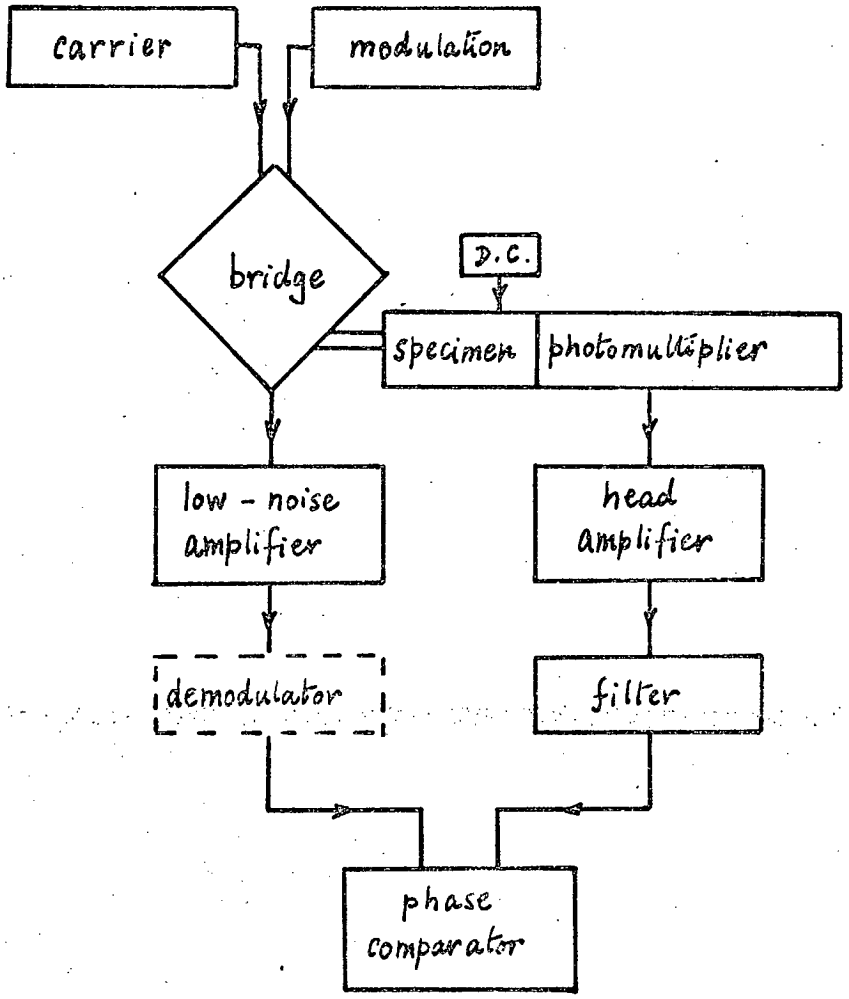

Sec.3.1. Fig.1 - Block diagram of the phase-comparison experiment

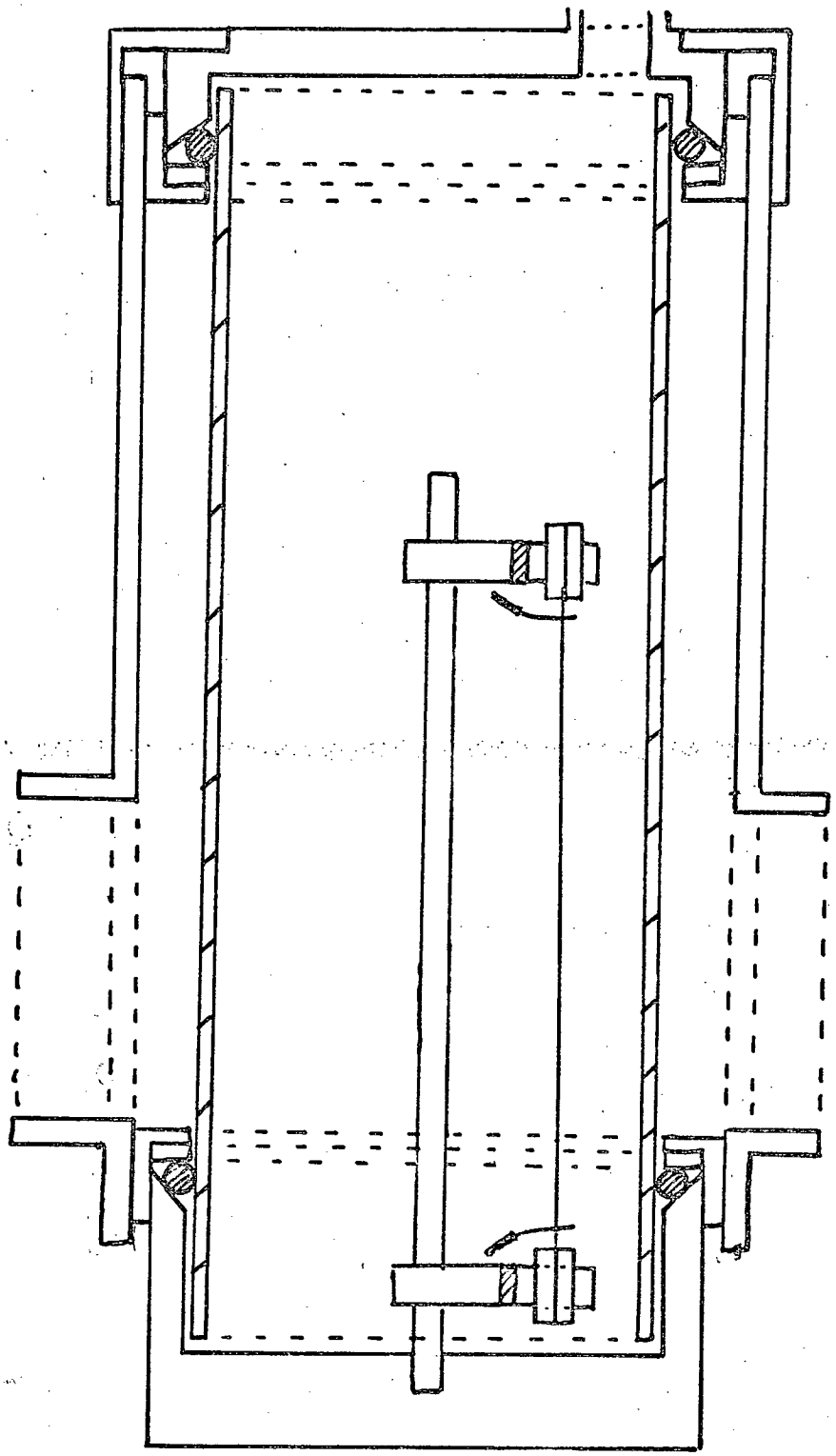

Sec.3.2.1. Fig.1 - Specimen chamber (dummy not shown)

of a Pyrex glass tube of 5 cm diameter equipped with brass endpieces and O-ring vacuum seals. In use, the chamber was evacuated using a 2-stage rotary pump. The lower endpiece was bored to take the various electrical connections via glass/metal insulating seals soldered into the endpiece. The specimen, in the form of a wire of pure polycrystalline gold, was typically of nominal diameter 50 μm, and about 5 cm in length. It was mounted vertically with its ends clamped between brass grips contained in terminal blocks, the upper one insulated with neoprene sheet from the central supporting column, and the lower one similarly insulated from the lower endpiece. The main heating current for the wire was fed in via these terminal blocks. There was similar provision for a dummy wire on the opposite side of the central column, and an aluminium separating sheet could be introduced so that light from the dummy did not reach the light detector. In the earlier experiments, however, a dummy was not used.

Potential leads of the same gold wire were spot welded to the specimen (and dummy, where used) using an Ewald Instruments spot welder on a setting of 80 volts on the low range, and minimum contact-arm pressure. These leads were generally attached so that they were about 5 mm from the end grips. The potential leads were quite short, about 5 mm, and were taken to the lead-out seals by thicker gold wire (diam. 500 μm). These arrangements were required because these leads had to bear the carrier-frequency current, and it was therefore necessary to keep down their

resistance without introducing a dissimilar metal at a point where temperature modulation could have introduced a spurious thermoelectric voltage.

After mounting, specimens were annealed for about 1 hour at a temperature of roughly $^{2}/_{3}\ T_{m}$ under vacuum.

3.2.2 The heating current supplies

The D.C. component of the heating current was supplied by a 6 volt car battery with a variable series resistor for coarse control, and a further resistor as a fine control. The A.C. component was obtained from a Hewlett-Packard type 202C low-frequency oscillator, giving a usable frequency range from 1 Hz to the maximum of $\sim$1 kHz set by the carrier system. For frequencies above 20 Hz, extra power could be obtained using one channel of an Armstrong A20 stereo amplifier. The A.C. and D.C. components were superimposed in the resistance bridge. Typically, the R.M.S. modulating current was about $^{1}/_{5}$ of the D.C. component, which was itself of the order of 100 mA.

3.2.3 Design requirements for the carrier-frequency system

It was decided to design the carrier-frequency system to operate at 100 kHz. This frequency was low enough for skin depth problems to be negligible (even on the large 2mm specimens used in the work on zinc mentioned in section 3.1 above), and for the design of bridges to be fairly simple, not requiring special high frequency techniques. At the same time, the frequency was high enough to be well above the maximum frequencies of modulation contemplated - a few kHz at most - so that

carrier separation was easy. Also, phase shifts of the carrier introduced in the selective low-noise carrier-frequency amplifier would not introduce significant phase shifts of the modulation waveforms.

3.2.4 The carrier-frequency supply

In its final form, the 100 kHz oscillator was a transistorised crystal-controlled multivibrator, as shown in the circuit diagram (Fig.1). The output from this was amplified and passed through a tuned transformer T_1 and fed to the power stage, consisting of a push-pull valve arrangement working into a second tuned transformer T_2 designed to match the input impedance of the resistance bridge. The resulting waveform was reasonably free from harmonics (< 1%) which could overload the low-noise amplifier used as detector in the bridge. Power up to 25 W could be delivered, though for the application described here much lower power sufficed.

3.2.5 The low-noise amplifier

In order to achieve the required low-noise performance, careful design of the first stage was required. Low-noise, low-distortion triode valves were selected, working in cascode to minimise the effect of anode-grid capacitance. In addition, bandwidth limitation was required to reduce noise. The bandwidth selected was ±1.5 kHz about the carrier frequency, and the necessary pass-band shaping was effected according to the design procedure of Belrose (1956). A sweep-frequency oscillator trace of the pass-band is shown in Fig. 1. In the early version of this amplifier, the bandwidth limitation was carried out by filtering

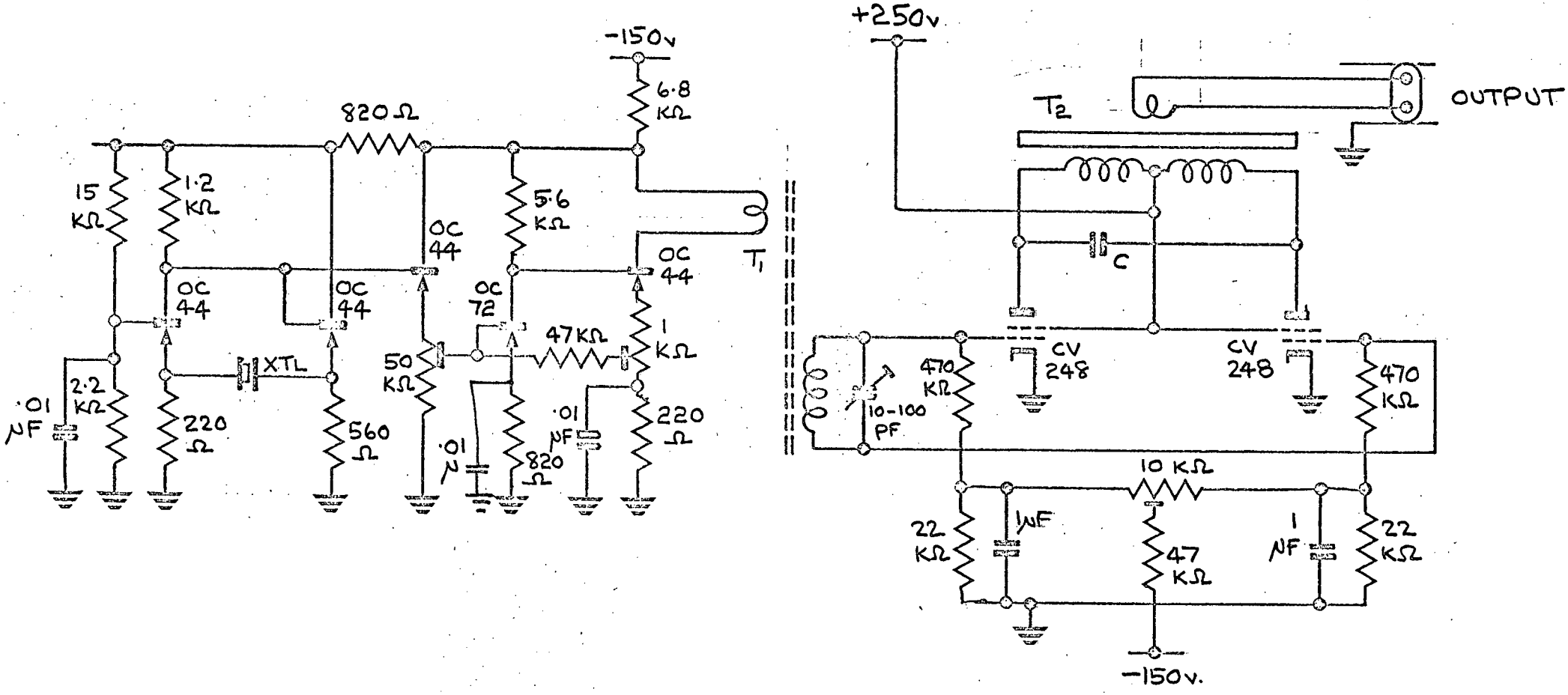

Sec.3.2.4. Fig.1 - 100 kHz carrier-frequency supply

subsequent to the first, cascode stage. This version, while usable, was subject to overloading by small unwanted input waveforms at frequencies outside the pass-band. These waveforms arose through imperfect separation of the A.C. heating voltage from the carrier frequency, and the early form of resistance bridge was designed to enable these spurious voltages to be balanced out. In the final version of the low-noise amplifier (Fig.2) the filters were incorporated in the cascode stage; this version was not as subject to the overloading difficulty, and the resistance bridge could accordingly be simplified. The noise output of this amplifier was measured, with the input shorted, to be equivalent to approximately 30 nV at the input; this compared favourably with the corresponding value, $\sim$ 60 nV, measured on the previous version. On both amplifiers, the gain was of the order of 10^3. Particular attention was paid to the screening of the first stage of these amplifiers in view of the possibility of oscillation, and the bases of the cascode valves were enclosed in a separate shield. The amplifiers were used on an antivibration mount, consisting of a lead base covered with plastic foam, to which the amplifier was strapped; this minimised difficulties due to microphonic behaviour.

3.2.6 The resistance bridge

The earlier form of the resistance bridge is shown in Fig. 1. Each set of upper ratio arms consisted of fixed wire-wound resistors with a variable wire wound potentiometer at the apex. One set of ratio arms was used to introduce the A.C. heating current in a symmetrical way,

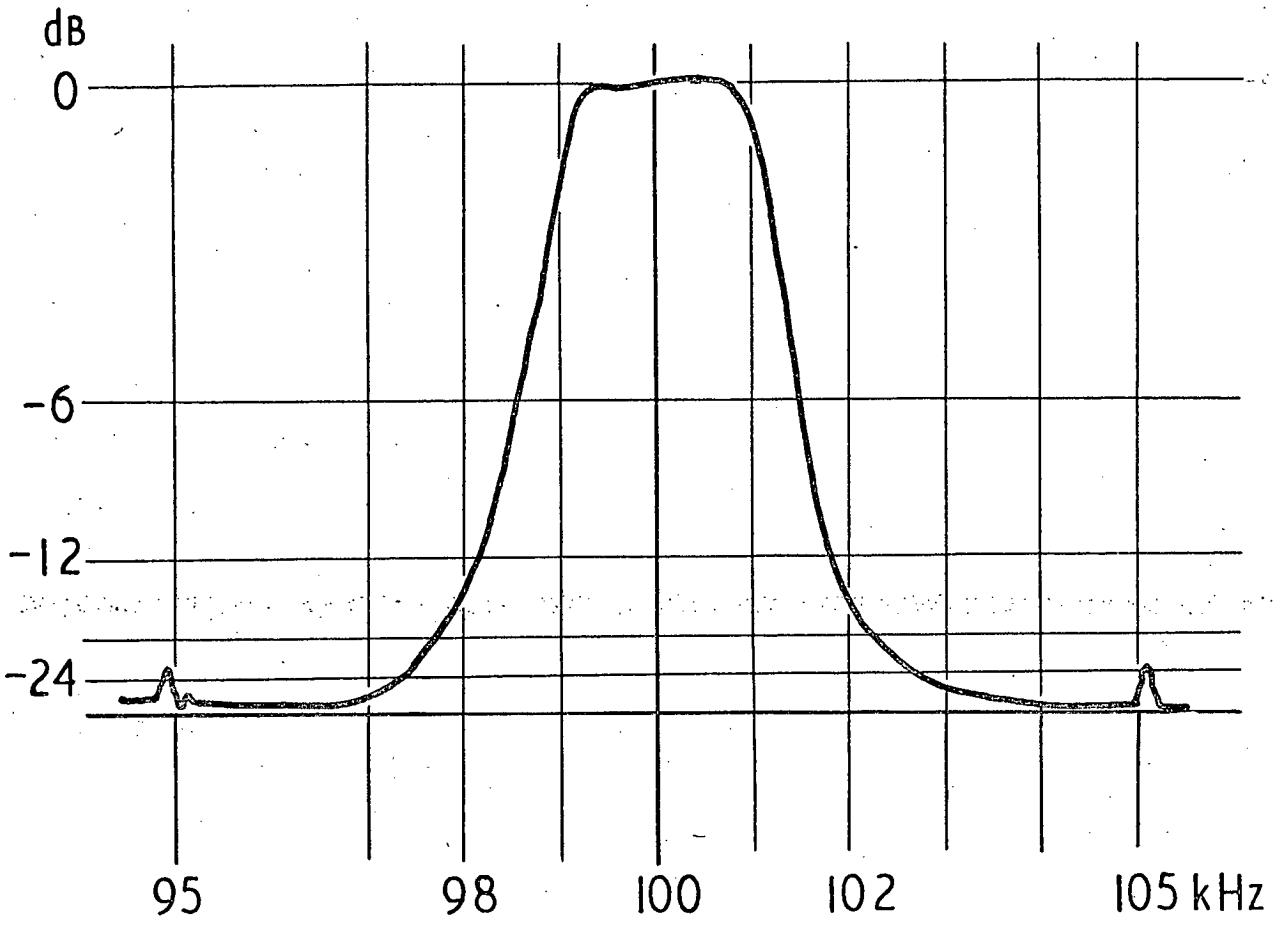

Sec.3.2.5. Fig.1 - Pass-band of low-noise amplifier

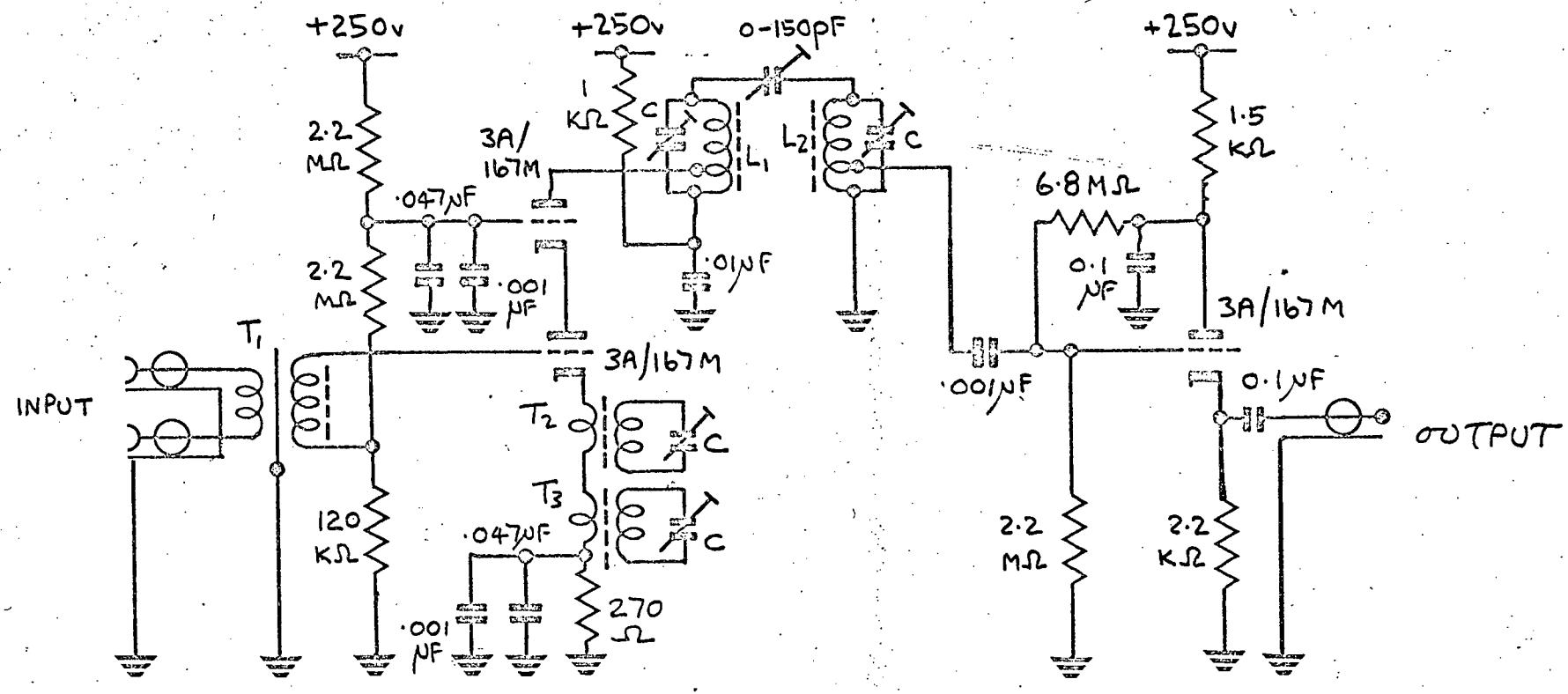

Sec.3.2.5. Fig.2 - The low-noise amplifier circuit

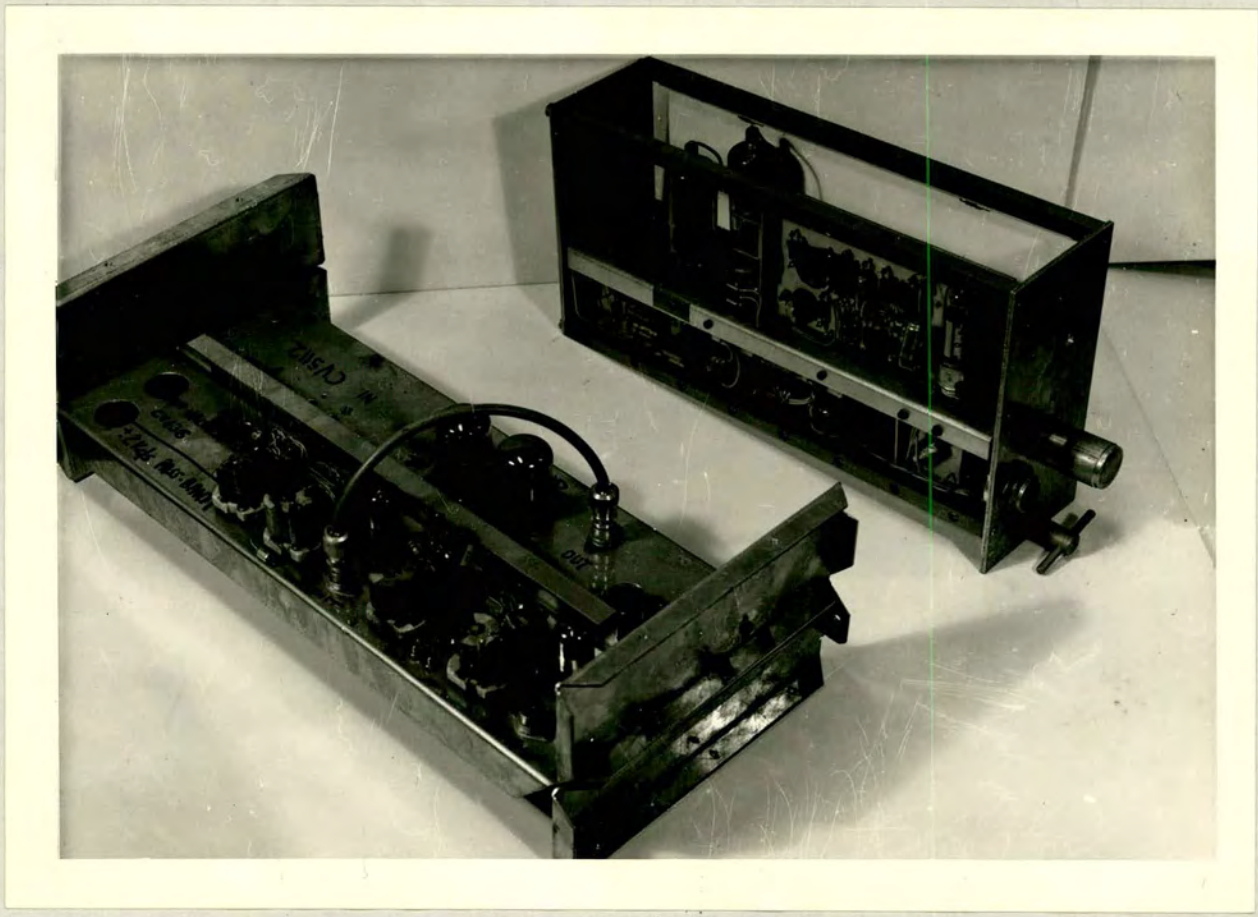

Sec.3.2.5. Fig.3 - Carrier supply unit and (left) low-noise amplifier

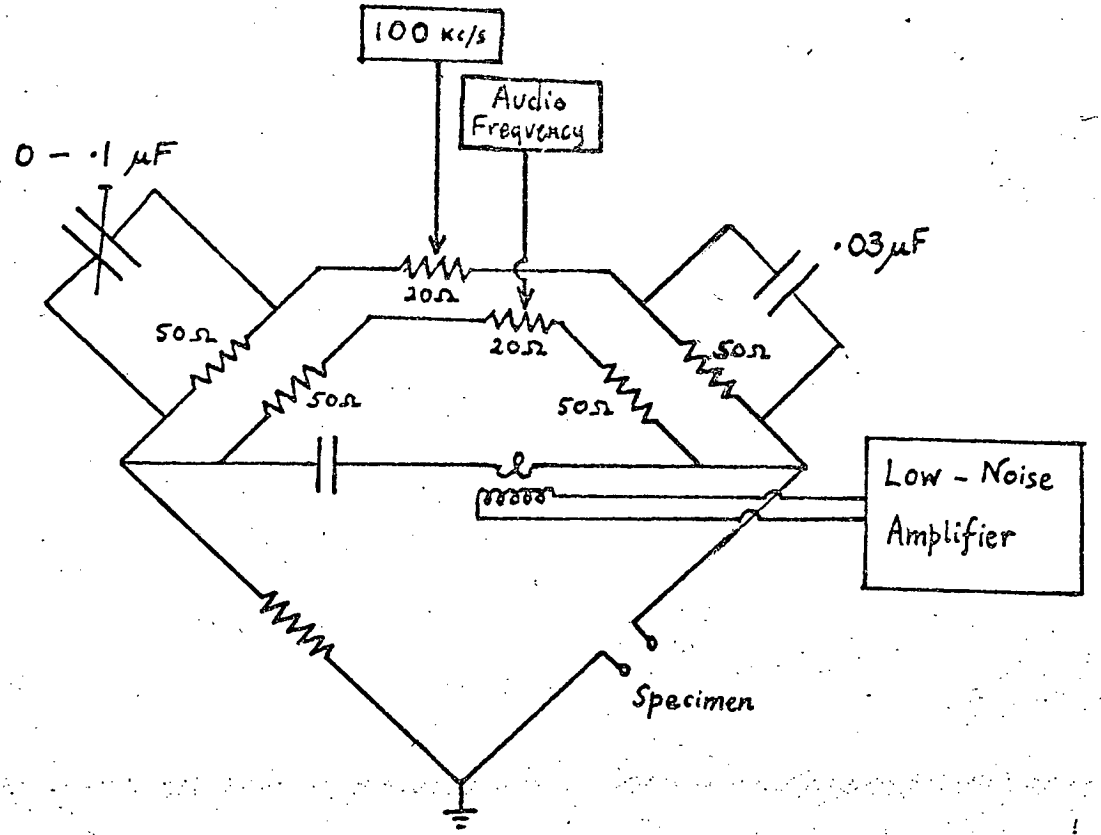

Sec.3.2.6. Fig.1 – Earlier form of resistance bridge

so that only a small voltage at the modulating frequency appeared across the bridge output. The other set was used for the carrier frequency and was equipped with the capacitors indicated, so that the bridge could be balanced at the carrier frequency. The specimen was connected into one lower arm via its potential leads, the other arm consisting of a dummy resistor sufficiently massive to be unaffected by the A.C. heating current that flowed through it. The dummy resistor could be changed to suit different specimen wires; for most experiments it was 2.5 Ω. The output of the bridge was taken, via a blocking capacitor and tuned transformer, to the low-noise amplifier.

All connections to the various components were screened, using coaxial cable for joining the aluminium die-cast boxes in which the ratio-arm resistors were housed. These screens were connected to a single common earth point, thus avoiding earth loops as far as possible.

The action of the bridge was as follows. The capacitance and resistance balance controls were adjusted to give zero output when the specimen wire was at its mean temperature. The excursions of the specimen temperature from this mean unbalanced the bridge so that a carrier frequency signal appeared; the bridge output was then as indicated in Fig. 2(a) A slight change in mean temperature was then made, introducing a permanent unbalance in the bridge, the degree of which depended on the instantaneous resistance of the specimen. The output was then as indicated in Fig. 2(b), the effect of the sinusoidal temperature variation being to modulate the

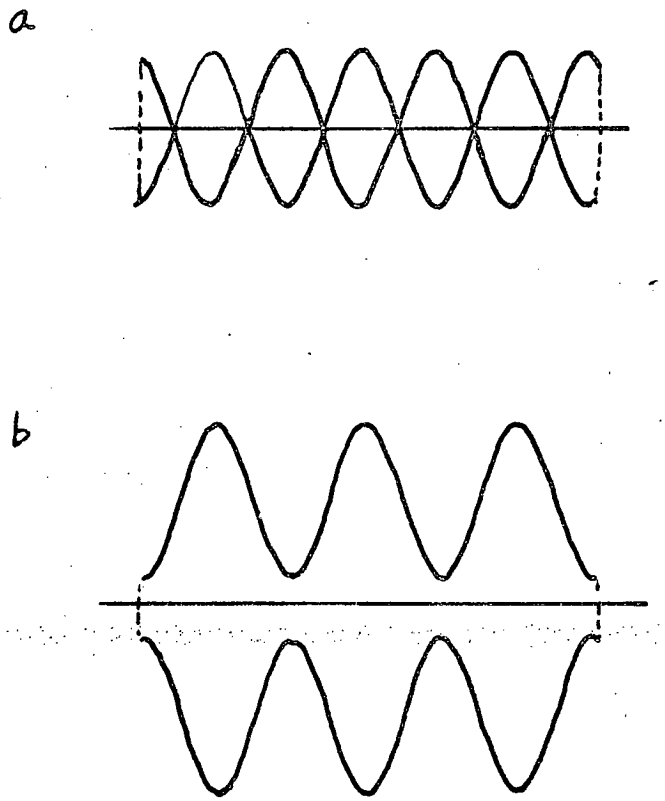

Sec.3.2.6. Fig.2 - Output of resistance bridge

(a) at balance
(b) slightly out of balance

carrier frequency output.

The sensitivity of the bridge could be adjusted by varying the amount of carrier-frequency current flowing; an upper limit here was set by the requirement that the potential leads should not be heated significantly. Also, the carrier frequency itself heated the specimen so that for a given mean temperature the D.C. component had to be reduced. This increased the ratio of the A.C. and D.C. components, so increasing the second-harmonic distortion. The R.M.S. carrier frequency current was generally in the range $\frac{1}{10}$ to $\frac{1}{4}$ of the D.C.

3.2.7 The photomultiplier system

The photomultiplier tube was used in conjunction with Harwell 1000-series electronic equipment, a head amplifier being used for the output. The feedback circuit of this amplifier was modified to extend the pass-band to below 10 Hz. At the other end of the pass-band, the risetime of $\sim$ 1 μs was adequate. The output from the head amplifier was passed through a 5 section low-pass L-C filter with its pass-band limited to 3 kHz. The sensitivity of the system was adjustable within limits via the E.H.T. voltage applied to the photomultiplier tube.

The photomultiplier tube was arranged so that light from only the central part of the specimen fell on its sensitive surface. The specimen chamber and photomultiplier were enclosed in a light-tight metal shield.

It must be remarked that this kind of system, with a filter giving pronounced phase-shifts at the measurement

frequency is not really suitable for a phase-comparison experiment. It was intended only for rough measurements pending the acquisition of synchronous (phase-sensitive) equipment.

An important consideration is that the output from the photomultiplier system should follow without distortion the temperature changes at the wire's surface. The output of such a tube increases steadily with increase of wire temperature and may therefore, for small temperature changes, be expanded in a Taylor series about the mean temperature. For the relatively large temperature excursions used in this experiment ($\sim \pm 10$ K), a linear approximation was inadequate, and the square term introduced appreciable second-harmonic distortion. This increased the difficulty of phase comparison.

3.2.8 Phase comparison

The signals from the low-noise amplifier and from the photomultiplier system were compared using a Tektronix 555 dual-beam oscilloscope, triggering both beams from the modulating signal generator. Using the expanded trace facility, with ideal waveforms, this method is capable of a resolution of perhaps 1° on signals nearly in phase. It was therefore thought suitable for preliminary experiments to test the system, and it was hoped that the resolution would be just adequate to detect vacancy relaxation effects at the higher temperatures.

3.2.9 System performance

Measurements with this system proved difficult,

particularly because of the resistance bridge. The resistive and capacitative balance controls were not independent in action, causing difficulties in balancing. Also the specimen chamber was separated from the bridge components by coaxial leads of some 15 cm length, causing instability. This general lack of compactness of the bridge increased difficulties due to pick-up and hum voltages. The system was therefore modified as set out below.

3.3 The modified experimental apparatus

3.3.1 Comparison with the earlier system

In the modified system, the same photomultiplier equipment was used. Changes were made to the heating current supply arrangements, and a new resistance bridge was constructed. These changes are detailed below. Also the newer form of the low-noise amplifier was used.

The resistance bridge was completely re-designed to work as a transformer bridge, as shown in Fig. 1. The specimen chamber was bolted to a die-cast aluminium box so that direct connections could be made from the bridge elements to the lead-through pins in the base of the specimen chamber. The ratio arms consisted of the centre-tapped primary winding of a close-wound transformer, wound on a ferrite ring some 5 cm in diameter. This winding was of 300 turns in each half, and carefully arranged to be as symmetrical as possible. The centre of the winding was earthed and formed the common earth point for screens. The output from the bridge was taken via a 10-turn secondary

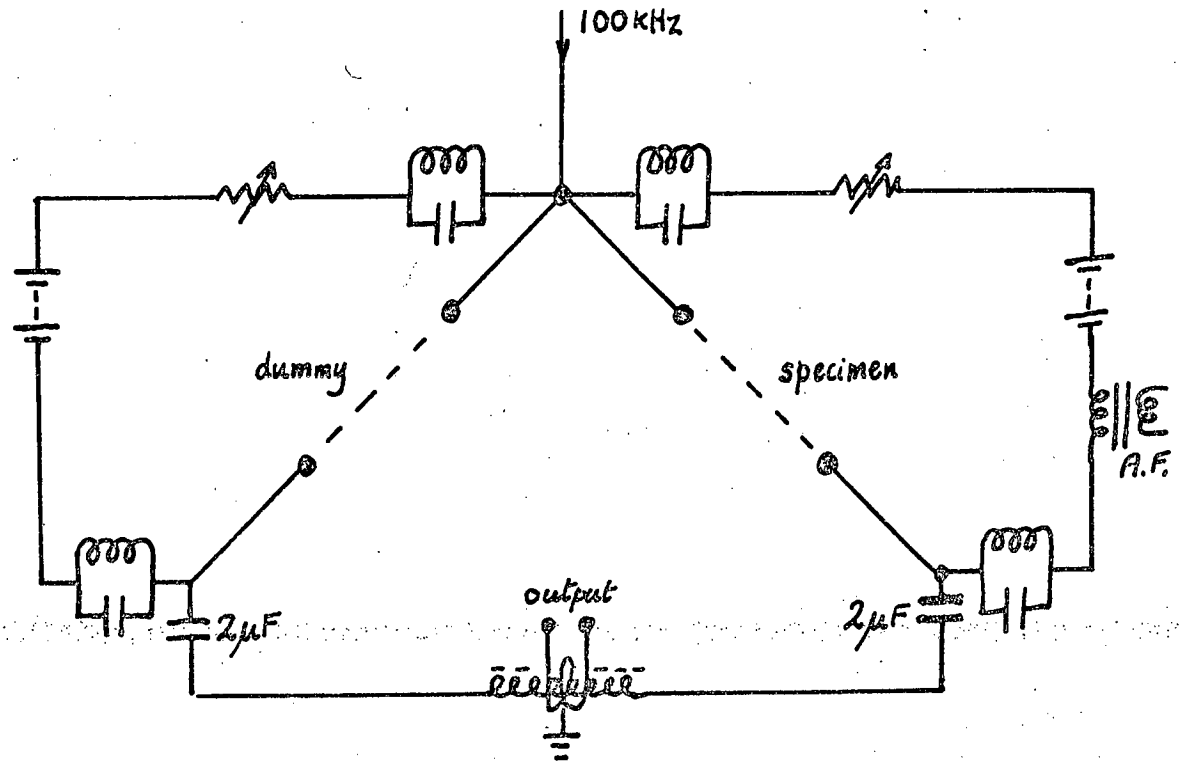

Sec.3.3.1. Fig.1 - Modified form of resistance bridge

winding to the low-noise amplifier. The specimen wire was balanced by a dummy wire from the same batch.

The current supply arrangements are also shown in Fig. 1. Independent D.C. supplies were arranged for specimen and dummy. The D.C. for the specimen was led through the secondary of the output transformer of the Armstrong audio-frequency amplifier previously used to supply the modulating current. In this way, the A.C. was superimposed on the D.C. The dummy was fed with D.C. only. An arrangement of band-stop filters tuned to the carrier frequency was used to prevent the carrier-frequency current from flowing in the D.C. supply networks. The D.C. was prevented from flowing in the bridge circuit by the isolating capacitors shown, which were of negligible impedance at the carrier frequency.

In use, the bridge was balanced at the carrier frequency by varying the D.C. supplied to the dummy, and hence altering its temperature and resistance. Any residual capacitative unbalance was small, because of the symmetrical design of the bridge, and the degree of unbalance would have been acceptable. However, this too was generally balanced to zero, using a decade capacitor box across either the dummy or specimen, as required. This could then be left undisturbed during measurements. The carrier frequency output thus depended solely on the instantaneous difference between the varying specimen temperature and the fixed dummy temperature. A further advantage of this new form of bridge was the much improved stability, resulting from compact design.

3.3.2 Experimental measurements

The chief difficulty in making measurements with the system was noise, in both signals. The sensitivity of the apparatus was estimated by calculating the expected amplitude of temperature excursion for the known electrical conditions and using the published values for the specific heat of gold. The noise levels on the signals were then estimated from the oscilloscope traces as fractions of this amplitude. The noise level in the resistance measuring system corresponded to a temperature change of approximately 0.5 K in the specimen, with the maximum allowable carrier-frequency current. Ideally, the noise level should have been negligible compared with the temperature modulation of the specimen. This would have involved modulation levels of say ±50 K. These levels are undesirable on three grounds. Firstly, they are not small compared with the mean temperature, and considerable complications ensue. Secondly, even at low frequencies $\sim$ 10 Hz such large modulations involve large values of modulating current, not much smaller than the D.C., and consequent severe second-harmonic distortion. Thirdly, at these large excursions, the assumption that the photomultiplier output varies linearly with wire temperature breaks down, so that more distortion is introduced.

In the photomultiplier system, the noise level, even after filtering, was worse, corresponding to about 5 K. The bandwidth of the associated filter was therefore reduced, with a cut-off at 150 Hz. This brought the noise level down to roughly the same order of magnitude as the

resistance system noise, but at the cost of preventing any measurements involving a frequency sweep, because of the frequency-dependent phase shifts introduced.

All measurements had therefore to be made at fixed frequencies, and $\sim$ 20 Hz were selected, being still just high frequency as far as thermal relaxation was concerned, but affording the maximum temperature excursion for a given modulating voltage. The amplitude of temperature variations was reduced to roughly $\pm$10 K. This compromise gave reasonably sinusoidal, though noisy, waveforms which were compared using the oscilloscope as detailed above. Since the absolute phase difference of the waveforms had no meaning because of the filtering, a comparative technique was used whereby the mean specimen temperature was increased by a step of 50 K, thereby changing the vacancy relaxation time and theoretically introducing a phase difference. The size of the temperature step was limited by the limited dynamic range of the low-noise amplifier, which began to saturate when the bridge was much out of balance. After the step, the bridge was re-balanced by increasing the dummy temperature. The step increases were repeated, covering the range $\sim$ 1000 K - 1200 K. Temperatures were estimated from the resistance ratio of the dummy knowing the D.C. current supplied to the dummy at balance and the corresponding D.C. voltage across the dummy, measured potentiometrically. (Resistance ratios for gold were obtained from the results of Meechan and Eggleston (1954).)

No phase shifts were detected during this process, though the resolution was poor, and could have masked such

shifts. The resolution was estimated at $\pm 5^{\circ}$ at the lower end of the temperature range, decreasing to $\pm 2\frac{1}{2}^{\circ}$ at the upper end because of the improvement in the photomultiplier signal. In view of the expected magnitude of phase shift under these conditions, these results were not significant.

3.4 The application of phase-sensitive detection techniques to the experiment

It was realised that in modulation experiments generally, the answer to the problem of noise lay in the advent of the phase-sensitive detector. The action of such a device is now well known: in an ideal detector, a reference input waveform, derived from the generator of the modulating waveform, controls a high-speed electronic switch. The signal of interest, containing information about the specimen at the modulation frequency, but contaminated by noise, is also fed to the detector. The action of the switch is to multiply the signal waveform by a square wave at the reference frequency. The output of the device is time-averaged over an integration period t_I, say, when input signals not coherent with the reference waveform are averaged to zero. Coherent signals give a D.C. ouput, depending only on amplitude and phase relative to the reference waveform. The device thus acts as a band-pass filter, the pass-band being centred on the reference frequency. The advantage of this system is that the bandwidth is of the order of $1/t_I$ and may be made as small as required to eliminate noise, subject of course to the stability of the experiment. A further advantage is that a second harmonic of the modulating frequency present in the signal will average to zero; as we have seen, such distortion was typically present

in the phase-comparison experiment signals.

Phase measuring equipment utilising this principle of synchronous switching was becoming commercially available in the U.S.A. as the experiment was being developed, e.g. the apparatus made by AD-YU Electronics Inc., employing a dual-channel synchronous filter (Type 1034) before the phase meter (Type 405) and having a claimed accuracy of $\pm 0.4^{\circ}$ overall. Such equipment was expensive ($\sim$ £2000) and, though attempts were made in 1965 to obtain this or similar equipment on a trial basis, they were not successful. As was mentioned in section 1.5, outright purchase of phase-measuring equipment for this experiment was not thought justified, particularly as the equipment was specialised, and no other application to existing projects was apparent.

Trials were subsequently made with a phase-sensitive detector constructed to the original design of Faulkner and Stannett (1964), but this work was overtaken by the decision to concentrate on the specific heat measurements.

It is, however, of interest to sketch the application of such instruments to the experiment. The modulating current is relatively free from noise, and is thus a suitable reference waveform. The resistance and light-detector signals are, because of thermal relaxation, nearly in quadrature with the reference, and would each give small outputs, sensitive to small phase shifts, when fed to the phase-sensitive detector. The amplitudes of the signals are measured by noting the outputs after shifting the reference waveform through 90°. The phase-difference of interest can then be calculated.

For the phase-difference measured in this way to be interpretable directly as due to vacancy relaxation, it is

necessary that the systems producing the signals shall not themselves introduce any significant phase shifts, or, if this ideal is not attainable, then the phase shifts must be reproducible and known. The most important source of unwanted phase shifts was in the light-detection system, since this operated at the modulation frequency. Development of this system, using solid-state radiation detectors and amplifiers with a frequency range extending down to D.C., was begun for use on the phase-comparison experiment, culminating in the instrument described in a following section (4.2.4) and used for the specific heat measurements. The phase-shift introduced by this instrument is $< \frac{1}{2}^{o}$ for frequencies in the range 0-50 Hz, and can be found by calibration to an accuracy of $\pm\frac{1}{2}^{o}$ up to 1000 Hz, at which frequency the phase shift is 11^{o}. A further source of unwanted phase-shifts comes from mechanical vibrations of the specimen wire, as discussed more fully in section 4.4.3. They arise because of thermal expansion effects, and, by moving the wire relative to the detector, generate a spurious modulation generally not in phase with the genuine modulation. They can however be overcome by choosing the frequencies of modulation to be sufficiently far from important resonance frequencies.

In the resistance measurement system, phase-shifts at the carrier frequency are not significant. The amplified output from the bridge may be passed through a simple diode detector and, without smoothing, be fed directly to the phase-sensitive detector, which then extracts the component at the modulating frequency. A more sophisticated procedure is to use a second phase-sensitive detector as a demodulator, using the carrier-frequency itself as reference. The restriction of bandwidth can be effected simply by

using a detector time constant $t_I \sim 1$ ms corresponding to a bandwidth of $\sim \pm 1$ Hz. This enables the use of a much simpler low-noise amplifier than the instruments developed here, with their elaborate tuned circuits, and a commercial instrument such as the Brookdeal 450, would suffice. An arrangement of this kind is indicated in Fig. 1, using also the Brookdeal phase-sensitive detectors.

The technical problems involved in the phase-comparison experiment have thus been overcome in principle, and an accuracy of $\pm 1^{\circ}$ at least seems attainable, combining commercial instruments with the light-detector and carrier-frequency-bridge systems developed in the present work.

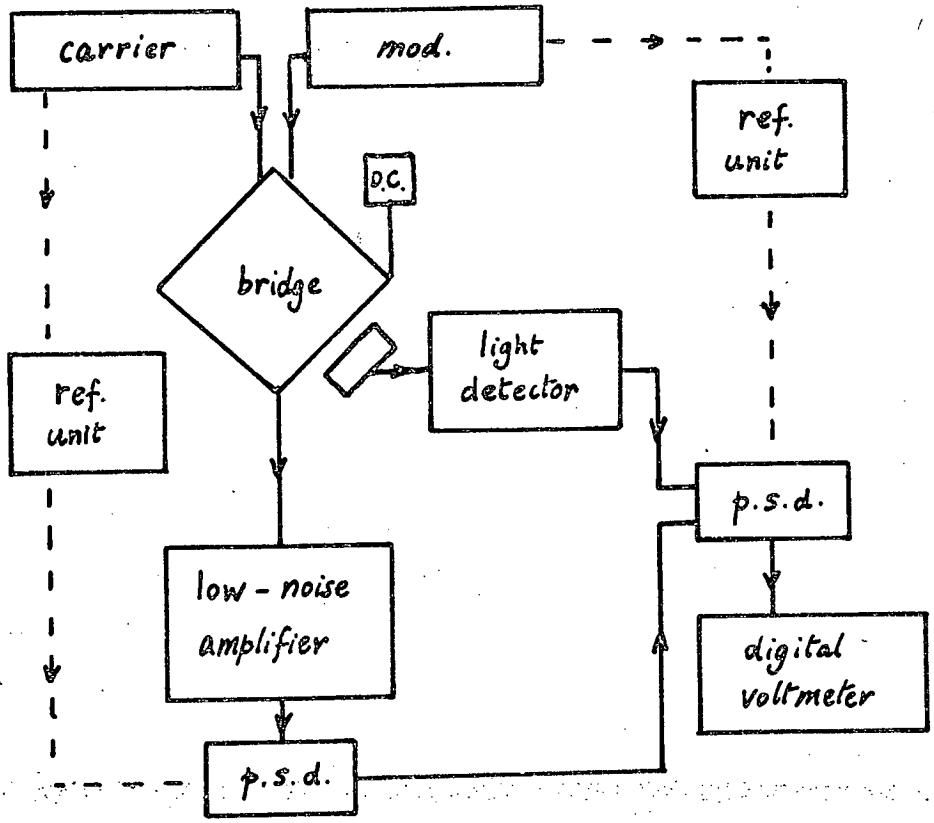

Sec.3.4.1. Fig.1 - Application of p.s.d. techniques to the phase-comparison experiment

4. The Specific Heat Experiments

An outline of the background to this work has been given in sections 1.6 and 1.7. In what follows, an account is given of the reasons for choosing the particular experimental method, the apparatus is described, and the various calibrations and preliminary measurements are set out, leading on to an account of the main experiments themselves. Since much of this section necessarily consists of detail, it may be of assistance to draw attention particularly to sections 4.5.3, 4.5.4 and 4.5.6, in which the results appear that have significance in regard to vacancy behaviour. Sections 4.5.3 and 4.5.4 deal with the measurements to investigate the possible dependence of the specific heat on frequency, while section 4.5.6 deals with the absolute measurements of the magnitude of the specifc heat. A summary of the results is given in section 4.5.7.

4.1 General Considerations and Choice of Method

4.1.1 Methods of measuring specific heat

The general methods of measuring specific heat at high temperatures can be categorised as follows: 1) drop calorimetry, 2) adiabatic calorimetry, 3) micro-cooling calorimetry, 4) pulse heating methods, 5) the modulation method. A review is given by Hoch (1970). In method 1), a specimen heated above the required temperature is rapidly transferred to a calorimeter, where the heat evolved in cooling is measured. In 2), the specimen is suspended in a container acting as an adiabatic shield. The rise in temperature of the specimen is determined as a known addition of energy is made. In 3), the specimen is lowered into an assembly held at a constant temperature some tens of degrees below that of the specimen. Unless heat is evolved because of some energy release in the specimen, the latter cools exponentially. The specific heat is determined from the cooling rate. All these three methods have in common that they require fairly elaborate experimental precautions relating to furnace and calorimeter design and (in 1) and 3)) relating to transfer of the hot specimen. Further, they involve rather massive specimens, and slow changes in temperature. They are therefore generally unsuitable for measuring vacancy relaxation effects. They have the advantage that specific heats are measured directly,

and have been used to measure quasi-equilibrium vacancy concentrations, though the difficulty of extrapolating the "baseline" specific heat of the hypothetical vacancy-free crystal is considerable since the accuracy is not usually better than $\sim$ 1%. In method 4), pulse heating, a specimen generally in the form of a thin wire is maintained at a steady temperature by passing a steady current. A short pulse (typically 5 ms - 500 ms in duration) of extra electrical power raises the temperature of the specimen. The temperature rise is determined indirectly, via the change in resistivity. It will be seen that in this form the pulse-heating method is very similar to 5), the modulation method as described in section 2. The particular advantage of the modulation method is that, because the heating is periodic, the techniques of phase-sensitive detection can be used for signal recovery. This is reflected in the rather poorer accuracies (typical ±5%) claimed for pulse methods, compared with perhaps ±1% for the modulation method.

These considerations make the modulation method an obvious choice for vacancy relaxation studies, provided that the frequency range encompasses the relaxation peak, and provided that the accuracy is sufficient.

4.1.2 Choice of modulation technique

The choice for the present experiments involved the possible methods for measuring the temperature modulation, as described in section 2.4.1: 1) the bridge techniques of Kraftmakher et al., 2) measurements of the third-harmonic voltage, 3) the carrier-frequency technique and

4) the radiation detector technique. The adoption of 4) was conditioned by the fact that it was the simpler of the two techniques (3) and 4)) which had been used for the phase-comparison experiment. For the accurate measurement of amplitude, the requisite stability would have been hard to achieve in the carrier-frequency system. The possibility of using solid-state radiation detectors (instead of a photomultiplier tube) was an additional attraction, for advances in design had reduced their response time. Finally, the technique seemed potentially very sensitive, if noise effects could be dealt with by phase-sensitive detection: the variation of light output with temperature is rapid, and small temperature differences should therefore be detected more easily than by resistance methods. A higher melting point material than gold appeared to be required, however, to increase the light output.

4.1.3 Outline of the experimental method

A block diagram of the arrangement is shown in Fig.1.

A solid-state photovoltaic junction diode was chosen as radiation detector. Compared with the photomultiplier, it had the advantage of not requiring an EHT supply, which avoided the problems of stabilising this supply for the amplitude measurements required, and also simplified the design of the associated amplifier. This amplifier was required to have a frequency range from D.C. up to the maximum to be used in experiment; this maximum was set by the response time of the detector, and by the fact that at high frequencies the amplitude of the temperature changes becomes too small for accurate measurement. An upper limit

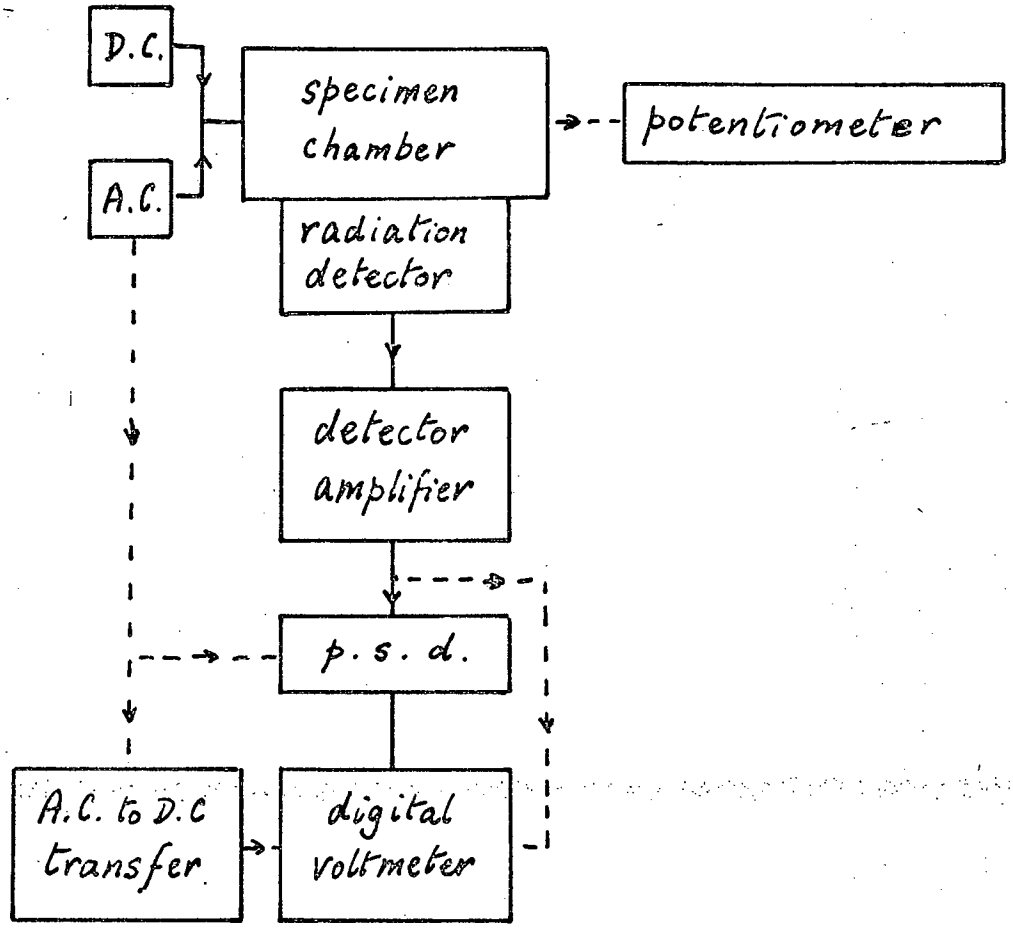

Sec.4.1.3. Fig.1 - Block diagram of the specific heat experiment

of 1 kHz was anticipated.

The specimens were to be of platinum wire, chosen for its melting point (2042 K compared with 1336 K for gold) and because of its face-centred-cubic-structure, which meant that its vacancy properties, scaled according to the melting point, might be compared with the better-known properties of gold. It was therefore preferred over metals with higher melting point, but different structure, for which large specific heat enhancements had also been reported (section 1.6).

Modulation of the specimen temperature was to be effected by known superimposed A.C. and D.C. and the amplitude of the corresponding output from the radiation detector amplifier was to be measured using a phase-sensitive detector and digital voltmeter to determine the magnitude of this modulation. For this, the detector system would be calibrated by making small, known changes in the D.C. heating current, the consequent changes in mean temperature being determined by potentiometric measurements of the specimen resistance, knowing the dependence of resistance on temperature. It was this calibration requirement that necessitated the detector amplifier's D.C. sensitivity.

Using this procedure, it was intended (1) to look for any variation of specific heat with frequency at all practicable temperatures, and (2) to measure the absolute specific heat, to compare the results particularly with those of Kraftmakher et al.

4.1.4 Trial experiments

The first experiments were made in 1968 to test the feasibility of the proposed technique, and will be described only briefly. The specimens were of ∿ 50 μm platinum wire, heated with superimposed A.C. and D.C. and maintained under vacuum essentially as in the phase-comparison experiment. The radiation detector was a photovoltaic junction diode and amplifier similar to that described below.* The electrical measurements were made using a conventional valve A.C. meter for the modulating current and an Advance digital voltmeter, with A.C. measuring capability, for the detector output.

Measurements of the variation of detector output with frequency were made; this verified the thermal relaxation behaviour of the wire within ∿ ±3% in the frequency range 30 Hz - 3000 Hz. Because of noise, these measurements were made at fairly high temperatures > 1400 K. The upper frequency was limited by the detector response time to ∿ 300 Hz.

Although no vacancy relaxation effects were observable, the trials were sufficiently encouraging to warrant the purchase of the phase-sensitive detector system described below, and it was decided to carry out the experiments indicated in the preceding section.

4.2 Apparatus

In this section, the experimental system is described component by component. Test and calibration procedures relating

* See section 4.2.4.

to these components individually are also described.

4.2.1 The specimen and specimen chamber

Specimens were of 0.002 inch nominal diameter (∿ 50 μm) thermopure platinum wire, supplied by Johnson, Matthey & Co. Ltd., London, and having a stated purity of 99.999%. The specimen chamber was essentially as described in section 3.2.1. but arrangements were made to accommodate specimens of increased length ∿ 150 mm. It is shown in Fig. 1. Potential leads of the same platinum wire were spot welded to the specimen some 150 mm apart. A travelling microscope was used to determine this distance, as it was required for calculations of the specimen mass. The ends of the specimen were then soldered to stout current leads of enamelled copper wire mounted in the specimen chamber so as to support the specimen in a vertical position. It was found best to offset the lower end of the wire some 10 mm from the vertical through the upper end. This allowed most of the wire to hang vertically when heated, permitting free thermal expansion. A similar procedure was carried out for a short dummy of wire of length ∿ 60 mm. The end effects for both wires were made as similar as possible by standardising the distances between potential leads and the adjacent ends of specimen or dummy, typically at ∿ 3 mm. Specimen and dummy were separated by an aluminium shield which prevented light from the dummy reaching the radiation detector. These arrangements are shown in Fig. 2. The various electrical leads were carried out of the vacuum chamber via the lower endpiece.

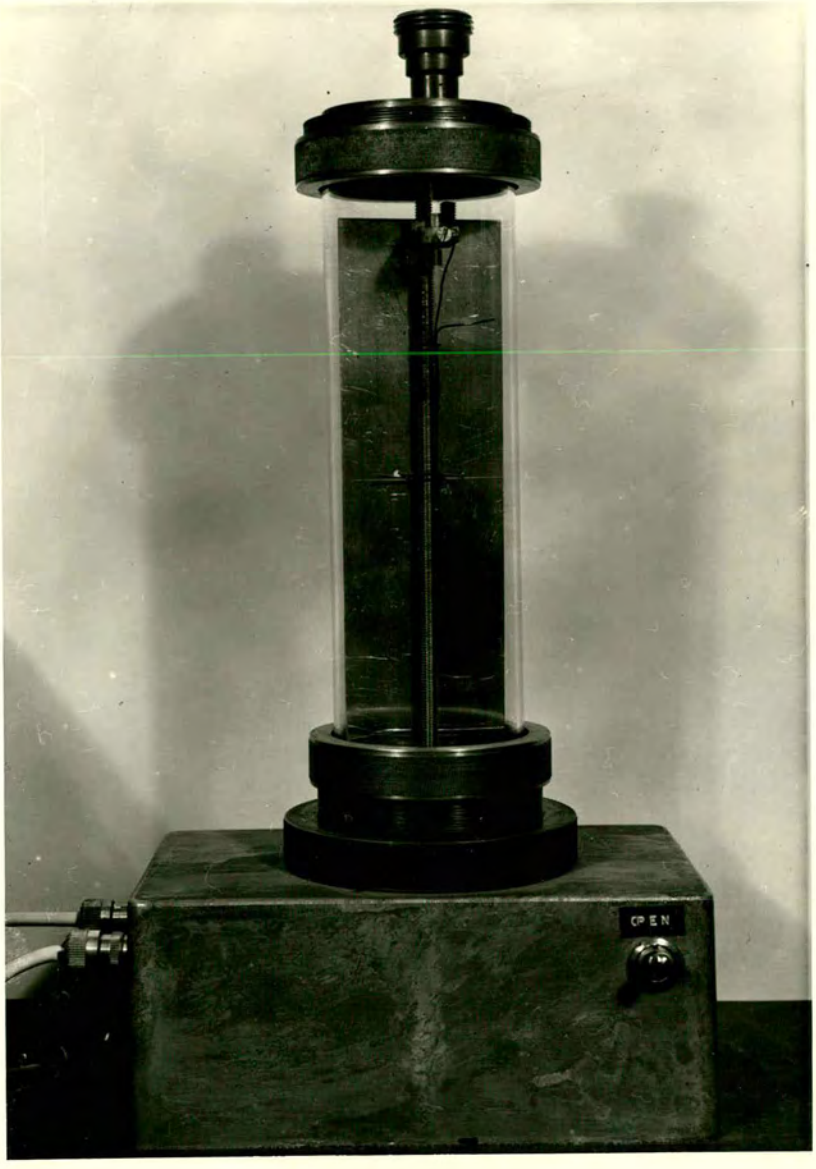

Sec.4.2.1. Fig.1 - The Specimen Chamber

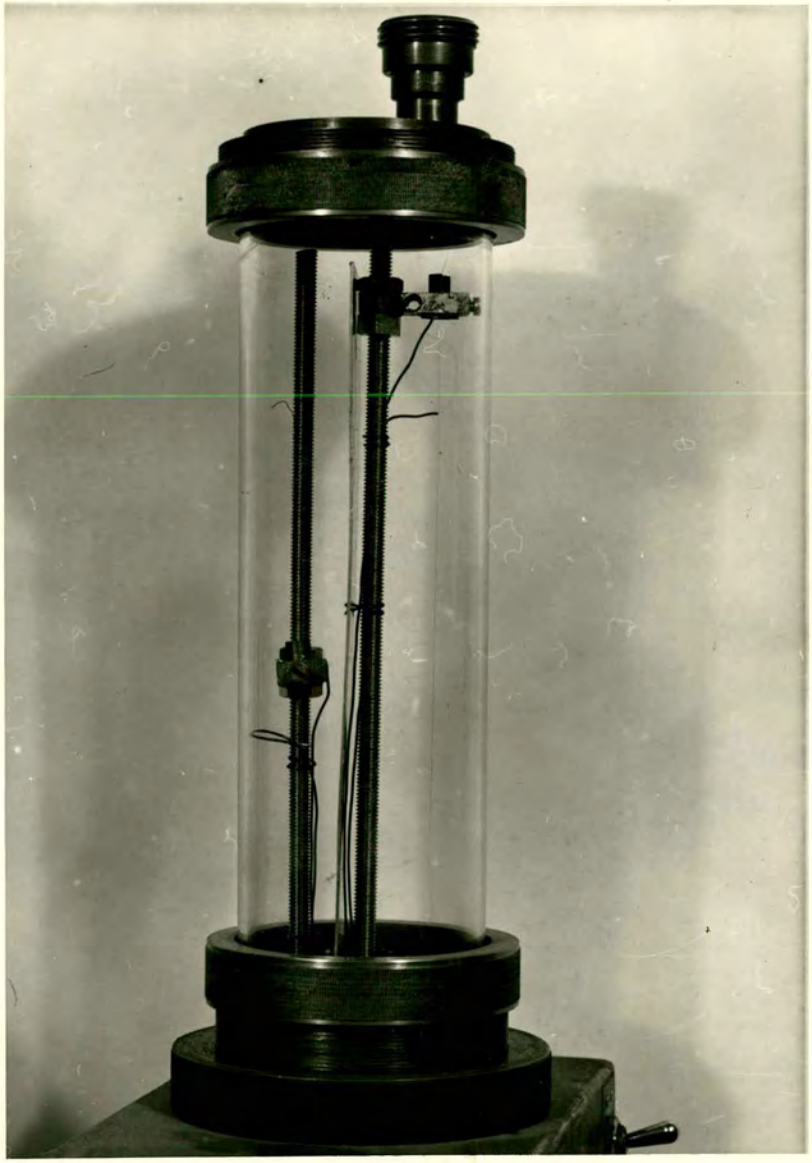

Sec.4.2.1. Fig.2 - Specimen and dummy arrangement

The specimen chamber was mounted on a diecast aluminium box carrying a toggle switch enabling the dummy to be short-circuited if required. It was surrounded by a light-tight shield of brass tubing which carried the radiation detector described below. The whole assembly stood on a stout shelf mounted on the wall of the laboratory. The apparatus was evacuated using a DR1 two-stage rotary vacuum pump connected via a flexible pipe which passed through a massive concrete block; this had the effect of isolating the apparatus from the pump vibrations. In use, this arrangement proved satisfactorily stable, the specimen wire maintaining its position relative to the radiation detector during experimental runs. The vacuum attained was $\sim 10^{-2}$ torr, at which pressure calculation and experiment showed the residual gas to have a negligible effect on the thermal conditions of the wires at the temperatures used. A general view of the system is shown in Fig. 3.

4.2.2 Heating current supplies and associated equipment

The arrangements by which specimen and dummy in series were fed with superimposed D.C. and A.C. are shown in Fig. 1. The heating currents were measured by use of a 1 Ω standard resistor (Tinsley, oil-filled). Screened leads were used for this circuitry, care being taken to avoid earth loops.

The D.C. heating current in the range 100 mA - 350 mA was supplied by a Solartron power supply (type AS1412) used on its 500 mA range, usually with a voltage limit of 30 V. This supply incorporates a series-regulation element which, in the "constant current" mode of operation

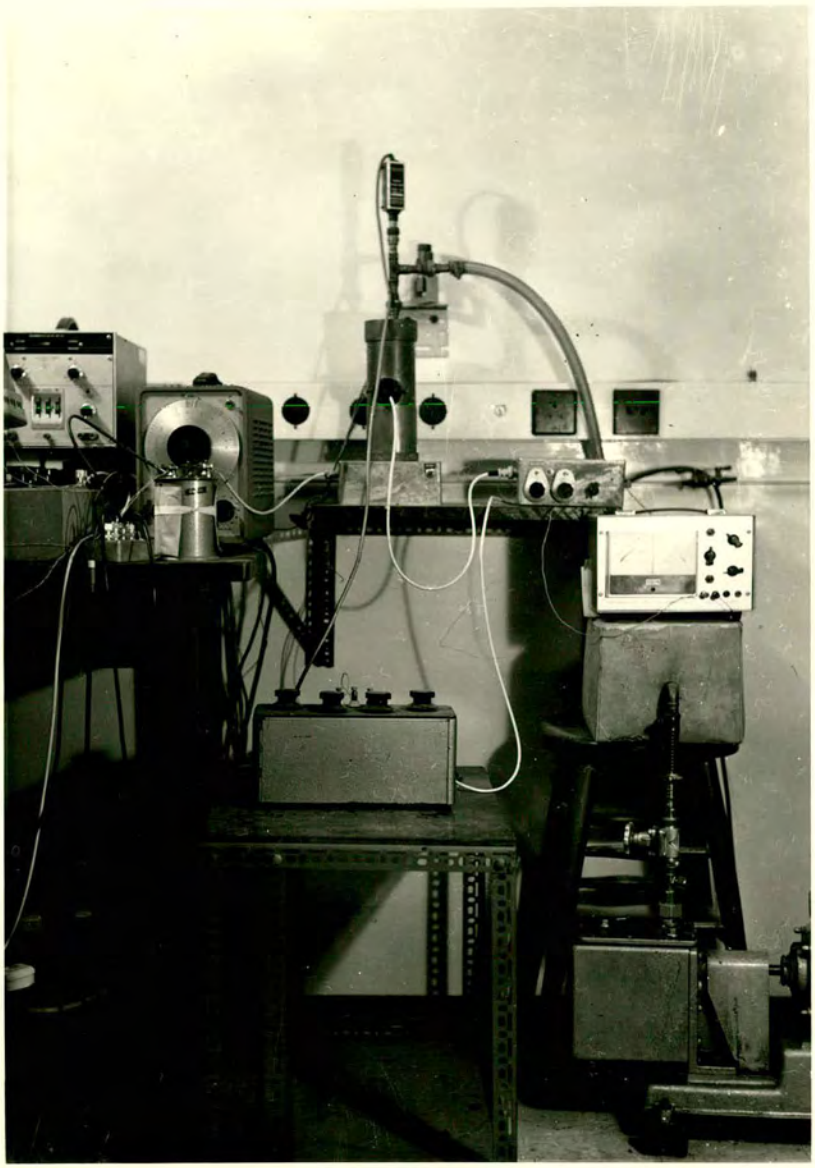

Sec.4.2.1. Fig.3 - General view of the system

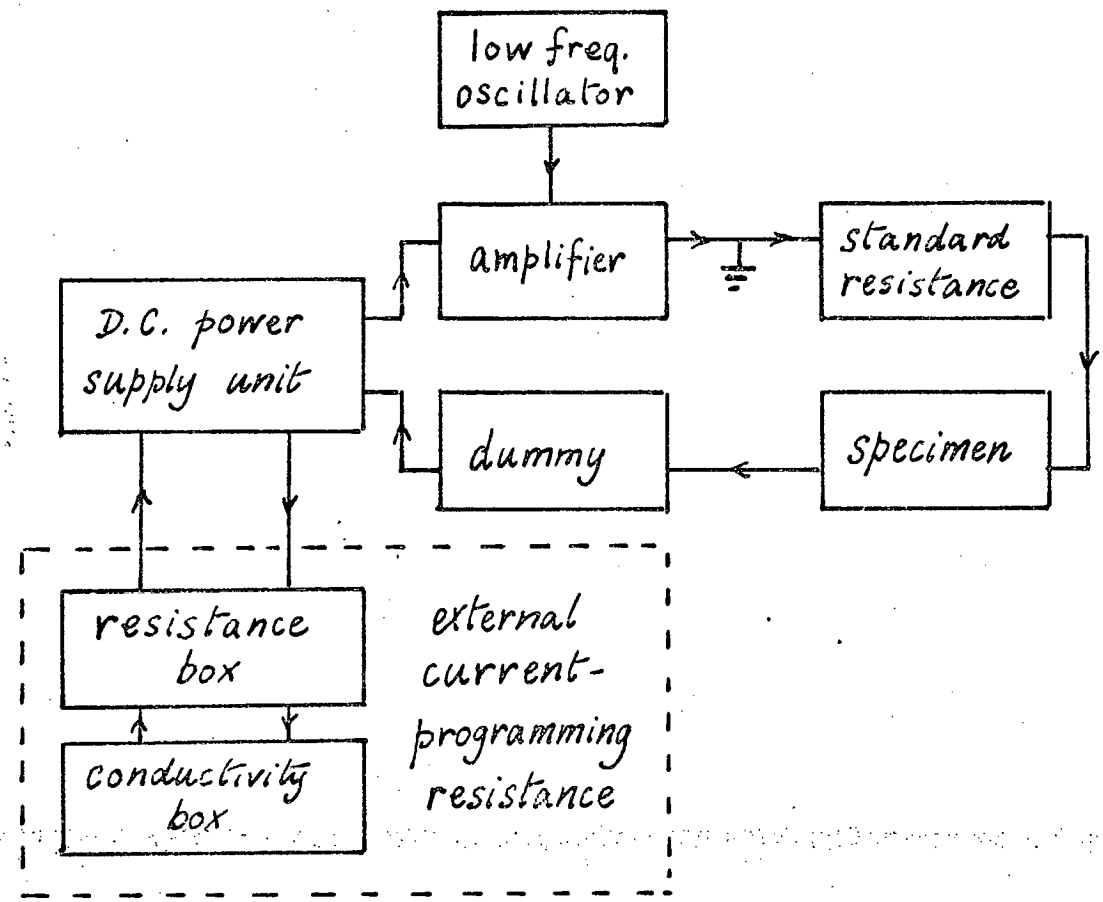

Sec.4.2.2. Fig.1 - Heating current supply arrangements

employed for these experiments, is controlled by a bridge circuit comparing an internal reference voltage with that developed across a sensing resistor carrying the delivered current. Apart from giving excellent current stability, this allows control of the current by alteration of the sensing resistor. The "external current programming" circuit used is shown in Fig. 1 : a low-resistance decade box (Sullivan dual-dial, non-reactive, .05% grade) was used on its 10 x 1 Ω and 10 x 0.1 Ω dials to select the current required for a desired mean temperature. Small changes in this mean temperature as required for calibration of the radiation detector were produced by use of the conductance box in parallel with it (Sullivan non-reactive .1% grade); the 10 x 0.01 mho and 10 x 0.001 mho dials were usually employed for this. The 1 hour stability of the current was $\sim$ 1 part in 10^5 after a warm-up period including at least 1 hour at the desired current. This was achieved only after cleaning the low-resistance-box switches, and using soldered connections on the current-sensing circuit. Currents could be reset to this accuracy after changes made using the conductance box, but naturally the resetting accuracy after use of the low-resistance box was much less because of the low resistance involved. However, currents could be set to within a few mA of the expected values; once so set, the low-resistance box was left untouched until all measurements at that current had been completed. The relationship between measured current and external programming resistance is shown in Fig. 2 and is seen to be substantially ideal.

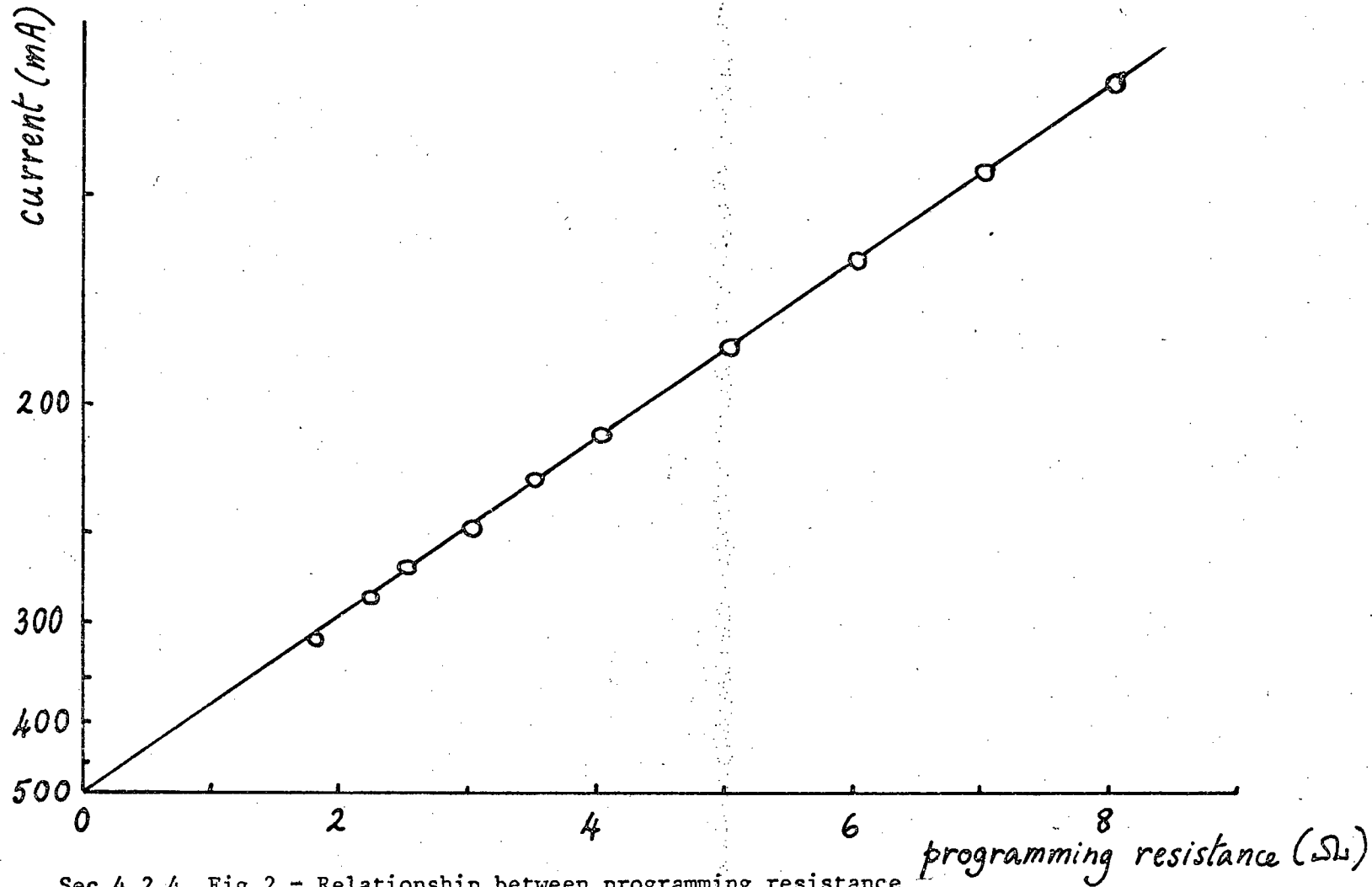

Sec.4.2.4. Fig.2 - Relationship between programming resistance and heating current

The A.C. heating current was superimposed on the D.C. by feeding the latter through the secondary winding of one output transformer of an Armstrong audio amplifier, type A20, substantially as in section 3.3.1. A 5 Ω, 5 W load resistor was permanently connected across this output to protect the transformer in case of an open circuit (e.g. due to specimen failure). This amplifier had a frequency range of 20 Hz - 12 KHz at low specified distortion (< 1%). The current-carrying capacity of the winding (3 Ω tapping) was at least 2A (before onset of core saturation) and so little extra distortion was introduced at the currents used. The amplitude stability of the A.C. current was ∿ 1 part in 10^3 over a 1 hour period. Currents were measured using a Dynamco digital voltmeter type DM2022S with an A.C. convertor assembly consisting of the low-frequency amplifier module type A1 and r.m.s. detector module type B1. The root-mean-square sensing meant that harmonics of 1% amplitude in the heating current affected the readings by only 0.01%, and that this source of error could be neglected. The accuracy of the measuring system was specified as better than 0.1% over the frequency range used.

The frequency of the A.C. heating current was found using an S.E.L. digital counter/timer. On a 10 s count period, this gave accuracies of better than ±0.1% at frequencies of 100 Hz or over.

4.2.3 The D.C. potentiometer

Measurements of the D.C. potential differences across the potential leads of specimen and dummy, and across the

Sec.4.2.3. Fig.1 - Arrangements for D.C. potentiometry

1 Ω standard resistor, were made using a Tinsley vernier potentiometer type 5590B working from a current controller type 5750 and standardised against a Weston standard cell. The null-detector chosen (a wall-mounted Tinsley reflecting galvanometer) was of sufficiently long period that it was unaffected by the unbalanced A.C. flowing through it; tests showed that this A.C. flowing alone produced no deflection. A damping resistor of 1000 Ω was connected across it.

Typical values of specimen voltage and dummy voltage were ∿ 10 V and ∿ 5 V respectively, and a 10:1 potential divider was used (consisting of two .01% resistance boxes (Sullivan non-reactive) set at 90 kΩ and 10 kΩ) to bring these within range of the potentiometer. The standard resistor voltage was 100 mV - 500 mV, and could therefore be measured directly. These voltages could be measured to ∿ 2 parts in 10^5, corresponding to ±200 μV for specimen and dummy, and ±20 μV for the standard resistance voltage. Better accuracy was not warranted in view of the current stability.

For determinations of the specimen and dummy resistances when at room temperature, the current was reduced to ∿ 10 mA using a 1000 Ω series resistor. The corresponding voltages were measured directly on the x 0.1 range of the potentiometer. The accuracy for these voltage measurements was ∿ 2 parts in 10^4.

4.2.4 The radiation detector and associated equipment

This equipment is shown in Fig.1 and Fig.2.

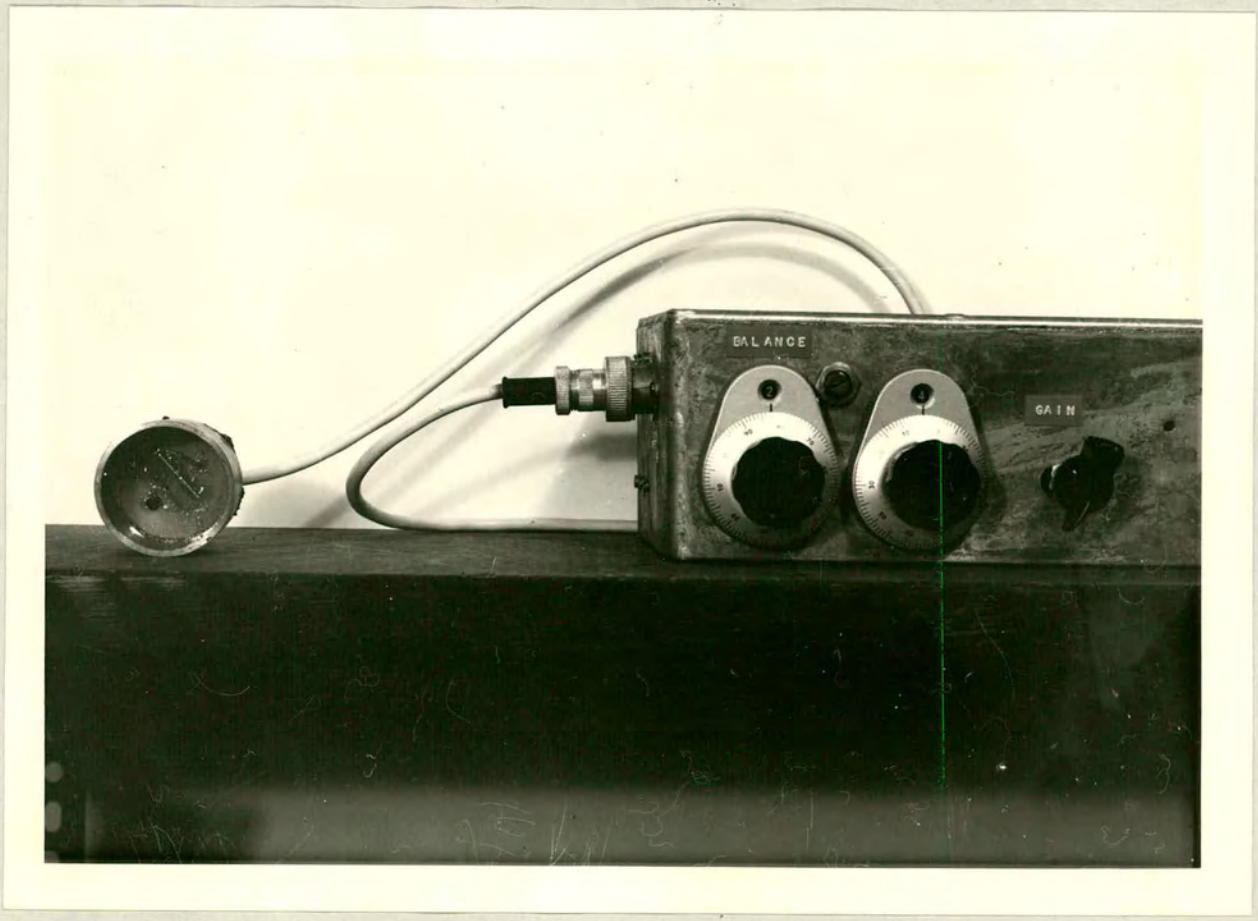

Sec.4.2.4. Fig.1 - The radiation detector and associated amplifier

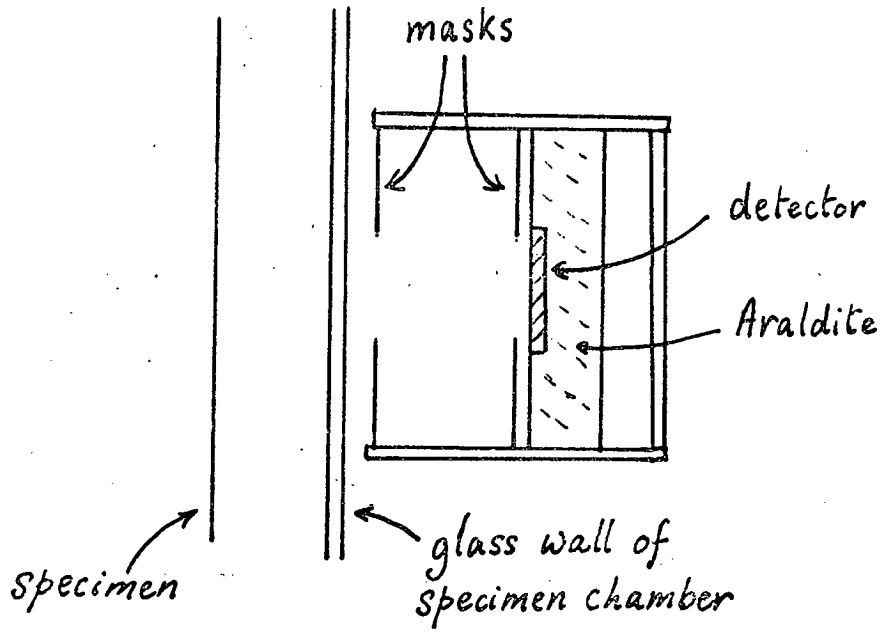

Sec.4.2.4. Fig.2 - Radiation detector geometry

The radiation detector selected was a Ferranti type MS2 silicon photo-voltaic junction diode, chosen for its spectral response (determined from the manufacturer's published data) and for its short response time. For devices of this type, this depends partly on the transit time of the carriers, which is kept small by using a thin junction, and partly on the junction capacitance which can be reduced by reducing the area of the device. The diode selected had a rectangular working area 19 mm x 11.5 mm (and was thus substantially smaller than that used in the trial experiments of section 4.1.4 which had a circular area 30 mm in diameter). In use, the diode was connected across a load resistor, the voltage across which was amplified. The value of this resistor also affected the response time, and a compromise between sensitivity and response time had to be reached. A load resistor of 390 Ω was used giving an overall response time of 30 μs for the system. Under these conditions, the overall response was governed essentially by the amplifier response time, which then avoids any difficulty due to possible dependence of the detector response time on light intensity or spectral distribution. This aspect of the performance was tested using a chopped light beam from a tungsten-filament lamp, and recording the output of the detector amplifier using a Tektronix 545 oscilloscope. Fig. 3 shows typical traces corresponding to the rise and fall of the light intensity, the upper trace corresponding to a lower value of the load resistor, and giving correspondingly faster response.

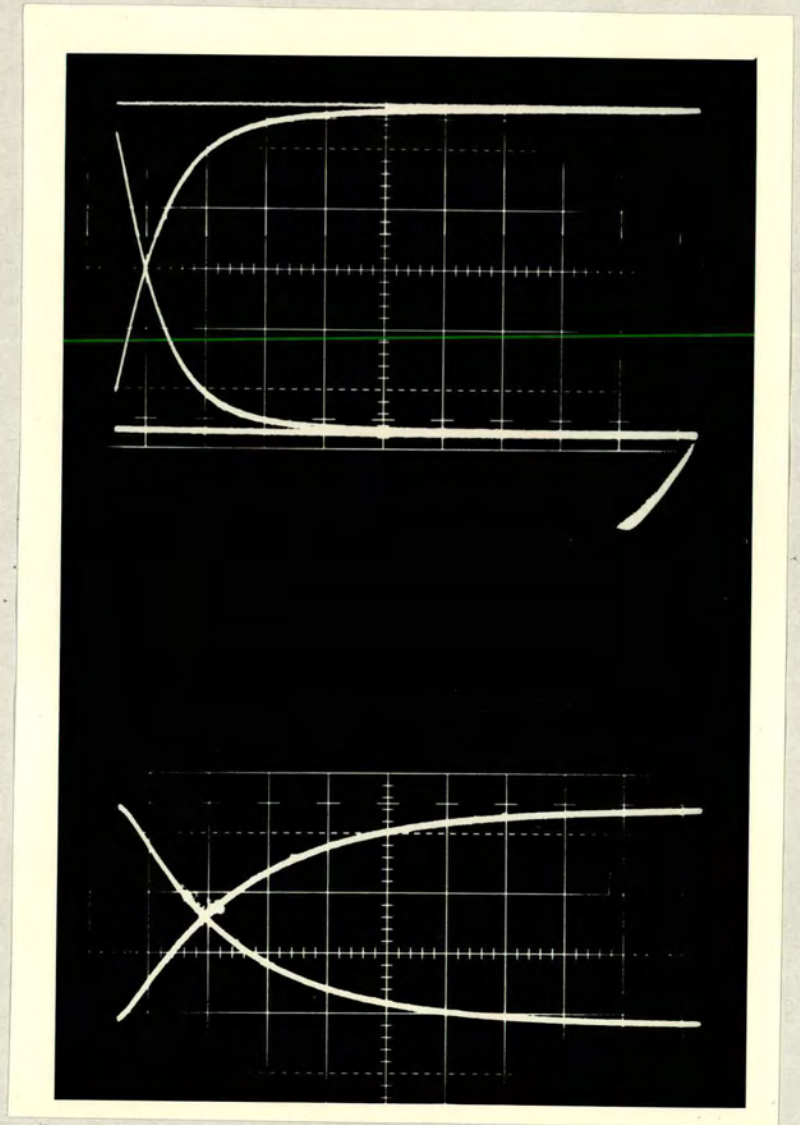

Sec.4.2.4. Fig.3 - Response of detector system to chopped beam, showing decrease of response time as the load resistor is decreased

The dector was mounted in a brass tube using 'Araldite' resin, and this tube also carried an assembly of two diaphragms placed between the specimen wire and the detector. That nearest the wire had a rectangular slot cut in it some 20 mm x 5 mm, the long side being horizontal, and ensured that only light from the central portion of the wire could fall on the detector. The large width of the slot allowed for small lateral movements of the wire. The rear diaphragm consisted of a horizontal slit which could be changed to vary area of the detector on which light could fall. This allowed a variation in sensitivity from the maximum, when the full area was in use, down to $\sim$ 0.1 of this.

The detector amplifier circuit is shown in Fig. 4.* It was powered by a separate stabilised supply working from dry batteries. The amplifier had D.C. sensitivity, so that it could be used to monitor changes in average temperature of the wire, for calibration and as a check on unwanted variations. The D.C. voltage output from the detector was balanced against a variable reference voltage from a calibrated internal helical potentiometer of 10 turns. The amplifier was thus designed as a differential amplifier. Particular care was taken to avoid drift in the input stage (due to temperature changes) and a dual transistor was selected for this reason; similarly, resistors and potentiometers of equal temperature coefficient were used. A transistor acting as constant-

* Acknowledgement is made to J. P. Weight for his technical help in the design and construction.

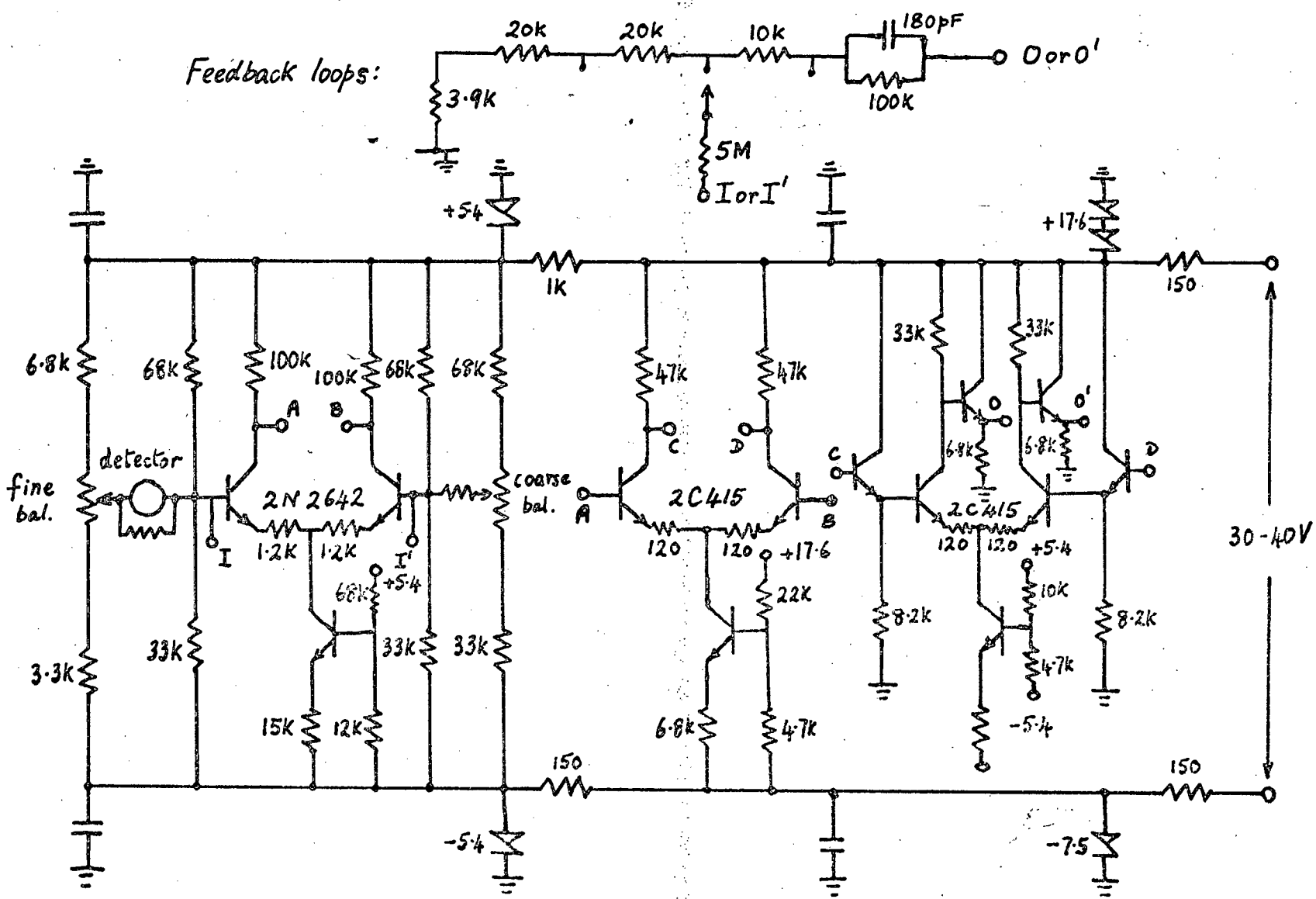

Sec.4.2.4. Fig.4 - The detector amplifier circuit

current generator was provided in the emitter circuit to improve common-mode rejection of changes in supply voltage. In this first stage, collector current was kept low to minimise noise. Similar considerations applied to the design of the remaining two stages. The output of the amplifier was fed out via emitter-followers. A negative-feedback loop was provided between output and input. This stabilised the voltage gain at approximately 40 dB and served to define the pass-band. It also gave the necessary good linearity.

The double-sided output of the detector amplifier was connected to a battery-operated transistorized multimeter (Levell type TM9B) of high impedance (1 MΩ) working on a -5 V to +5 V range with centre zero. This was used as a null-detector to determine an approximate balance point for operation of the amplifier corresponding to each particular light intensity. It also served as a rough indicator for the temperature changes used in calibration, and as a monitor of average specimen temperature generally.

For measurements of the output of the detector amplifier, earthing requirements necessitated the use of the single-sided output. Two kinds of measurements were made. For the D.C. measurements made during calibration, the output was fed via a smoothing network to the Dynamco digital voltmeter described in section 4.2.3. This smoothing network was required to remove the superimposed noise and A.C. from the output, and is shown in Fig. 5 . A time constant of 8 s was found satisfactory, and this was

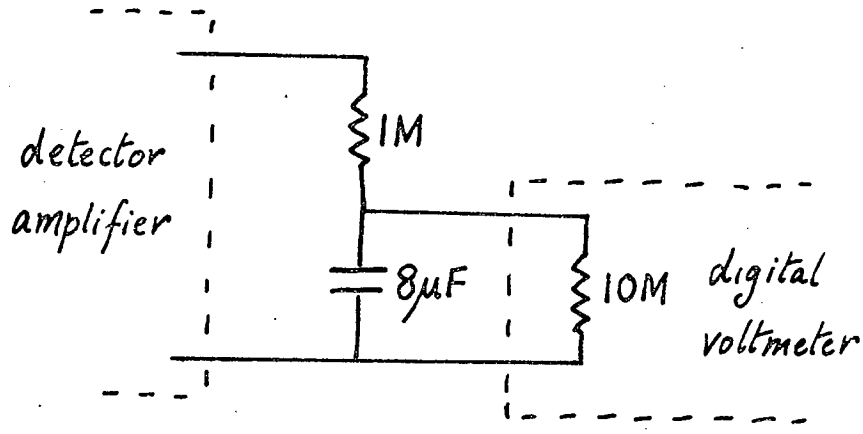

Sec.4.2.4. Fig.5 - Smoothing circuit for D.C. measurements

achieved by using a low-leakage 8 μF mica capacitor fed through a 1 MΩ resistor of 1% grade (Dawe resistance box type 200J). The voltage across the capacitor is proportional to the output voltage of the detector, the constant of proportionality being determined from the known input impedance of the digital voltmeter. On the 0-39.999 volt range this was specified as 10 MΩ, giving a nominal conversion ratio of 10:11. This ratio was checked by using the 0-3.9999 V range (with impedance > 100 MΩ) to measure suitable voltages and comparing with the values calculated from the smoothing circuit measurements. The agreement was better than 0.01%.

For measurements of the A.C. component of the output, the phase-sensitive detector system described below was used.

4.2.5 The phase-sensitive detector system

The idealised action of phase-sensitive detectors (p.s.d.'s) has been briefly described in section 3.4; there it was also remarked that their advantages for this work include not only their insensitivity to noise, but also their insensitivity to second-harmonic distortion.

The p.s.d. chosen was a Brookdeal type 411 used in conjunction with the Dynamco digital voltmeter. This p.s.d. is designed for frequencies in the range 1 Hz - 1 MHz and at the frequencies used the switching action was substantially ideal. For the accurate amplitude measurements required, exceedingly good linearity is needed from the instrument even at input signals corresponding to only $\frac{1}{10}$

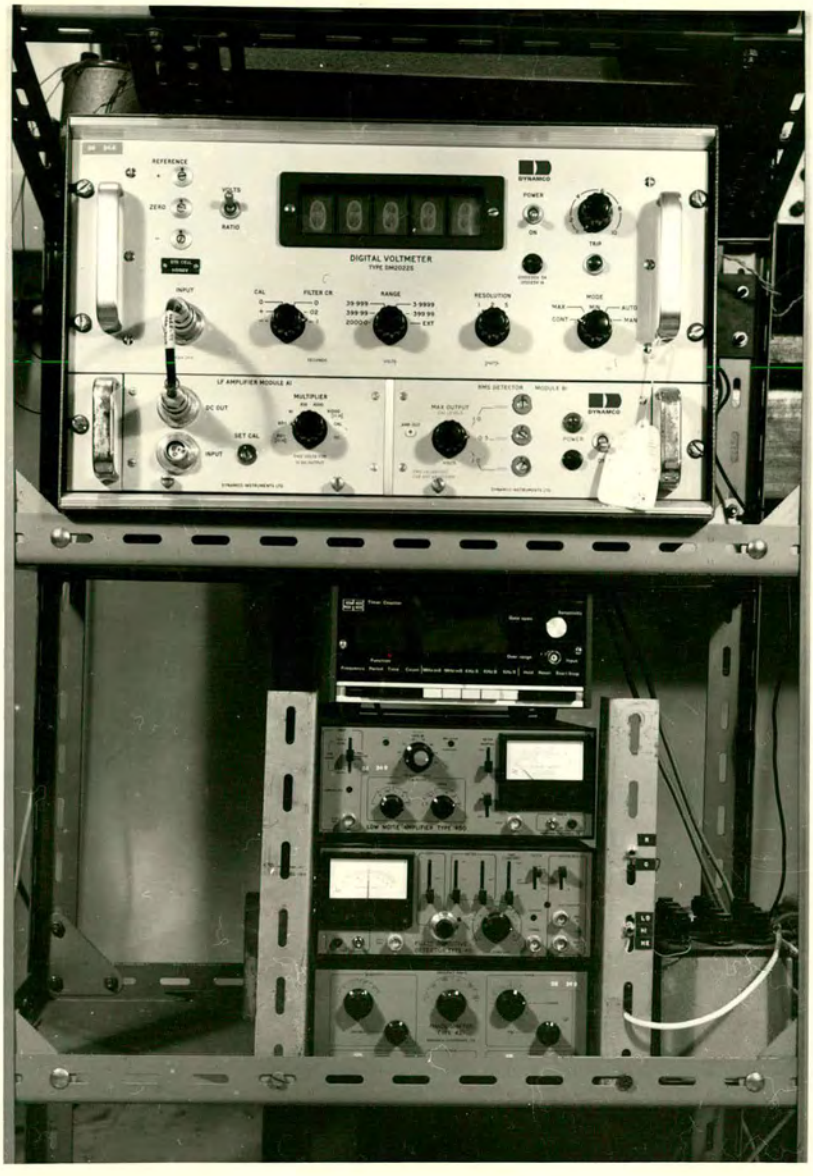

Sec.4.2.5. Fig.1 - The phase-sensitive detector system

of the full-scale output. The instrument chosen had a specified non-linearity < 0.03% of full-scale (as measured by the intermodulation method) and could therefore be used down to $\frac{1}{10}$ full scale with < 0.3% error. The instrument was supplied calibrated to give a full-scale output of 10 V D.C. for a sine-wave input of 1 V (R.M.S.). This calibration was tested using the Dynamco A.C. digital voltmeter described in section 4.2.2, and was found to be accurate within 0.1% at full-scale. The linearity was similarly checked, and found to be within the specification at $\frac{1}{10}$ full-scale provided the zero was carefully set. These tests were made using a detector integration time constant τ_I of 3 s, as used in the experimental measurements.

The input to the p.s.d. was either direct from the radiation detector amplifier, or, for the lower signal levels, via a Brookdeal low-noise, low distortion amplifier (type 450). This instrument provided switched, calibrated voltage gains of 30dB-70dB nominal, by 10dB steps. The calibration of these switched gains was carried out by use of an insertion-loss technique using an Avel decade ratio transformer type 4TR2D. Typical calibration curves, for the 30dB and 40dB gain positions used in the experiment, are shown in Fig. 2. The measurements were taken using the Dynamco A.C. digital voltmeter to compare the test signal and the output from the low-noise amplifier, fed with the test signal attenuated in known ratio by the transformer. The transformer ratio was adjusted by use of the decade switches to give approximate equality of these voltages compared. These calibration curves were

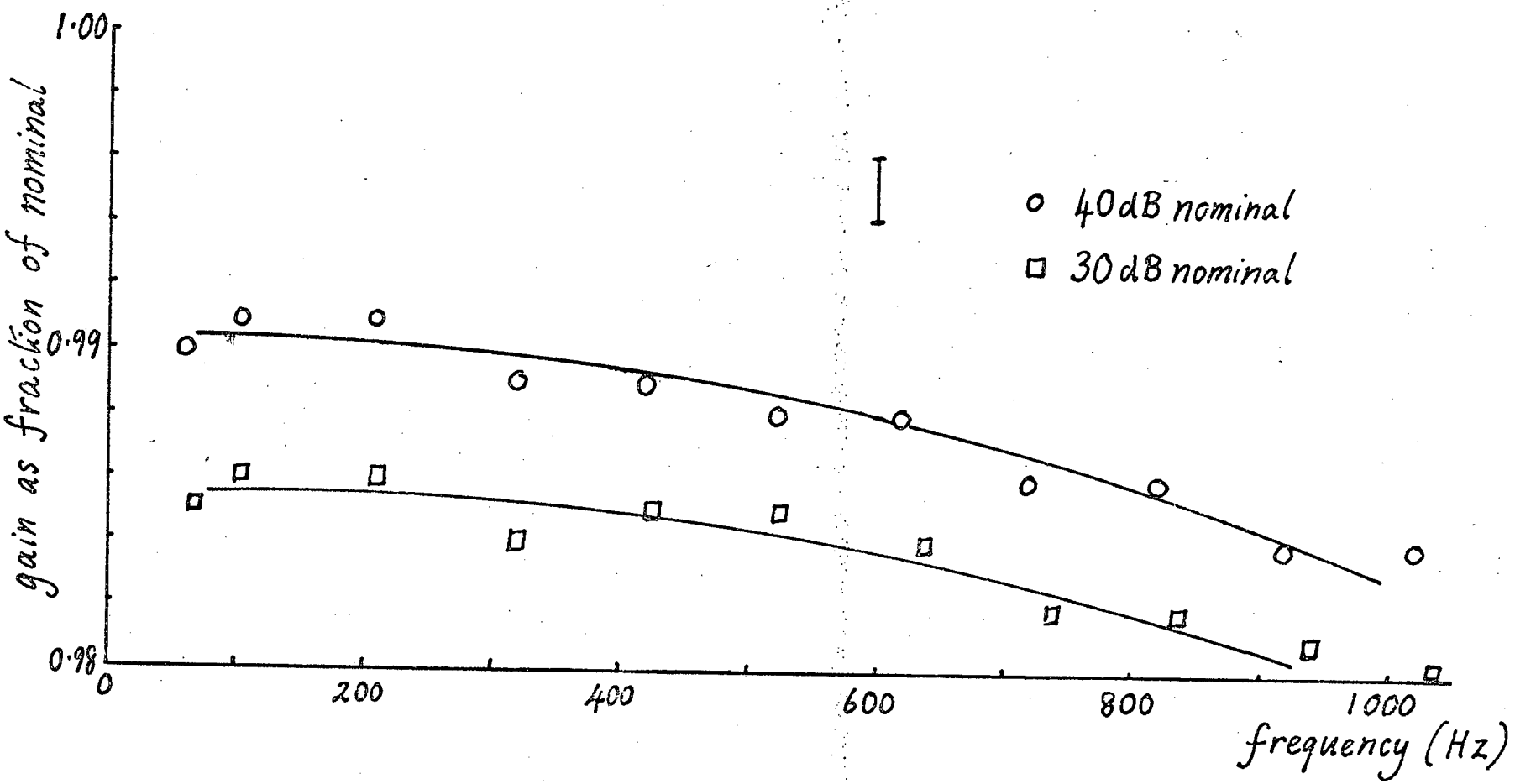

Sec.4.2.5. Fig.2 - Calibration curves for the low noise amplifier

taken with the same low-noise amplifier internal filter settings as used in the experiment. The amplifier had, for noise-reduction purposes, a bandwidth that could be limited by this internal band pass filter. The low- and high-frequency cut-off points were selected to be well outside the frequency range. The curves shown correspond to the 1 Hz and 10 KHz settings and were used for measurements in the 200-500 Hz range. Satisfactory agreement was also found in the experiments themselves when changing amplifier ranges if the appropriate calibration curve was used, thus providing an additional check. The calibration factors determined from the curves were reproducible, and taken as accurate to $< 0.3\%$.

The reference signal for the phase-sensitive detector was derived by the circuit shown in Fig. 3. A.C. from the output transformer of the modulating current supply amplifier was passed through a simple R-C series circuit. The voltages across resistor and capacitor were approximately 90^{o} out of phase; the input of a Brookdeal Phase Shifter type 421 could be switched across either, the R-C circuit then acting as a 90^{o} phase-shifter. The magnitudes of the resistor and capacitor were chosen to give approximately equal voltages across them at the design frequency, and three such R-C pairs were provided for frequencies $\sim$ 100 Hz, $\sim$ 300 Hz and $\sim$ 1 Hz respectively. The impedance of each components at the design frequency was small compared to the input impedance of the Brookdeal phase-shifter, and the phase-shift produced was within $\frac{1}{2}^{o}$ of 90^{o}. This phase shift was determined using the heating

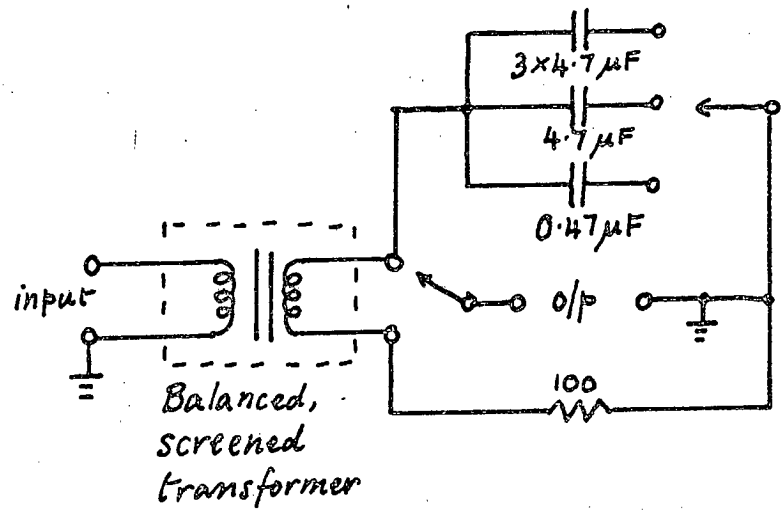

Sec.4.2.5. Fig.3 - 90° phase-shift network

current waveform as signal, with reference set at $\sim 45^{\circ}$ phase difference, and noting the outputs before and after shifting the reference through the nominal 90°. The Brookdeal phase-shifter itself provided fine and coarse controls for phase over rather more than 180°, and variable amplification to provide an output level suitable for the reference channel of the p.s.d. In the interests of consistency of p.s.d. switching, this level was adjusted always to be just below the maximum permitted as indicated by an overload neon on the phase-shifter.

The procedure used for amplitude measurements of a signal was to adjust the variable phase-shift to give a zero output from the p.s.d., signal and reference were then 90° out of phase. The 90° phase-shift was then operated, giving an output corresponding to either 0° or 180° phase-difference between signal and reference. In either case, the output was a measure of the amplitude of the signal. The fractional error introduced by a small error ϕ in the 90° phase shift was $(1 - \cos\phi) \simeq \frac{1}{2}\phi^2$ i.e. .02% for $\phi = 1^{\circ}$. In practice, no detectable error was introduced, as tested by looking for an increase in output on adjustment of the fine-phase control.

The above procedure was rather slow, particularly when long integration-time constants (such as 3 s) were in use, since the full procedure had to be used each time the frequency was changed. The difficulty may be avoided with more modern equipment, not available at the time of purchase of that described above. The type 422 reference-signal generator would replace the reference signal arrangements above.

It has built-in 0^{o}, 90^{o} and 180^{o} phase-shift output terminals. The phase can also be varied continuously either manually or by an externally-applied voltage. If this voltage is derived from the output of a second p.s.d. using the output of the phase-shifter as reference and having the signal as input, the output from the 90^{o} terminal will be maintained at 180^{o} relative to the signal, and can be used as reference signal in the primary measuring p.s.d. (An apparently simpler solution is to derive the reference by 90^{o} phase-shift of the voltage across a sensing resistor in the specimen current circuit, and subsequent amplification using an amplifier with sensibly zero phase-shift. The difficulty here is that it relies on the radiation detector output and the modulation current being 90^{o} out of phase, and this is not always true.)

4.3 Measurements of the Mean Temperature

4.3.1 Introductory

Measurements of specimen mean temperature were needed not only for interpretation of the specific heat measurements, but also for radiation-detector calibration. For the first purpose, an absolute measurement accurate to a few degrees was needed, while for the second, accurate measurements of small changes of mean temperature ($\pm \sim 10$ K) were required. The required information was obtained from resistance measurements at the working temperatures and at room temperature; these were converted to temperatures using an assumed dependence of resistance on temperature, as explained below.

4.3.2 The electrical resistivity of platinum

Where pure metals are concerned, reliable results for the variation of resistivity with temperature are often available. In the case of platinum, while the resistivity at moderate temperatures is well known, the region between ∿ 1500 K and the melting point has been explored much less extensively. Roeser and Wensel (1941)[a] give values to 1500°C (1773 K) which are confirmed up to 1700 K by the work of Jain, Goel and Narayan (1968) as far as variation with temperature is concerned. Data above 1773 K appear to be lacking.

Kraftmakher and Lanina (1965) in their work on the specific heat of platinum required to know the resistance as a function of temperature in the high temperature region. They used published values of "total emissivity" (i.e. emittance) of platinum to calculate the temperatures of wires held above 1500 K by Joule heating in vacuo, measuring the resistance R. Their results for $\alpha = (1/R_{ice})(dR/dT)$ differed by not more than 2% from specimen to specimen, and are shown in Fig. 1. Temperatures below 1500 K and above 1000 K determined similarly agreed with the values obtained from the quadratic expression given by Roeser and Wensel (1941)[a]. A further check was made by heating a wire to the melting point.

The procedure used by Kraftmakher and Lanina raises some questions. The references they give for the emittance data are confusing. The first ("Handbook of Thermophysical

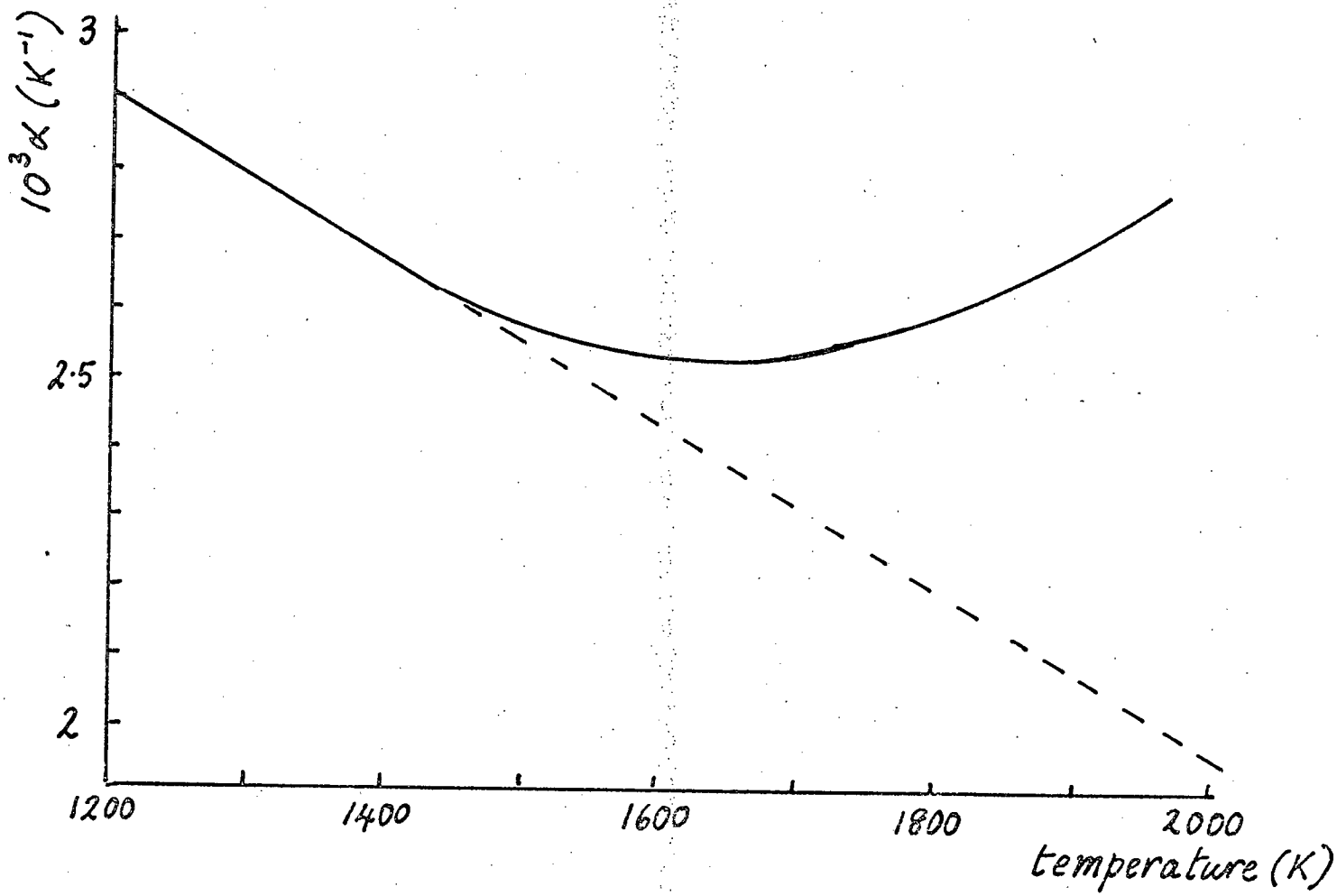

Sec.4.3.2. Fig.1 - Temperature coefficient of resistance for platinum, after Kraftmakher and Lanina

Properties of Solid Materials, Pergamon 1961") appears to give only total normal emittance ε_{nt} instead of the total hemispherical emittance, ε_{ht}. The other ("Temperature its Measurement and Control in Science and Industry, Reinhold, N.Y., 1941") gives recommended values for ε_{ht} (appendix p.1314) but only to 1500°C (1773 K). In the same volume, the article by Worthing pp. 1164-1187 refers to several determinations of ε_{ht}, though only that of Davisson and Weeks (1924) goes above 1500 K, reaching 1700 K. Total normal emittances are given to 1950 K (Foote, 1915), but the distinction between ε_{nt} and ε_{ht} is not negligible; at 1500 K, $\varepsilon_{ht} \sim 0.13$-$0.15$, while $\varepsilon_{nt} \sim 0.17$-$0.18$. Since the temperature in Kraftmakher and Lanina's experiment is determined from the power balance, these variations in ε are significant and would lead to differences in estimated temperature of ~ 45 K. An additional difficulty is suggested by the work of Jain, Goel and Narayan (1968). They measured ε_{ht} for different samples of "pure" platinum, and found that the values differed by as much as 20% from sample to sample; moreover, the variation of ε_{ht} with temperature also depended on the sample. This suggests that the agreement reported by Kraftmakher and Lanina was to some extent fortuitous.

In these circumstances, since one of the main objects was a comparison with the work of Kraftmakher and Lanina, their values of α were used to extrapolate the published values of r_e (Roeser and Wensel 1941) starting at 1000°C (1273 K). The values of α were taken from the table given by Kraftmakher (1966). The results are shown in the table below:

Table 4.1

Resistance ratio $r_e = R/R_{ice}$ for platinum

Temperature		Mean *		
°C	K	$\alpha \times 10^3$ (K^{-1})	Extrapolated r_e	r_e †
1000	1273	2.76	(4.395)	4.395
1100	1373	2.65	4.671	4.672
1200	1473	2.56	4.936	4.937
1300	1573	2.53	5.192	5.190
1400	1673	2.55	5.444	5.431
1500	1773	2.62	5.699	5.660
1600	1873	2.72	5.961	-
1700	1973		6.233	-

* Kraftmakher (1966)

† Roeser and Wensel (1941)

Up to 1500 K, there is no significant difference between the extrapolated and the published values of r_e. At 1773 K, the difference, 0.7%, corresponds to $\sim$ 10 K. The extrapolated values of r_e were used in the experiments described below to determine temperatures. Values of ε_{ht} were also determined as a check on the procedure, as described in section 4.3.8.

4.3.3 End effects

The most satisfactory way of eliminating the end effects in hot-wire measurements is to use potential leads

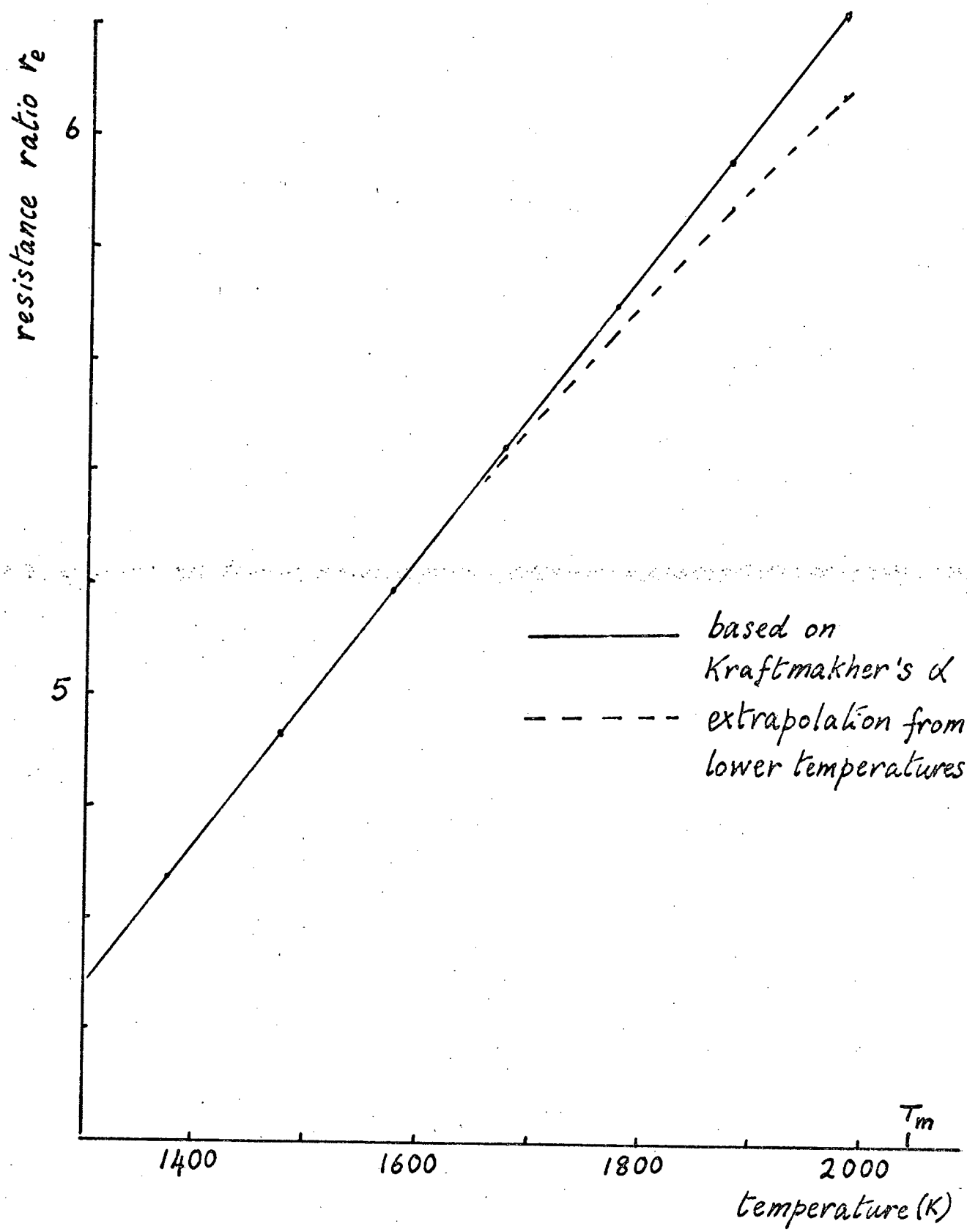

Sec.4.3.2. Fig.2 - Resistance ratio for platinum as a function of temperature

sufficiently far from the ends to be in the uniform-temperature region, and sufficiently thin compared with the specimen to cause no significant disturbance to that uniformity. In the present experiments, the specimen wires were, at 50 μm diameter, so thin that potential leads of the requisite thinness (say ∿ 5 μm) were not practicable. The potential leads used were of the same material and diameter as the specimen, and therefore conducted away a significant amount of heat. Further, for a reason which will be discussed in section 4.4.3 , they were mounted rather close to the end supports, at a distance (5 mm) which, although enough to avoid most of the end effects, was not large compared with the characteristic scale of the temperature variation near the end (∿ 2 mm). The use of a dummy of the same wire and having the same end-arrangements meant that by subtraction of specimen and dummy resistances end effects could, if equal, be eliminated entirely. Further, a check on the magnitude of such effects could be made, giving an estimate of the uncertainty in the measurements due to variation in end effect.

For example, at 1450 K, with a 154 mm specimen and 62 mm dummy, measured resistance ratios r_{sp}, r_{du} were obtained for specimen and dummy respectively

$$r_{sp} = 4.846 \qquad r_{du} = 4.775$$

while by subtracting the measured resistances of specimen and dummy the value $r_{sp-du} = 4.898$ was obtained. As expected $r_{sp-du} > r_{sp} > r_{du}$. The differences were

significant: $r_{sp-du} - r_{sp} = .052$, about 1%, while $r_{sp-du} - r_{du} = .123$. The ratio of these differences was $\sim 1/2.4$, which correlated well with the ratio of specimen and dummy lengths (2.41). It was concluded that the end effect error was reduced by using r_{sp-du} and was < 0.1%. At higher temperatures, the end effects are even smaller. At the lowest temperatures used ($\sim$ 1200 K) the specimen end effect is still < 2%, and end effects in r_{sp-du} < 0.2%, the last figure corresponding to < 3 K. These results indicated that even with a fairly long specimen (150 mm) and use of potential leads, the use of the dummy was a significant improvement.

4.3.4 Room temperature measurements of resistance

For measurements of the specimen and dummy resistances at room temperature, the specimen chamber was opened to atmospheric pressure. Measurements of the air temperature were made using a certified mercury-in-glass thermometer reading to 0.1°C, the bulb being in the vicinity of the mid-point of the specimen wire. The light shield of heavy brass tube acted also as a thermal-shield, and stable temperatures were obtained after about 1 hour, changing by not more than 0.1°C during the potentiometric measurements then made. These were made using the technique described in section 4.2.3. The measuring current, $\sim$ 10 mA, was chosen to be well below the minimum current at which wire-heating effects were observed ($\sim$ 50 mA), and no significant variations of measured resistance were observed using currents in the range 5-20 mA. The accuracy of the

resistances determined in this way was $\sim$ 3 parts in 10^4 so that the difference in specimen and dummy resistance was determined to $\sim$ 5 in 10^4.

These values were converted to equivalent resistances at $0^{\circ}C$ using the relationship, valid in the range $0\text{-}630^{\circ}C$ for platinum

$$r_e = 1 + A\theta + B\theta^2$$

where θ is the centigrade temperature and $A = 3.98 \times 10^{-3}\ ^{\circ}C^{-1}$, $B = -5.85 \times 10^{-7}\ ^{\circ}C^{-2}$. The values of these constants are taken from the manufacturer's data (Johnson, Matthey & Co. Ltd. 1952). This relationship gave consistent results when used at different room temperatures, and also gave $r_{100^{\circ}C}$ consistent with the value quoted by the wire supplier. The accuracy of the conversion was limited by that of the room temperature determination to $\sim$ 4 parts in 10^4. The overall accuracy of the resistances determined was $\sim$ 1 part in 10^3, and values could be reproduced to this accuracy provided the wires were not heated between measurements. The effect of heating is considered in detail below in section 4.3.6; the reproducibility from one measurement before heating to another after heating was a few parts in 10^3. This, therefore, limited the accuracy of the results.

4.3.5 Calculation of specimen parameters

The above values of resistance at $0^{\circ}C$ were used with the measured lengths of specimen and dummy to calculate the mass and surface area of the specimen and of the dummy,

assuming the resistivity of the platinum at $0^{o}C$ to be 9.81×10^{-8} Ωm and the density 21.40×10^{3} kgm^{-3} (Johnson, Matthey & Co. Ltd. 1952). The calculation assumes the wires are uniform cylinders.

The results were checked by weighing a known length of wire on a precision balance: 980 mm weighed 44.3 mg. The results were consistent within an allowance of $\sim$ 1% for variations in wire diameter. Because of the possibility of variations in wire thickness within the length of the specimen and dummy wires, it is somewhat difficult to estimate the accuracy of the calculated mass and area of the effective specimen defined as the difference between specimen and dummy. Accuracies of ±2% in these quantities will be assumed. Typical values were $\sim$ 14 mm^2 for effective specimen area and $\sim$ 4 mg for the corresponding mass.

4.3.6 Changes in specimen cold resistance after heating

Measurements made on fresh specimens which had been heated in vacuo for periods of a few hours showed that the resistance at $0^{o}C$ typically increased by a few parts in 10^{3}. The effect occurred at temperature as low as 1300 K. Saturation was observed after a total rise of $\sim$ 1% of the resistance at $0^{o}C$.

Polak (1967) observed this effect in platinum specimens heated in air; he also observed oxidation, a volatile oxide (PtO_2) being formed. In the present work, the oxidation was avoided by working in vacuo, the reaction rate with the residual gas being negligible (Fryburg, 1965). Absorption of the residual gas is however possible, and

the observed effects are attributed to this. (This explanation is in accordance with the proposal of Lovejoy (1964) who showed that a concentrated layer of impurity at the surface accounted for resistance-increase effects in heated platinum). There appeared to be no effect on the specific heat; in any case, because of the saturation behaviour, it was possible to work with specimens whose resistance at $0^{o}C$ had stabilised to $\sim$ 1 part in 10^{3}.

Evaporation effects are confined to much higher temperatures. A calculation based on the vapour pressure figures quoted by Smithells (1962) gave upper limits for the rate of loss of mass from 50 μm wire as $\sim$ 1% per hour at $\sim$ 1750 K, increasing by a factor $\sim$ 10 for each 100 K increase in temperature. This calculation assumes that the evaporation rate per unit area is the collision rate per unit area, and therefore overestimates the evaporation rate by a factor of perhaps 3-10. Appreciable (1 in 10^{3}) increases in resistance were not in fact observed in specimens heated to 1800 K for 1 hour, though above this temperature some evaporation occurred.

4.3.7 High temperature measurements of resistance

The resistance of specimen and dummy at high temperatures was measured by the technique described in section 4.2.3. The accuracy of the potentiometric measurements, 2 parts in 10^{5}, was fully adequate for absolute determination of the mean temperature, the limiting accuracy here being the determination of the resistance at $0^{o}C$, as discussed above. Absolute mean temperatures were

therefore regarded as being accurate only to about ±5 K.

For comparison of mean temperatures on the other hand, as needed in detector calibration, the precision of the high temperature potentiometric measurements was limiting. The resistance of the "effective specimen" (corresponding to the extra length of the specimen compared with that of the dummy) could be determined to $\sim$ 1 part in 10^4, so that, for 0.3% precision in measurement of a temperature interval, the interval needed to be at least 5 K. This temperature interval was usually increased to $\sim$ 20 K to allow some margin for current or other fluctuations. These calibrations are further discussed below.

The absolute mean temperatures determined from these measurements using the extrapolated resistance ratio values r_e of table 4.1 were checked as far as possible using an Evershed-Vignoles optical pyrometer. To adapt this for work on fine wires, a 10 dioptre converging lens was fitted adjacent to the objective lens to decrease the working distance and increase the size of the image of the specimen wire. The calibration is thereby unaffected, except for any absorption by the lens. Also, the geometry of a wire is such that if the radiation from it is diffuse and obeys the cosine law, the apparent brightness is that of a flat plate at the same temperature. Corrections were therefore made only for light absorption by the glass tube surrounding the specimen, and by the extra lens. Measured temperatures in the region above 1300 K were within 20 K of the resistance-derived values, taking values of normal

spectral emissivity $\varepsilon_{n\lambda}$ from Jain, Goel and Narayan 1968. Greater accuracy is not expected, since $\varepsilon_{n\lambda}$ varies considerably from sample to sample, and also depends critically on surface condition (see Jain et.al. and also the collection of data by Touloukian (1970)).

The temperature-current curve determined from the resistance measurements is shown, for typical specimens, in Fig. 1 . The variation from specimen to specimen is consistent with variations in radius $\sim$ 1%. A useful empirical curve is shown in Fig. 2 . The graph of log T against log i, where i is the total heating current and T is absolute temperature, is a straight line of slope nearly $\frac{1}{2}$; this corresponds to an emissivity ε proportional to T over the temperature range. The curve was extrapolated to determine the current required for any desired temperature near the melting point, to avoid melting the specimen by a too large current.

4.3.8 Measurements of total hemispherical emittance

The total hemispherical emittance ε_{ht} was calculated from the power dissipated in heating the specimen to a known temperature, knowing also the surface area. A correction was necessary for thermal expansion; values of mean expansion coefficient were taken from Smithells (1962) and extrapolated to temperatures above 1000°C (1273 K) using the results of Kraftmakher (1967) to 1500 K, and linear extrapolation thereafter. The linear expansion is 1% at 1200 K and increases steadily to 2% at 2000 K, using room temperature as the reference state. The

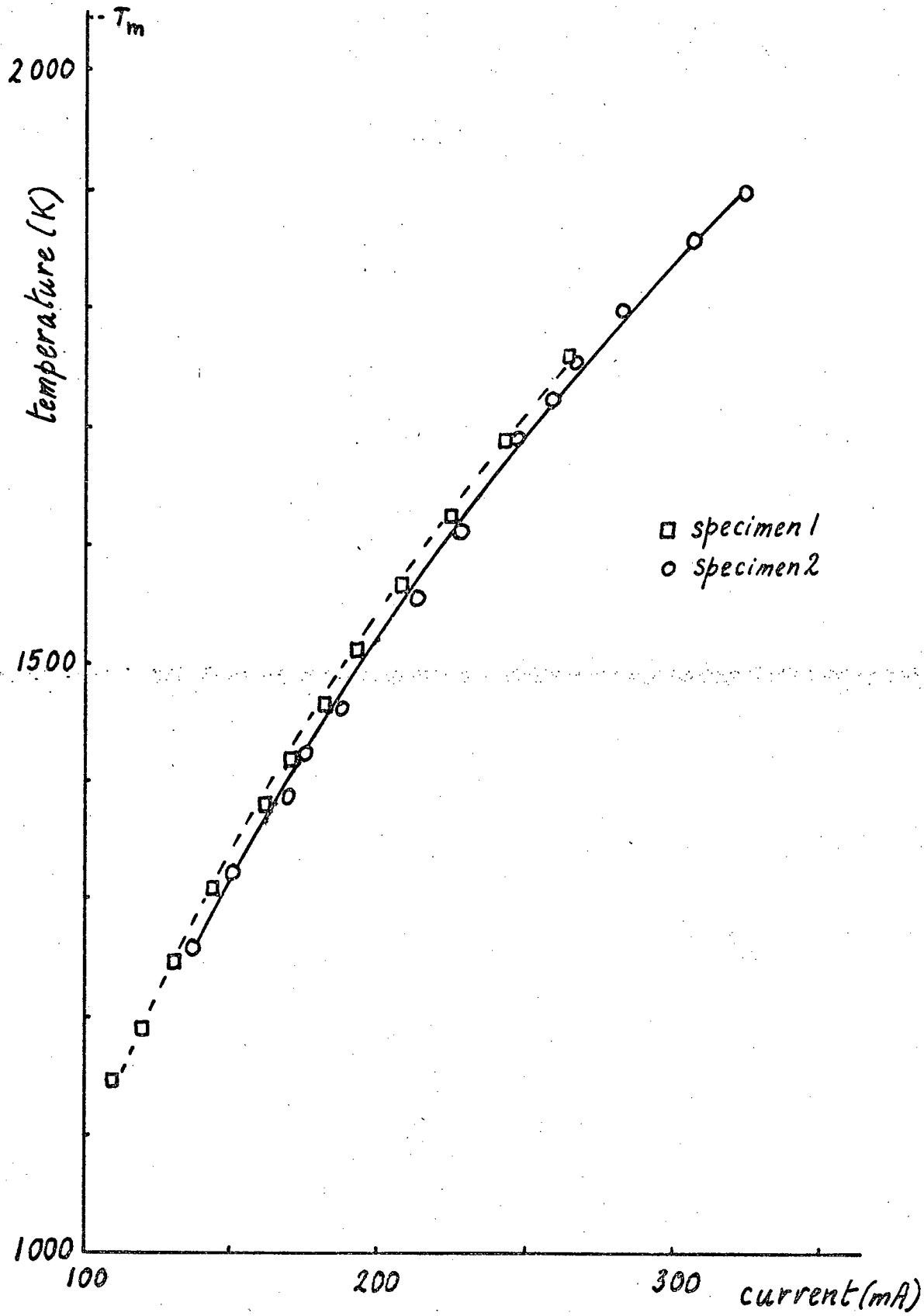

Sec.4.3.7. Fig.1 - Temperature/current curves for typical specimens

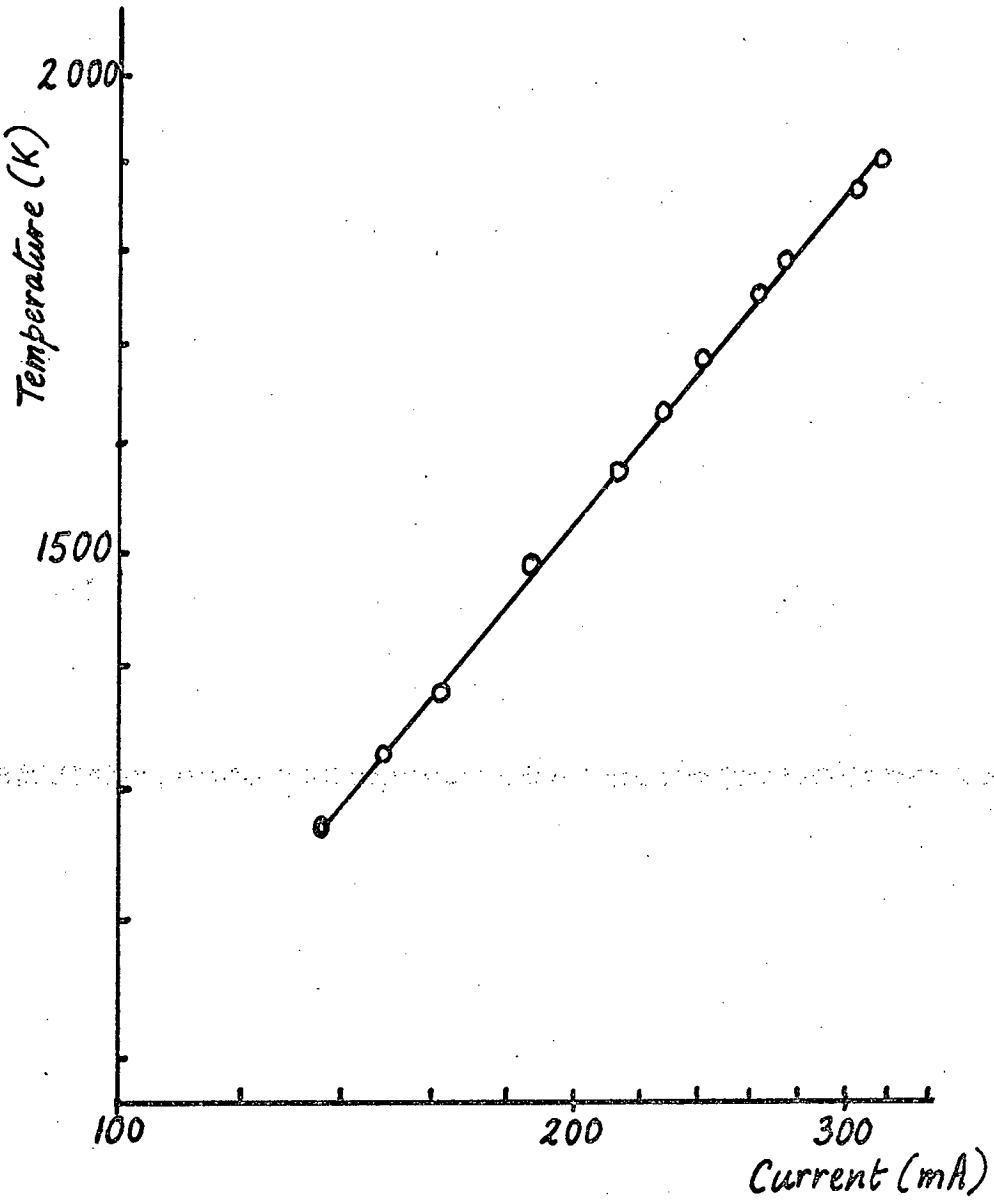

Sec.4.3.7. Fig.2 - Temperature vs. current-logarithmic plot

corrections to ε_{ht} are -2% and -4% at the respective temperatures, arising from the increase in area. No correction is required for the resistance changes due to expansion, as they are included in the resistance ratio values used to determine the temperature.

Measurements of ε_{ht} were made using D.C. heating alone, and also using combined A.C. and D.C. Typical results are shown in Fig. 1. for two different specimens. Results for the first are from a special emissivity run. They show no departure from a linear variation of ε_{ht} with temperature, and the agreement with the compiled values shown is satisfactory. On the second specimen, measurements were made over several weeks in the course of specific heat experiments. Though the scatter is somewhat larger, the results are satisfactory, except that a slight permanent increase in ε_{ht} was observed after heating above 1850 K. This is attributed to changes in surface condition of the wire. The uncertainty in the ε_{ht} values measured derives largely from the uncertainty in the wire radius; the overall uncertainty is $\sim \pm 5\%$, comparable with the usual uncertainties in the measurement of ε_{ht} (Touloukian 1970) and leading to uncertainties in the absolute temperature derived from a value of ε_{ht} of $\sim$ 20 K in the range of interest here.

4.4 The performance of the measuring system

4.4.1 General

The performance of the system was checked using the

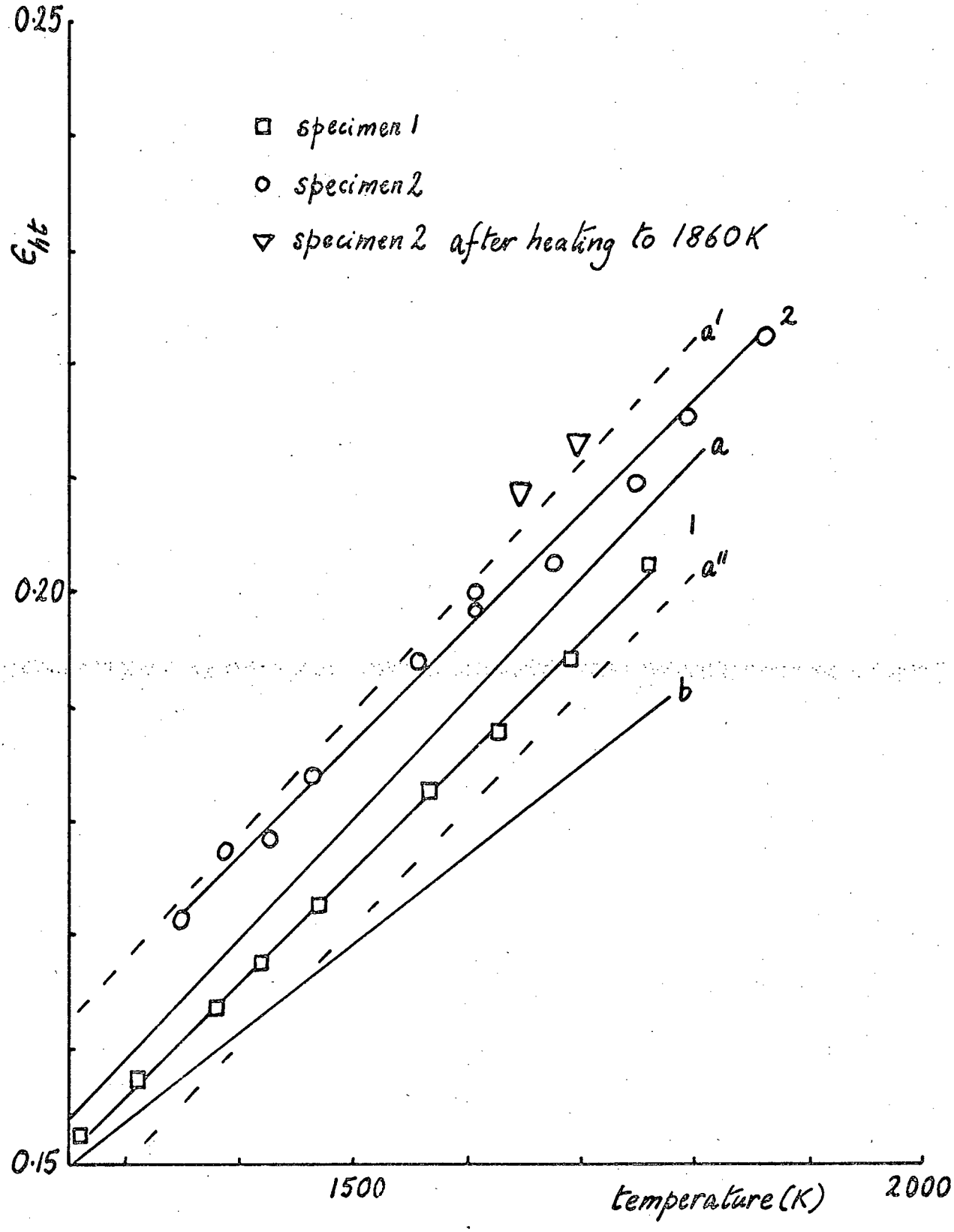

Sec.4.3.8. Fig.1 - Total hemispherical emittance

fact that at temperatures $\sim$ 1500 K, vacancy effects are negligible, and the specific heat of the specimen is independent of frequency. Under these conditions the theory of section 2.2 applies; in the high-frequency approximation we then have, from equation 2.13, that the magnitude of the temperature modulation is given by

$$|\theta_1| = \frac{2i_0 i_1 R_0}{\omega m c_p} . \qquad \ldots (4.1)$$

This equation formed the basis for the frequency and linearity checks described in the following two sections.

In addition, tests of noise, D.C. performance and drift were made over the working temperature range, as detailed in subsequent sections.

4.4.2 Linearity of the modulation measurement system

The A.C. linearity of the system constituted by the radiation detector and detector amplifier, low-noise amplifier (where used), phase sensitive detector and digital voltmeter, is crucial to any experiment in which frequency ω is varied with other factors constant; as equation 4.1 shows, such an experiment involves a range of $|\theta_1|$ values inversely proportional to the values of ω used. Compensating changes in i_1, the modulating current, can be made to restrict the range of $|\theta_1|$ values, but have other effects, such as changing the mean temperature (unless the D.C. heating i_0 is also adjusted) and changing the harmonic content of the output.

The system linearity was accordingly checked over a range of amplitude of $\sim$ 10:1 by varying i_1 at fixed

frequencies. It is important to maintain the specimen mean temperature constant during the experiment, since the temperature variation is being measured by a radiation detector whose output varies rapidly with temperature. This constancy was assured by varying i_o to return the D.C. output of the radiation detector to a fixed value, as measured by zero balanced D.C. output from the detector amplifier with the balance control at a fixed setting. This gave values of $(i_o^2 + \frac{1}{2}i_1^2)$ constant (to 1 part in 10^3), indicating that the mean temperature was kept constant by this procedure. Assuming the desired proportionality between $|\theta_1|$ and the A.C. output of the radiation detector system, V_{1d}, the quantity $V_{1d}/i_o i_1$ should be constant. Fig. 1 shows the variation of this quantity as a function of i_1/i_o at various frequencies, using the phase-sensitive detector without the low-noise amplifier. The integration time was 3 s, and the specimen mean temperature 1550 K. The results showed no significant departure from linearity within the experimental uncertainty $\sim$ 0.3%. The lower limit of the useful amplitude range is set by the phase-sensitive detector specificiation, which gives linearity within 0.3% at $^1/_{10}$ of full scale. The upper limit is set by the relative instability of i_1 compared with i_o.

Introduction of the low-noise amplifier contributed no significant non-linearity (< .05% full scale, as specified).

The range of temperature modulation amplitude used in the linearity experiments was up to a maximum of $\sim$ 5 K, at

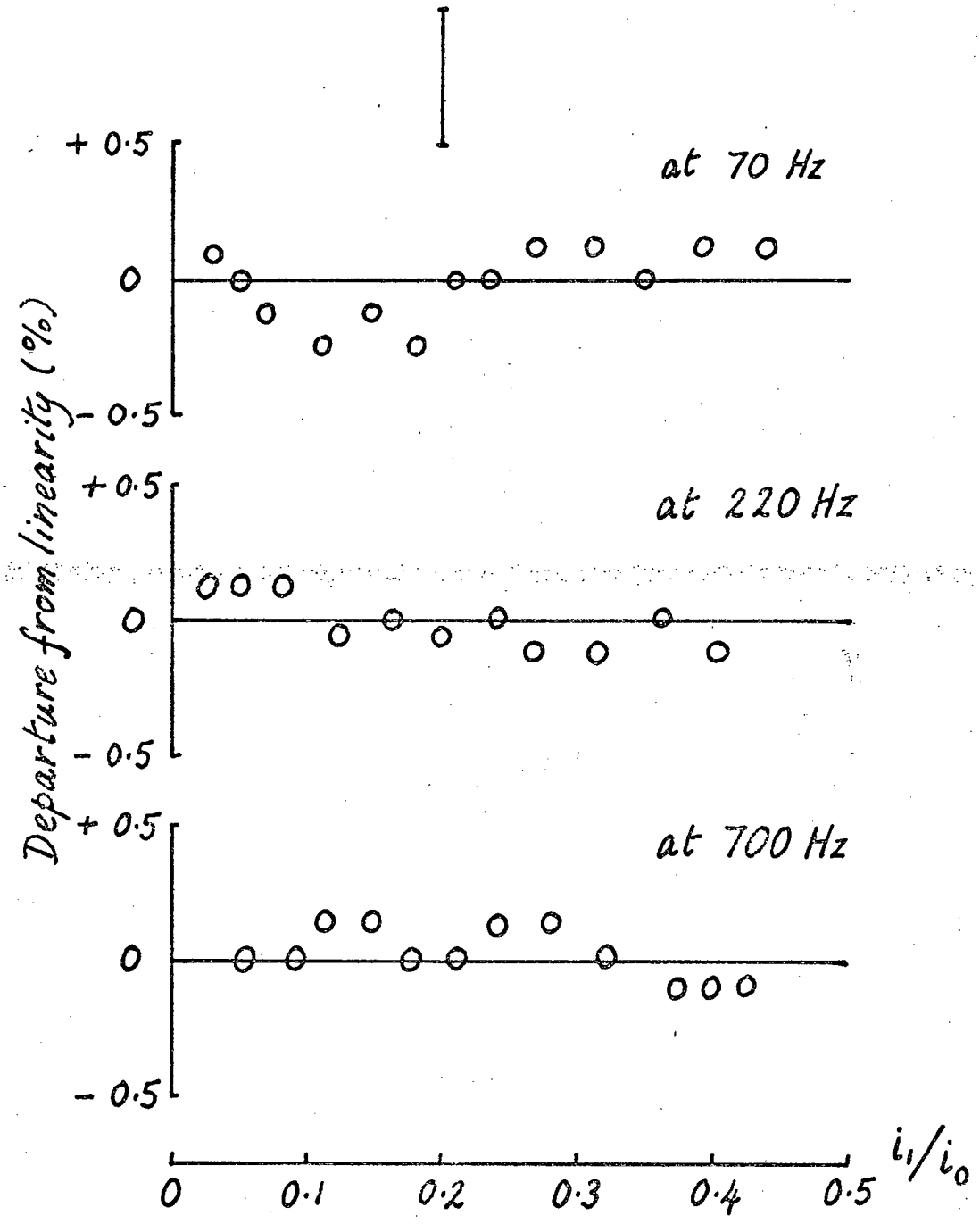

Sec.4.4.2. Fig.1 - Tests of system linearity

which the amplitude the non-linearity of the radiation detector specimen temperature is not sufficient to affect the results. This point is discussed further in section 4.4.5.

4.4.3 Frequency response of the system, including the effects due to mechanical vibration of the specimen

According to equation (4.1), if the modulation frequency ω is varied, keeping i_o and i_1 constant, the quantity ωV_{1d} should be constant. Experiments to test this were made, though to avoid having to reset i_1 exactly to a fixed value for each measurement, the quantity $\omega V_{1d}/i_1$ was determined, allowing only such small variations of i_1 from a fixed value as not to affect the mean temperature significantly.

Initial experiments were made using specimens some 80 mm in length, compared with the $\sim$ 150 mm specimens finally used. With these shorter specimens, although the constancy of $\omega V_{1d}/i_1$ expected was observed above $\sim$ 200 Hz, in the range 30 Hz - 200 Hz departures from this were observed. These departures were due to mechanical resonance vibrations of the specimen driven by the thermal expansion associated with the temperature modulation. The amplitude at the fundamental frequency was up to $\sim$ 1 mm with modulation currents $i_1 \sim 0.3\ i_o$. With the system then in use to define the acceptance angle of the radiation detector there was some restriction of the acceptance angle in the horizontal plane as well as in the vertical plane, and these horizontal movements of the wire changed the

proportion of light from the specimen falling on the detector. The changes so occasioned in the detector output were coherent with the changes caused by the genuine temperature modulation, and were therefore not removed by phase-sensitive detection. A typical fundamental-resonance curve is shown in Fig. 1. The resonance behaviour at higher frequencies was complex, other modes being excited. The amplitude of these vibrations was however much less than that of the fundamental, and the effect on the output negligible above 200 Hz.

No detailed studies of this phenomenon seem to have been made; other workers using the radiation output method have worked below the resonance frequency, using a spring tensioner if necessary to shift the resonance above the working frequency (Lowewenthal 1962). For the present work, this was not possible because of the need to work at high frequencies and temperatures near the melting point.

Various wire configurations were tried to eliminate the effect; the effect depends on the stiffness of the wire to provide the necessary storage of potential energy, and hanging the wire in a U-shaped loop was therefore tried. The difficulty here was that slow pendulum vibrations could occur, at frequencies of a few hertz, modulating the detector output at this frequency and providing sum and difference frequencies approaching the phase-sensitive detector pass band (unless very long integration times could be used). Another trial was of a specimen wire carrying at its lower end a weight of $\sim$ 1 g to take up the thermal expansion on heating to the mean temperature.

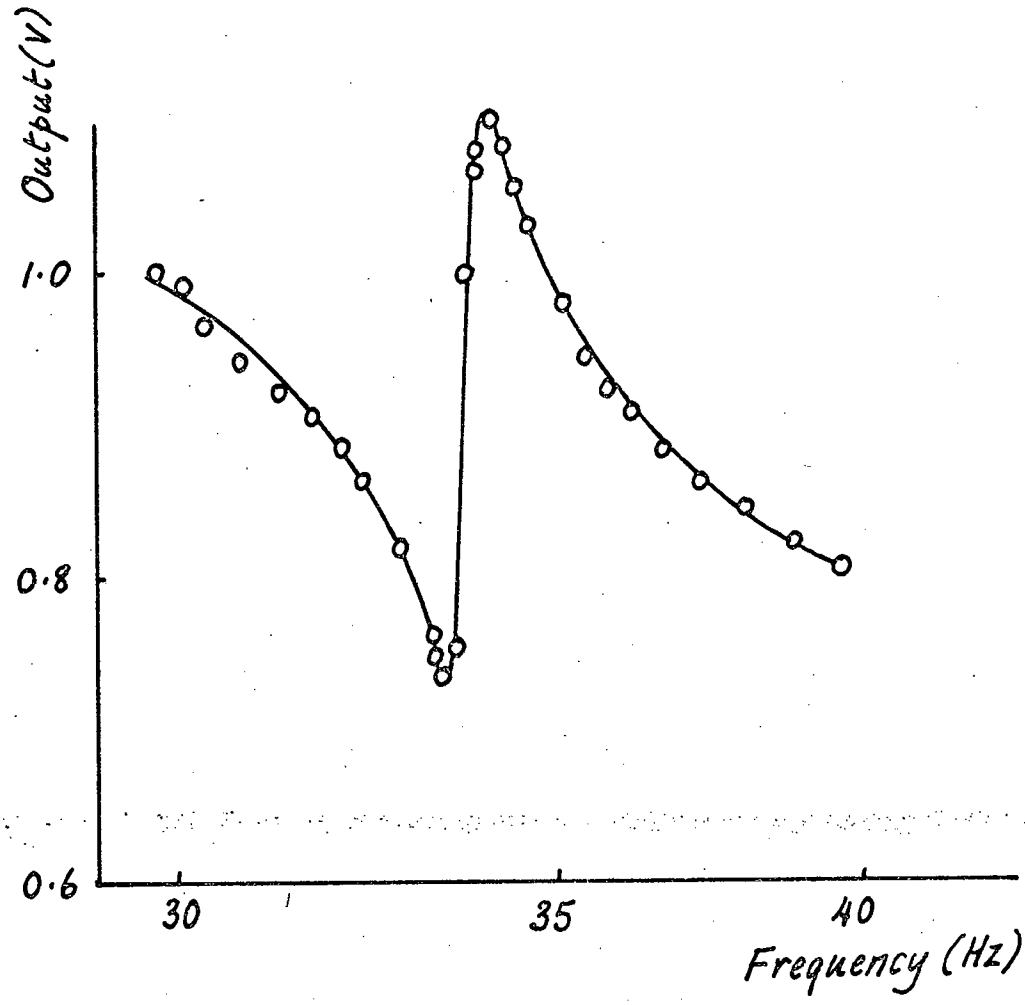

Sec.4.4.3. Fig.2 - Effect of mechanical resonance on detector output

The weight rested lightly against a nearly vertical PTFE strip to prevent pendulum oscillations. This did not suppress the thermal oscillations. Indeed, since the lower modes were now approximately harmonic because of the wire tension, sub-harmonic excitation of the fundamental was observed at the driving frequency of the first harmonic. This form of behaviour in non-linear oscillating systems has been discussed by Stoker (1950); for reference to similar phenomena, see the paper by Ludeke (1942).

The procedure eventually adopted was to use a fairly long ($\sim$ 150 mm) specimen mounted as described earlier (section 4.2.1) so that most of its length hung vertically from the upper support, and with its lower end offset some 10-20 mm from the vertical to allow for thermal expansion. This had the effect of displacing the fundamental resonance to $\sim$ 10 Hz. Also, the radiation detector geometry was altered to give negligible limitation on horizontal angle, using the system of horizontal apertures described in section 4.2.4. Fig. 2 shows the variation of the quantity $V_{1d}\omega/i_1$ for this arrangement. Above 200 Hz, no resonance effects are apparent, while down to 150 Hz the effects are small (< 0.3%). Below this frequency, the effects are not negligible. Apart from resonance effects, the behaviour follows equation 4.1 well.

A further complication is the finite rise-time of the radiation detector/amplifier system. The frequency behaviour of this system was checked using a phase-comparison method. The modulating current was used as reference waveform for the phase-sensitive detector via

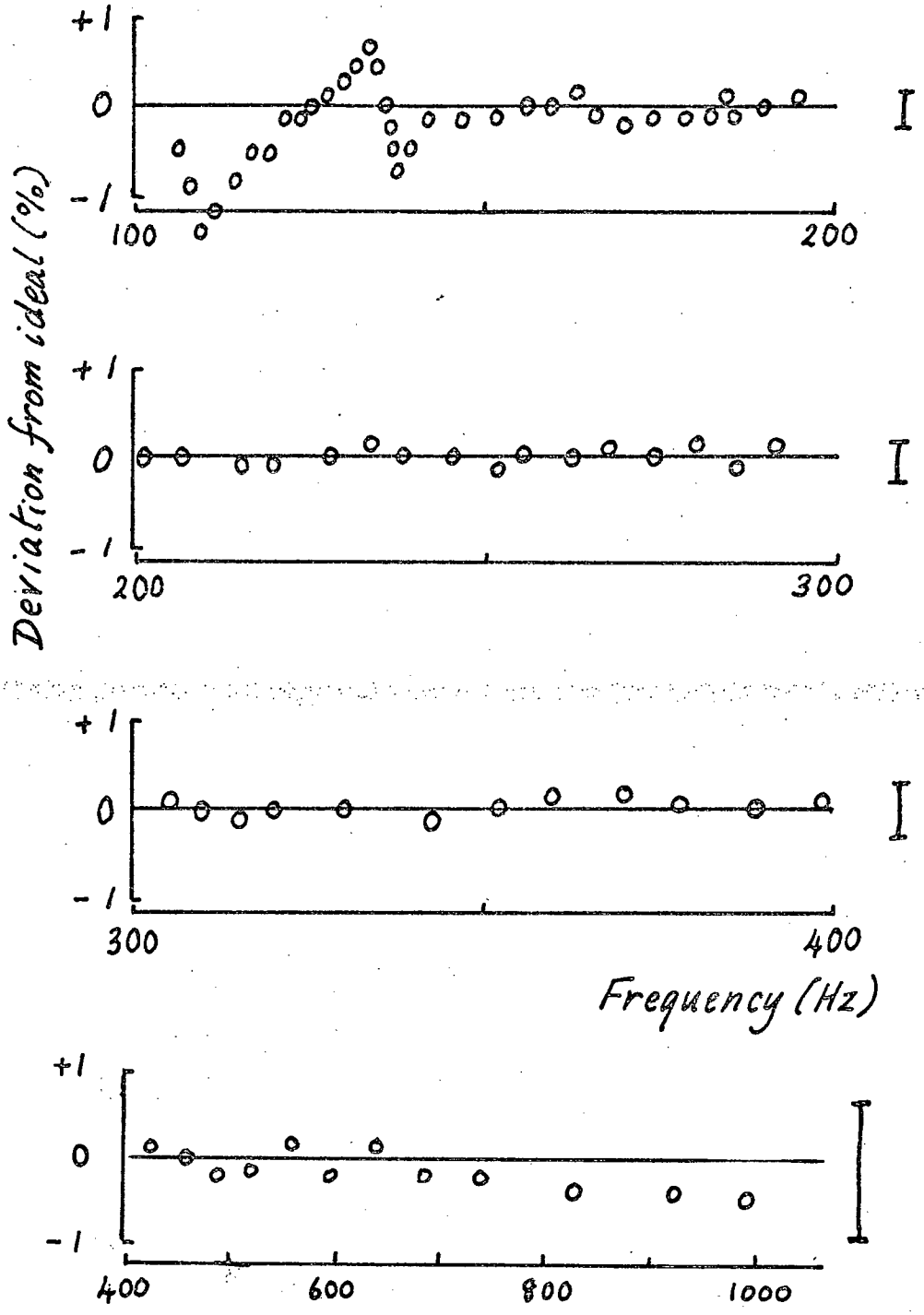

Sec.4.4.3. Fig.2 - Frequency behaviour of $V_{1d}/\omega i_1$ for modified geometry

the phase-shifter as usual. The voltage developed by the modulating current i_1 at a phase setting of $\sim 45^{\circ}$ was noted, after first measuring the amplitude of modulating current. The output from the radiation detector was then substituted as input, leaving the phase-shift untouched at its intermediate setting. The p.s.d. output was noted, and the amplitude of the radiation detector output next measured by the usual procedure of setting the reference to 90° phase difference giving zero output, and shifting through 90° using the switched phase-shift. The ratios of the respective p.s.d. outputs at the intermediate phase-setting to the outputs corresponding to the amplitudes of the respective waveforms give the cosines of the phase angles of these waveforms with respect to the intermediate phase. The phase angle between the waveforms themselves is thus deducible. Ideally, the angle should be 90°, assuming that the high-frequency approximation holds for the wire's thermal behaviour, and that the radiation detector system follows the temperature variation (lagging the current by 90°) without further phase lag. In fact, the finite rise-time of this system does cause a further lag, as can be seen in Fig. 3 , which shows as a function of frequency the amount ϕ_d by which the phase angle measured above exceeds 90°. The accuracy of measurement is $\sim \frac{1}{2}^{\circ}$, comparable with the accuracy obtained during calibration of the 90° phase-shift network (section 4.2.5); the above measurement procedure can be simplified somewhat if reliance is placed on this 90° shift network. It is then sufficient to set the reference to give zero

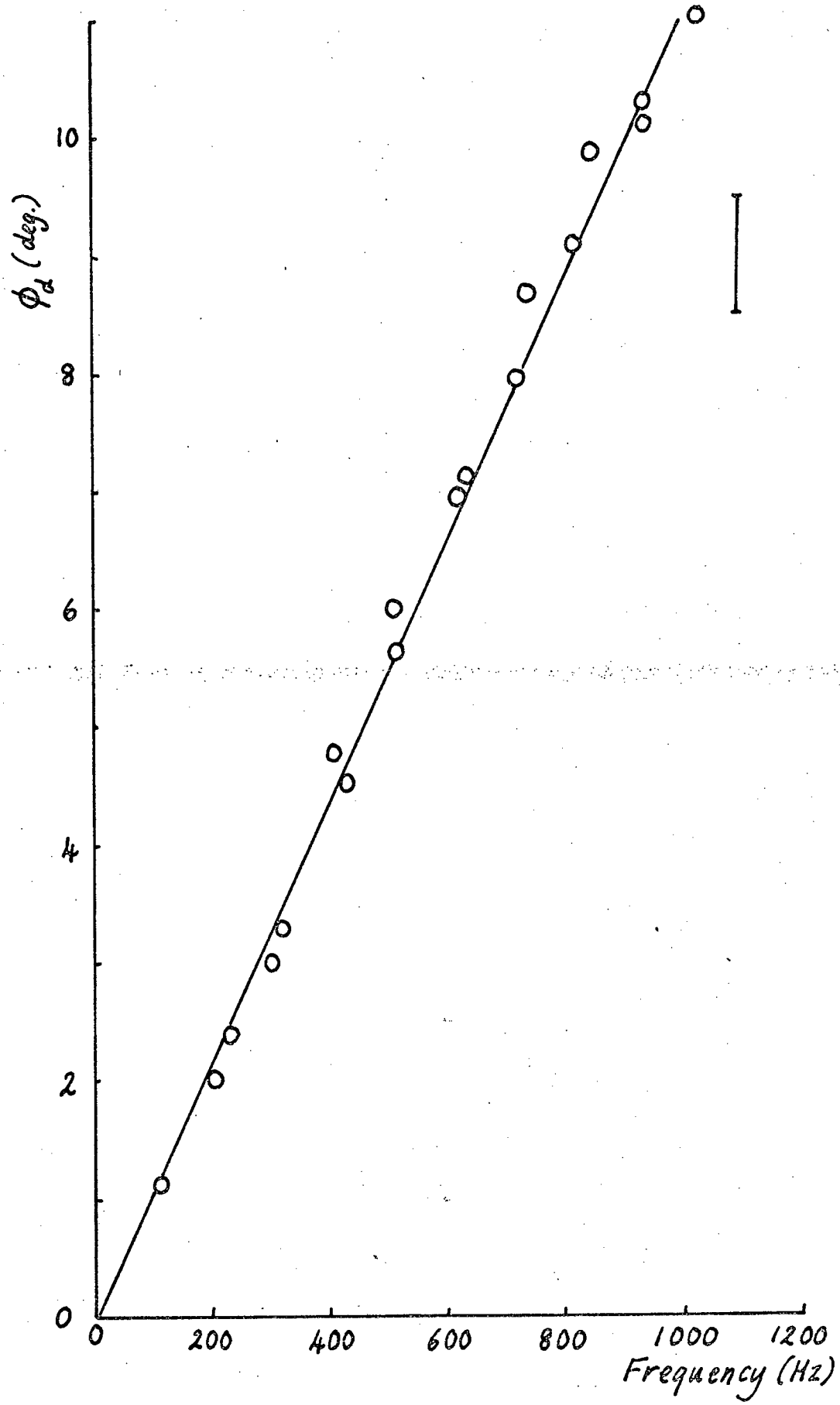

Sec.4.4.3. Fig.3 - Excess phase lag between current and detector waveforms

output using the current waveform as input, shift the reference through 90^{o} and substitute the radiation detector waveform as input. The ideal output is zero, and the actual output forms a sensitive measure of ϕ_d, since the ratio of this output to that corresponding to the amplitude of the radiation detector waveform gives sin ϕ_d directly. Both methods gave similar results. Moreover, the phase-angles were reproducible over periods of months, giving a reliable calibration procedure for the system.

Fig. 4 shows oscilloscope traces of the current and detector output waveforms at frequencies of $\sim$ 100 Hz and 1000 Hz, taken using the 'chop' mode of the 1A1 unit of a Tektronix 545 oscilloscope to illustrate the phase relationship. The 90^{o} phase difference is evident at the lower frequency, while at the higher frequency, the ($\sim 11^{o}$) phase shift is just visible.

Tests were made of the separate phase-shifts due to the radiation detector and detector amplifier. For this, the same method of using the p.s.d. described above was employed. The radiation detector was tested by loading it with the same resistance as in normal use, and amplifying the output using the Brookdeal low-noise amplifier alone. The internal filters were set at 1 Hz - 100 kHz to avoid phase-shifts in this amplifier, and the gain was 100 dB. Again, the phase shift observed was proportional to frequency (for the small angles measured), the shift being 5^{o} at 1000 Hz. The radiation detector amplifier was tested using an injected signal; it contributed the remaining shift. The rise-times corresponding to these phase-shifts

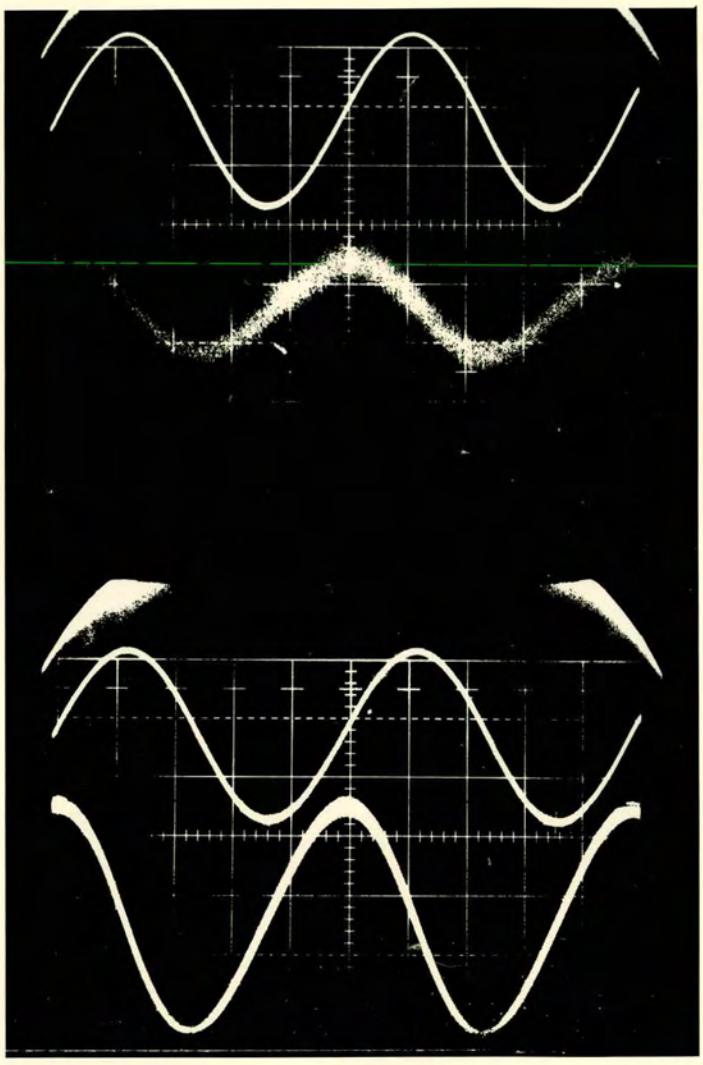

Sec.4.4.3. Fig.4 - Modulating current and radiation detector output waveforms

are ∿ 14 μs and ∿ 16 μs. Assuming they represent relaxation behaviour of the system, an overall amplitude correction can be calculated. As shown in Fig. 5, this is negligible (< 0.2%) up to 400 Hz, and small (< 1%) up to 1000 Hz. The observed frequency behaviour of the complete system is shown in Fig. 2, in which the deviation of $V_{1d}\omega/i_1$ from a constant value is shown to be negligible within the experimental uncertainty.

Over the frequency range 100 Hz - 1 kHz, no apparent effects arise due to any failure of the high frequency approximation to describe the thermal behaviour of the wire; any such failure would, of course, affect particularly the graph of ϕ_d against frequency at the low-frequency end. The absence of such an effect is consistent with the value τ_{th} = 300 ms for the wire's thermal time constant obtained below (section 4.5.2), for the phase error so introduced is only $1/\omega\tau_{th} = 0.3^{\circ}$ even at 100 Hz.

4.4.4 Noise

The noise on the output of the radiation detector amplifier under working conditions was measured at various temperatures using the Dynamco A.C. digital voltmeter; this, being r.m.s. sensing, gave an accurate means of estimating noise. The noise was measured using modulation frequencies of ∿ 20 kHz, well above the amplifier pass-band so that this did not affect the result; it was measured also with the input of the modulating current amplifier shorted, with similar results. In Fig. 1 the signal/noise ratio is shown for an intermediate frequency (∿ 250 Hz) at various temperatures approaching the lower

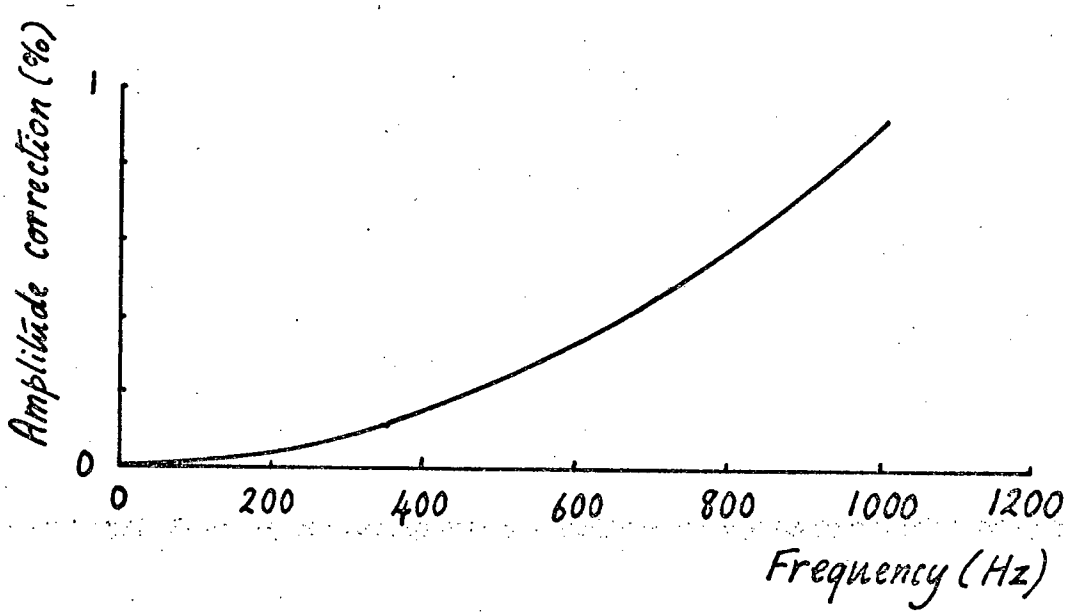

Sec.4.4.3. Fig.5 - Calculated amplitude correction for detector system

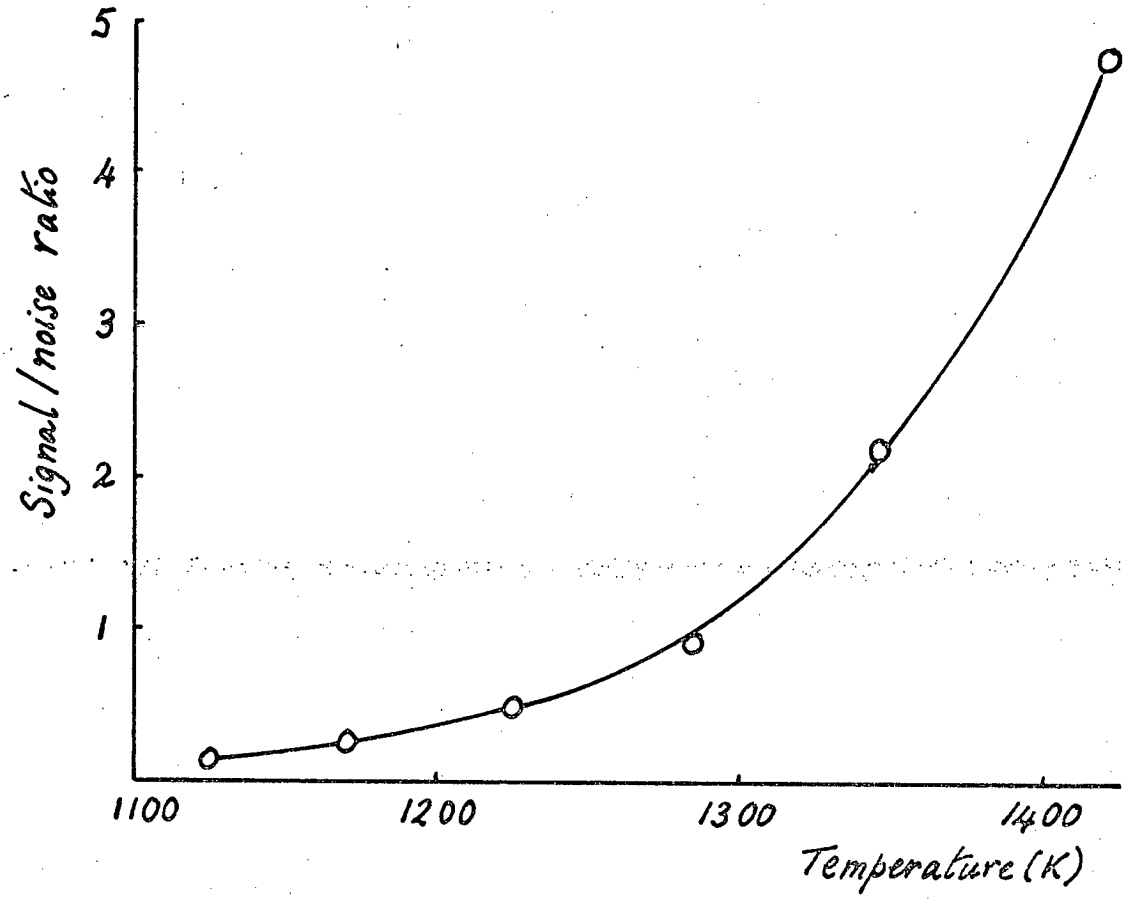

Sec.4.4.1. Fig.1 - Detector signal/noise ratio

limit of the apparatus. The modulation amplitude corresponds to a modulation current whose r.m.s. value is 10% of the direct heating current at each temperature. For the temperature range shown, this corresponds to an amplitude $|\theta_1|$ in the range 1 K - 5 K. The results indicate that the useful temperature range of the apparatus does not extend much below 1200 K, even using p.s.d. techniques. The reason for this is that the elimination of noise effects is not simply a matter of choosing a sufficiently long integration time; in order for the p.s.d. output to be a reliable measure of the signal input, it is necessary to avoid distortion or limiting of the input waveform during pre-detector amplification. A signal/noise ratio of less than unity therefore means that the output from the p.s.d. must be less than full-scale, and the linearity becomes suspect, particularly below $\frac{1}{10}$ full-scale. At temperatures of 1200 K and above, integration times of 1 s - 10 s were used to reduce the fluctuation in the p.s.d. output to an acceptable level. For most measurements, 3 s was used, as providing a final reading within 20-30 s, comparable with the reading times of the A.C. meter and the frequency counter, and reducing the noise fluctuations to $\sim$ 0.3%, or less at frequencies in the intermediate range.

Under the conditions of the experiment (signal/noise ratio $\sim$ 1 or larger) the noise rejection performance of the p.s.d., which is specified as < .01% is not a limiting factor.

4.4.5 The response to small changes of direct heating current

The effect of small known changes in mean temperature on the radiation detector output was measured using the Dynamco digital voltmeter in its D.C. mode, the signal being smoothed to remove the modulation and noise using the integration circuit (section 4.2.4) with a time constant of 8 s. The necessary small changes of direct heating current were made using a conductance box to vary the external current-programming resistance of the power supply, as described earlier (section 4.2.2).

Fig. 1 shows a typical result, in which the D.C. output V_{od} of the radiation detector is plotted as a function of resistance ratio r_e. The centre temperature is 1385 K and the temperature excursion covers a range of 50 K. The departure from linearity is evident, and arises because the light output from the specimen (evaluated according to the detector's spectral response) is a rapidly increasing non-linear function of temperature. The solid curve represents a parabolic fit to the data, and represents the experimental points adequately. From this fit, a value of dV_{od}/dr_e at the centre temperature can be estimated and knowing the value of $\alpha = dr_e/dT$ gives the detector sensitivity dV_{od}/dT at this temperature. Detector sensitivity as a function of temperature is shown in the semilogarithmic plot of Fig. 2. The curves shown may be crudely approximated by straight lines, indicating an exponential temperature dependence of the detector sensitivity. The separate curves correspond to the different masks used to reduce the area of the detector on

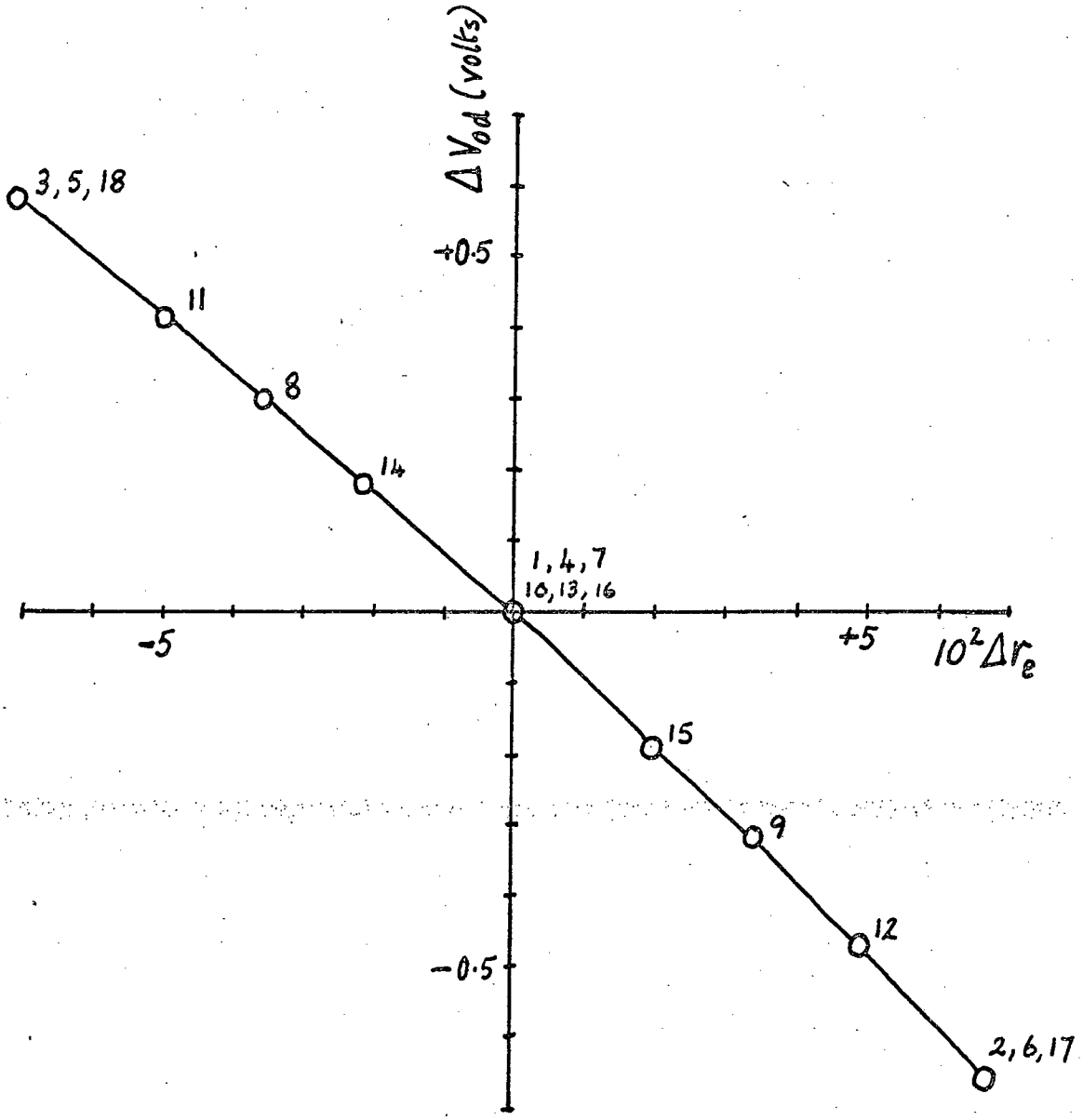

Sec.4.4.5. Fig.1 - Detector calibration curve
(The numbers associated with the points show the order in which measurements were made)

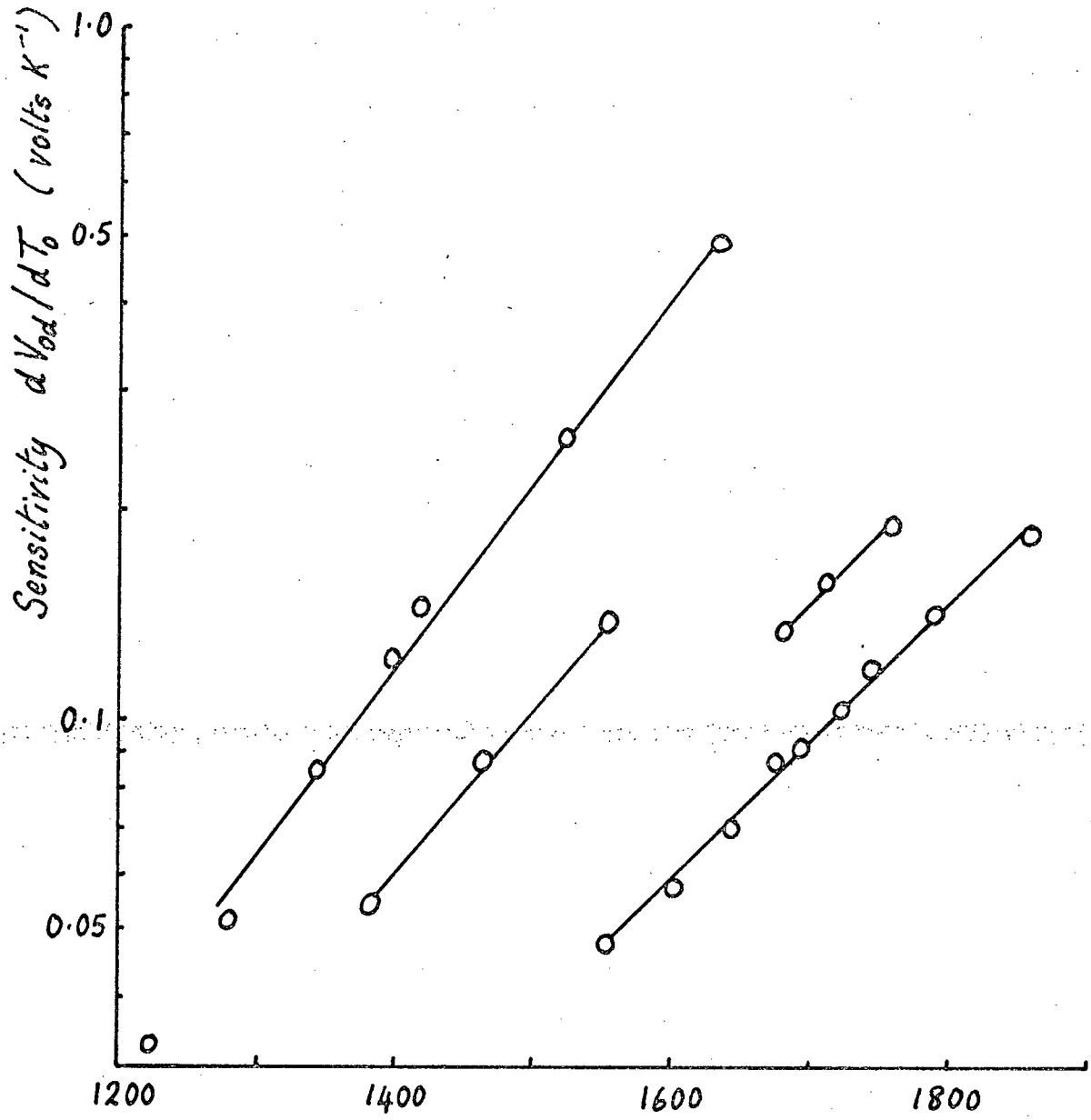

Sec.4.4.5. Fig.2 - Logarithmic plot of detector sensitivity

which light is allowed to fall; these curves all have essentially the same slope at corresponding temperatures, indicating no change in the temperature behaviour of the sensitivity due to masking. We may then write

$$dV_{od}/dT = A_d \exp(+\zeta T) \quad \ldots (4.2)$$

where A_d is a constant depending on the mask and $\zeta \simeq 6 \times 10^{-3}\ K^{-1}$.

This equation is useful in two ways. First, it allows one to predict roughly the temperature excursions for which linear, parabolic and higher-order fits to the output/temperature curve will be valid. In fact, it is evident from Fig. 1 that a linear fit will be valid only over such a small temperature excursion that accurate measurement of it is impossible because of the limitation of the D.C. potentiometry (see section 4.2.3). A parabolic fit is, however, not inconvenient, particularly if the calibration points are spaced nearly symmetrically about the centre temperature, for then the gradient derived from each such pair of points is a close approximation to the gradient of the curve at the centre temperature. An examination of the error involved in neglecting cubic and higher terms in the expansion of equation (4.2) in powers of θ_o, where θ_o is the excursion from the centre temperature, shows that for this error to be less than 0.1%, 0.3% or 1.0%, θ_o must be less than about 10 K, 20 K or 40 K respectively. For the present work, the limit on calibration excursions was chosen as ±20 K, giving the

best compromise. The A.C. temperature modulation amplitudes are of course substantially less than this, but still may be sufficient to provide some second-harmonic distortion (1% at $|\theta_1| \simeq 3$ K).

The second use of equation (4.2) is in providing an estimate of the required stability of the mean temperature, and hence also of the heating current. We find that as the fractional change in sensitivity with temperature is ζ, or about 0.6% K^{-1}, for measurements to 0.3% accuracy the temperature must be stable to $\sim$ 0.5 K. From the temperature/current curves, we find that dT/di is about 4 K per milliampere, and the current stability must be therefore better than $\sim$ 0.1 mA. This requirement is easily met by the current supply arrangements described earlier (section 4.2.2), but the temperature stability requirement generally is a stringent one, particularly at high temperatures when changes at the specimen surface cause drift effects. In view of this, it was decided that no attempt would be made to obtain a single calibration for the detector sensitivity to be used for all subsequent measurements at various temperatures; instead, the detector would have to be calibrated during each measurement of specific heat.

A further consideration which militates against a once-and-for-all calibration approach is that of geometrical effects due to wire movement. Any change in wire position may affect the detector sensitivity; in the absence of any slits restricting the horizontal acceptance angle of the detector, the importance of any such

movements is determined by their magnitude in relation to the distance from the wire to the detector $\sim$ 30 mm, movements of $> \sim 0.1$ mm being significant. In fact, this required stability was achieved, given the system for supporting the specimen chamber and keeping it free from external vibrations described earlier (section 4.2.1).

Wire movement also may lead to difficulty in relating the D.C. detector calibration results to the actual sensitivity when the detector is used in a modulation experiment. Since the modulation experiments are carried out well above the fundamental resonance frequency, the wire does not respond by any lateral movement to the 'driving force' occasioned by the thermal expansion associated with the modulation (unless, of course, it happens to be resonating in another mode). During D.C. calibration, on the other hand, the wire does move, to accommodate the thermal expansion associated with the temperature excursion. The thermal expansion coefficient is small ($\sim 10^{-5}$ K^{-1}) resulting in changes in lateral position during calibration of only < 0.01 mm; the change in detector output is $< 0.1\%$, compared with a change due to the temperature change of $\sim 30\%$. The systematic error expected from this cause is thus $< 0.3\%$. This estimate was checked by moving the radiation detector round the specimen wire, with constant modulation conditions. Although the detector output changed substantially due to the change in relative position of wire and detector, the ratio of A.C. output V_{1d} to the change in D.C. output ΔV_{od} remained constant, within an experimental error of

$\sim$ 0.3%, ΔV_{od} corresponding to a fixed temperature excursion of $\sim$ ±20 K. This indicated that ΔV_{od} was not seriously affected by wire movement. Any systematic errors arising from this cause would affect all measurements on a given specimen more or less equally, since the geometry of the arrangements remains constant during the series of experiments. The difference in the error is therefore probably negligible for studies of the temperature variation of specific heat on a single specimen, since the overall uncertainty is in any case $\sim$ 1%. For comparison of different specimens, the overall uncertainty is of course larger anyway. Any effect was minimised during the experimental runs by moving the detector round the hot wire until maximum indicated D.C. output was obtained, giving the position least affected by transverse wire movement. Although these precautions appear to have dealt with the effect during these experiments, it should be noted that use of a light detection system in which the input depended critically upon wire position (e.g. using narrow slits parallel to the specimen wire) could give rise to significant errors.

A further systematic error could arise through any non-linearity of the radiation detector and amplifier with respect to the D.C. changes used for calibration. The linearity of the detector amplifier was maintained using negative feedback, and was tested by introducing a D.C. offset using the internal potentiometric balance controls. A sensitive test of any non-linearity is to measure the A.C. output under fixed input conditions as the D.C. offset is

gradually increased. The A.C. output corresponding to typical modulation conditions is a small fraction of the available linear swing, and thus changes rapidly as the linear region is exceeded and the slope gain alters. Tests made in this way showed that the linearity was excellent (better than 0.1%) over at least the whole of the range represented by ±5 V D.C. balanced output. This corresponded to full positive and negative deflections on the Levell balance-indicating meter on 10 V centre-zero range, which thus gave a convenient indication of the allowable swing.

4.4.6 Drift in the measuring system

There are three main sources of drift in the experiment. Firstly, changes in the conditions affecting the specimen - changes in environment, heating currents or end effects. Secondly, there are secular changes in the specimen - evaporation etc. Finally, there are drifts in the measurement system itself. Here we shall consider only the last category of effects, dealing with the others in later sections.

Because of the stabilisation of the radiation detector amplifier power supply, and because of the balanced design of the amplifier, the A.C. gain was inherently stable, the most likely source of drift being the radiation detector itself. This was operated with a load resistance giving a reasonably flat output/ambient temperature characteristic, the variation being < 0.1% per degree in the $20^{o}C$-$25^{o}C$ region. The stability was checked using a modulated specimen at fairly low temperatures (1300 K - 1500 K) after a warm-up period of

$\sim$ 1 hour. No significant changes of A.C. output were observed over a 1 hour period.

The D.C. output stability is more subject to variations since the difference between the detector voltage and the internally-derived balancing voltage is amplified to give the D.C. output. Even so, the observed, drift rates were very small, usually corresponding to changes of $< 0.1\%$ in detector output per hour, equivalent to that resulting from a change in specimen temperature of ~ 0.2 K. As will be seen later, the measurement procedure allowed for any such drifts.

4.5 Experiments and results

4.5.1 Preliminary study - Drift behaviour due to the specimen

As discussed in section 4.2.2, the stability of the heating current for the specimen was very good, and observed drift effects at high temperatures were attributed to changes in the specimen itself. Below $\sim$ 1800 K, any such changes contributed drift effects which were only of the same order as those otherwise present in the experiment. Above this temperature, drift rates up to a few degrees per hour at 2000 K were observed. At fixed heating current, the measured resistance of both specimen and dummy decreased slowly with time; correspondingly, as the wires became cooler, the output of the radiation detector decreased. This decrease in output was less than would have occurred due to the temperature change indicated by the resistance measurements, confirming that the effective emittance of the specimen

had increased, and showing that the effects were not due to changes in the thermal environment.

Accurate estimation of these drift rates was complicated by the other causes of drift present, but there was evidence that the drift rate roughly doubled between 1850 K and 1950 K, corresponding to an activation energy of $\sim$ 2 eV. The increases in effective emittance were attributed to surface roughening caused presumably by grain growth or evaporation from preferred surfaces. No changes in the cold ($0^{o}C$) resistance could generally be measured to correlate with the high temperature measurements, because the accuracy of the room temperature measurements was only $\sim$ 1 part in 10^{3}. There was, however, a small increase of resistance at $0^{o}C$ to be observed in a specimen maintained at $\sim$ 1950 K for 12 hours and a trace of evaporated platinum on the wall of the specimen chamber. The removed specimen showed a marked roughening of the surface under a low power microscope (30x magnification).

For the purposes of the specific heat experiments, these drift effects were not serious as far as the specimen mass was concerned; they did however affect the sensitivity of the radiation detector, for which the temperature stability of the specimen required to be $\sim$ 1 K if serious effects were to be avoided. In the experiments described below, therefore, each experiment was planned to give a measurement of drift effects, and the results were dealt with so as to allow for a steady drift.

4.5.2 Preliminary study - The thermal relaxation time

A necessary preliminary experiment was to determine rough values for the thermal relaxation time τ_{th} of the specimen as a function of temperature, so that an estimate of the range of validity of the high-frequency approximation to the thermal behaviour of the wire could be made.

D.C. measurement of the specimen resistance as a function of heating current were made at various temperatures, noting the change of resistance caused by a small change of heating current. The corresponding temperature changes ($\sim \pm 20$ K) were obtained using the assumed values of temperature coefficient of resistivity as discussed in section 4.3.2. From the values of (dT/di) so obtained, τ_{th} was calculated using the procedure of section 2.2.1, equation 11, and using the values of c_p measured by Kraftmakher and Lanina (1965). (As will be seen later, the values of τ_{th} are not markedly altered if the results of the present specific heat experiments are used instead). The calculated values are shown in Fig. 1.

An approximate check of τ_{th} was made by using a Tektronix 545 oscilloscope to observe the time variation of the output of the radiation detector amplifier as a small change in specimen heating current was made. Only small changes in temperature (< 5 K) could be used, because the curvature introduced by the radiation detector temperature characteristic would otherwise have distorted the exponential relaxation. The accuracy of observation

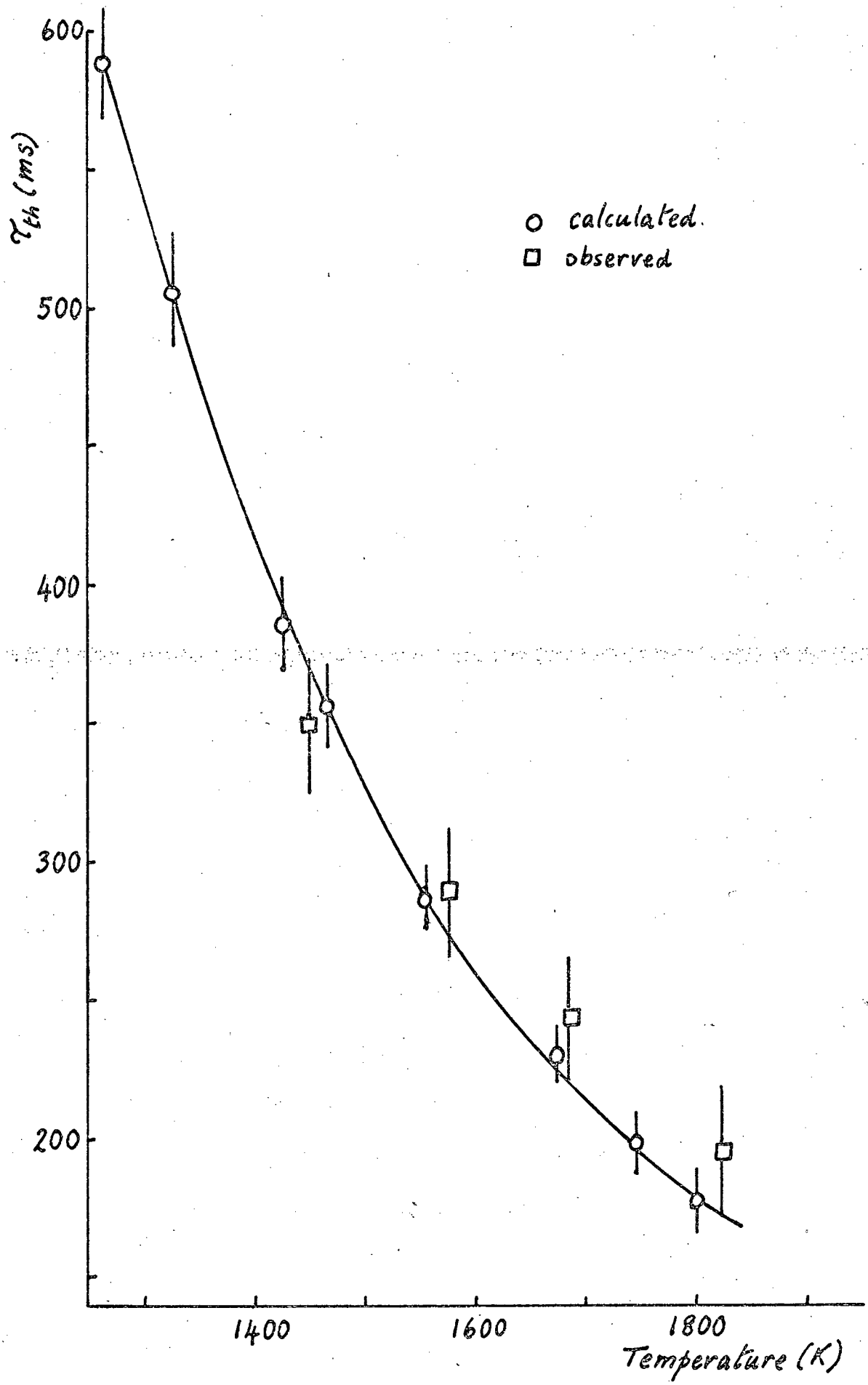

Sec.4.5.2. Fig.1 - Thermal relaxation time

was therefore not good because of noise, particularly at the lower temperatures. Since τ_{th} enters only in a small correction term in the specific heat experiments, the resulting confirmation of the calculated values was nonetheless adequate.

4.5.3 The frequency dependence of the specific heat - amplitude comparison measurements

By comparison with measurements of specific heat made at temperatures below $\sim$ 1500 K, high temperature measurements are expected to include a contribution due to vacancies which should relax out, according to the discussion of section 2.3, at frequencies large compared with $1/\tau_v$.

This effect was sought by making measurements of the A.C. detector output V_{1d} at various frequencies, keeping the heating and modulating currents fixed. As in section 4.4.3, where this experiment was described for a low mean temperature, the constancy of the quantity $V_{1d}\omega/V_1$ provided a measure of the constancy of C_p. Drift was allowed for by taking measurements in several batches of about ten, the measurements in each batch being at different frequencies spread through the range $\sim$ 100 Hz - $\sim$ 1000 Hz. Measurements from different batches at frequencies in the ranges 100 Hz - 200 Hz, 200 Hz - 300 Hz, etc. were averaged. Individual readings deviated not more than $\sim$ 1% from the means, the scatter tending to be larger over the 100 Hz - 200 Hz range because of small mechanical resonance effects. The overall accuracy of the comparison between different frequencies is also affected by linearity considerations,

since the high frequency measurements are necessarily at not more than 0.1 of full-scale output from the phase-sensitive detector. The overall accuracy is therefore ½% - 1% indicated in Fig. 1, which shows the results obtained. No correction is necessary for failure of the high-frequency approximation, since τ_{th} is long compared with $1/\omega$ under all experimental conditions ($\omega\tau_{th} \nless 90$).

No significant differences between the high-temperature and low-temperature frequency curves are apparent, and there is thus no evidence of vacancy relaxation effects. The significance of this null result can be assessed by considering the specific heat results (Fig. 2) of Kraftmakher and Lanina (1965) in conjunction with the vacancy relaxation curves of section 2.3.3 (Fig. 1).* It is estimated that the measurements would reveal an effect were the relaxation-peak frequency between 100 Hz and 1 kHz and were the vacancy contribution to the low-frequency specific heat 3% or greater. The results are therefore significant in excluding a vacancy relaxation peak in this range for measurement temperature above about 1650 K, provided that Kraftmakher's interpretation of the "excess" specific heat as due to creation and destruction of vacancies is accepted. In the same way, at 1850 K, where this "excess" specific heat reaches $\sim$ 10%, a relaxation peak would be detected if it lay within the range $\sim$ 30 Hz - 3 kHz. Alternative interpretations of these results will be discussed in section 5.

* Page 32

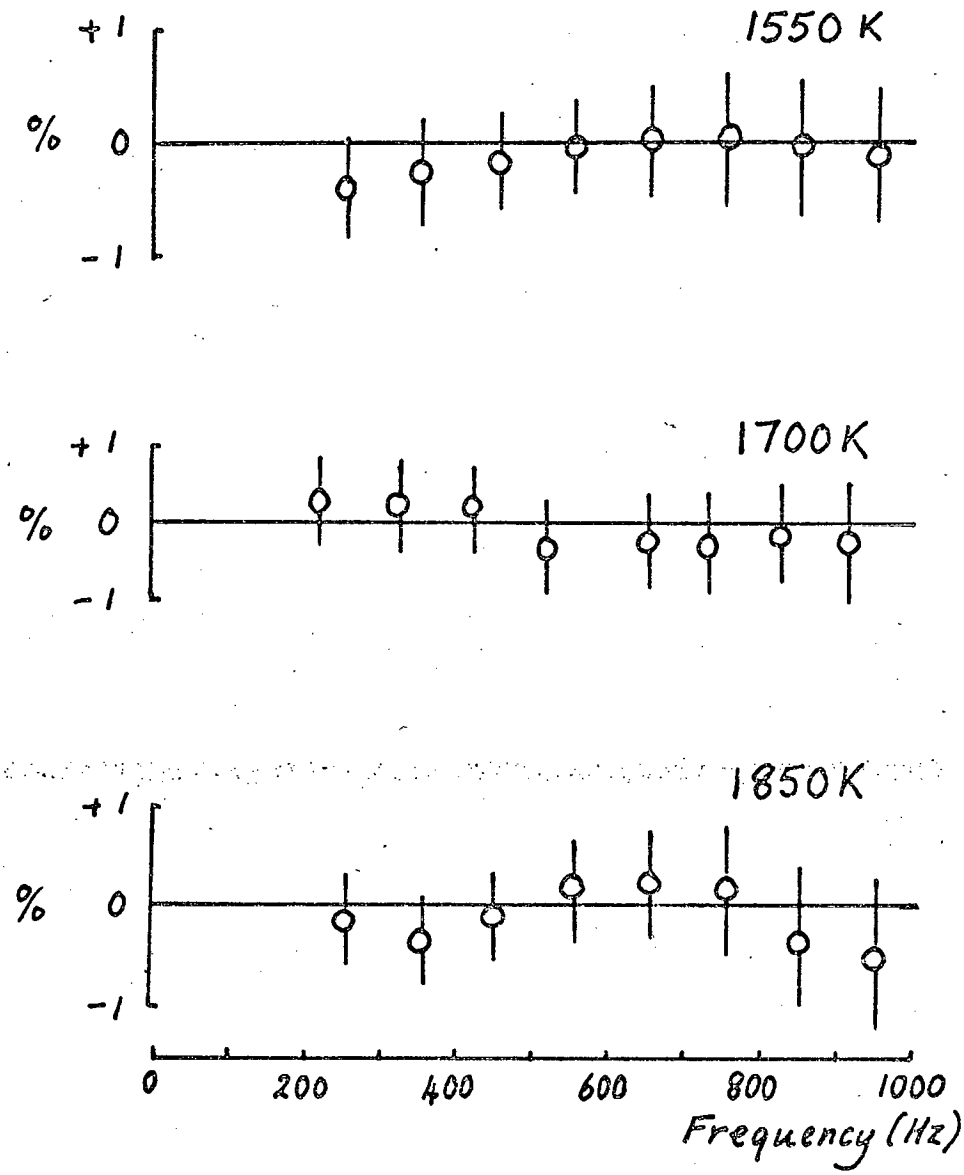

Sec.4.5.3. Fig.1 - Frequency dependence of specific heat

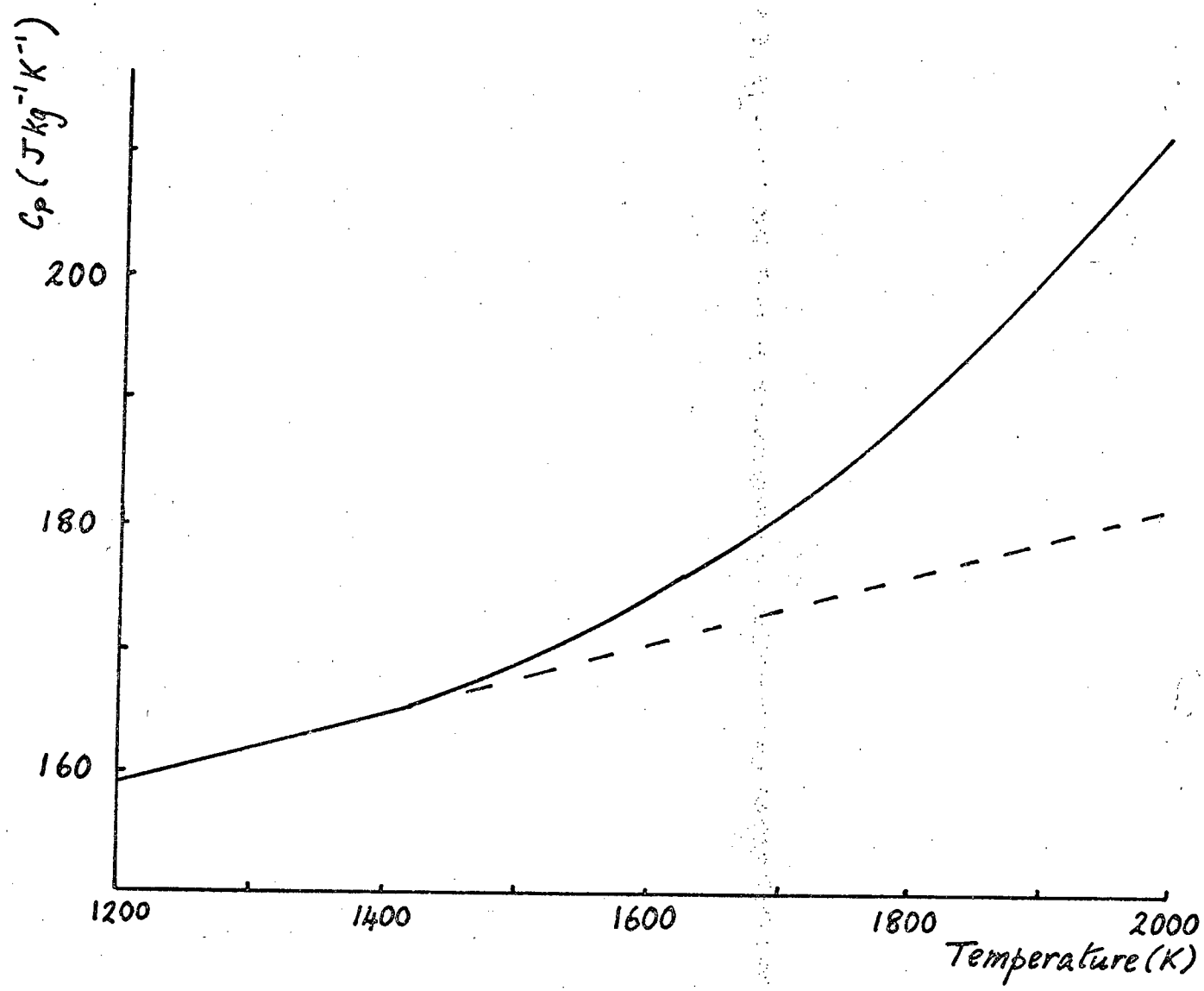

Sec.4.5.3. Fig.2 - High-temperature specific heat of platinum by the modulation method of Kraftmakher and Lanina

4.5.4 The frequency dependence of the specific heat - phase comparison measurements

Although the amplitude measurements described above are the most direct method of looking for a variation of specific heat with frequency, they have the disadvantage that there is no absolute reference for the comparison, and high and low frequency amplitudes have to be compared with each other; drift is therefore important.

This difficulty is overcome by seeking the relaxation peak by its effect on the phase rather than the amplitude. The vacancy relaxation causes the temperature modulation to lag behind the modulating current waveform, the phase angle behaving as indicated in Fig.2* of section 2.3.3.

The experimental method was as indicated for the low-temperature (1500 K) calibration of the radiation detector system in section 4.4.3, the Brookdeal p.s.d. system being used to measure the phase-difference between the modulating current waveform and the output waveform from the radiation detector amplifier. This phase-difference was measured for various frequencies in the range 100 Hz - 1 kHz at fixed temperatures in the vacancy region > 1500 K. The results obtained are shown in Fig. 1, where they are compared with the low-temperature calibration. The measurement accuracy was $\sim \frac{1}{2}^{o}$.

For these results, small corrections for finite thermal relaxation time τ_{th} are required, since the phase measurements are much more sensitive to relaxation behaviour involving small phase angles than are amplitude

* Page 33

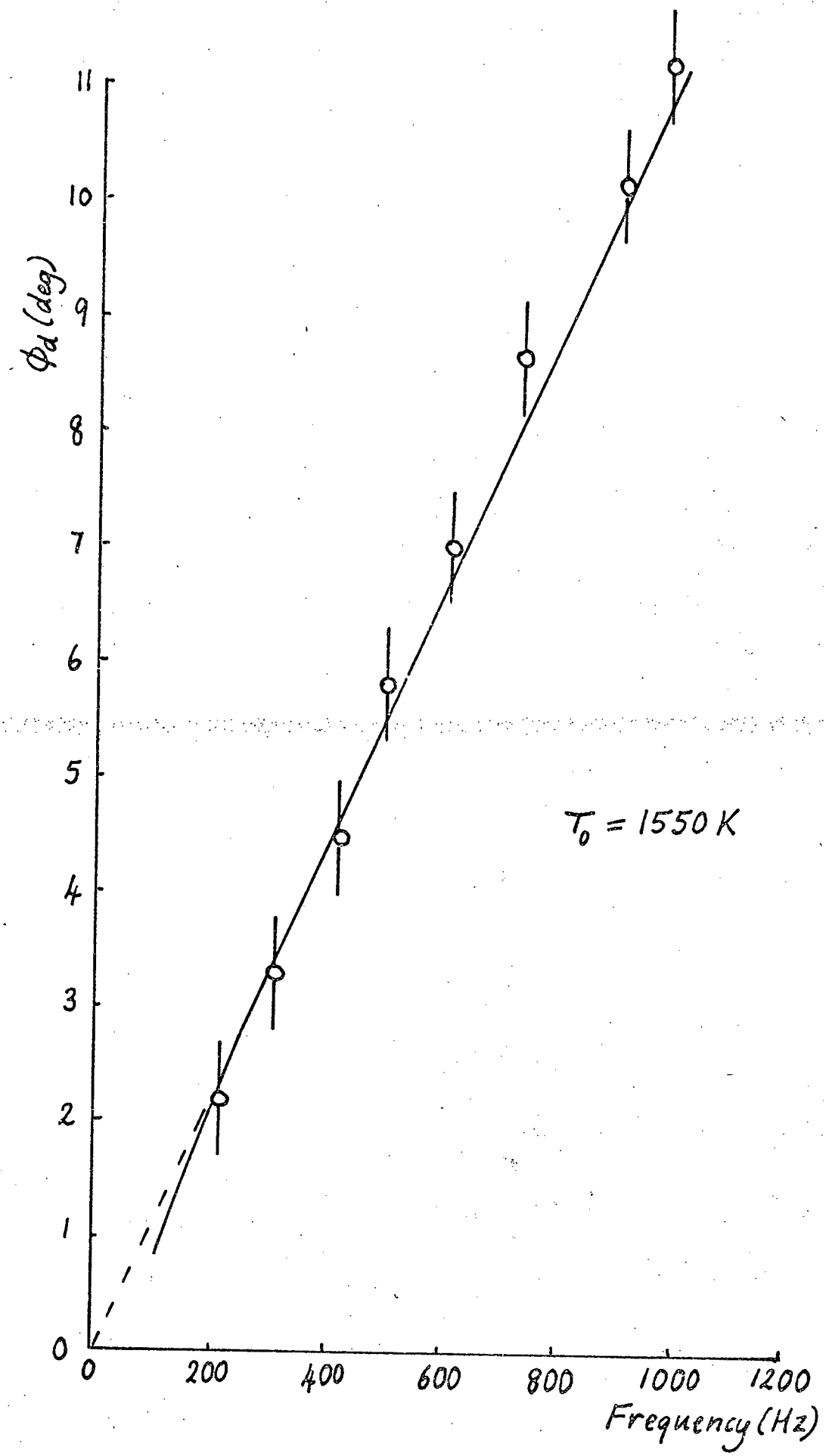

Sec.4.5.4. Fig.1a – Excess phase lag between current and radiation detector waveforms

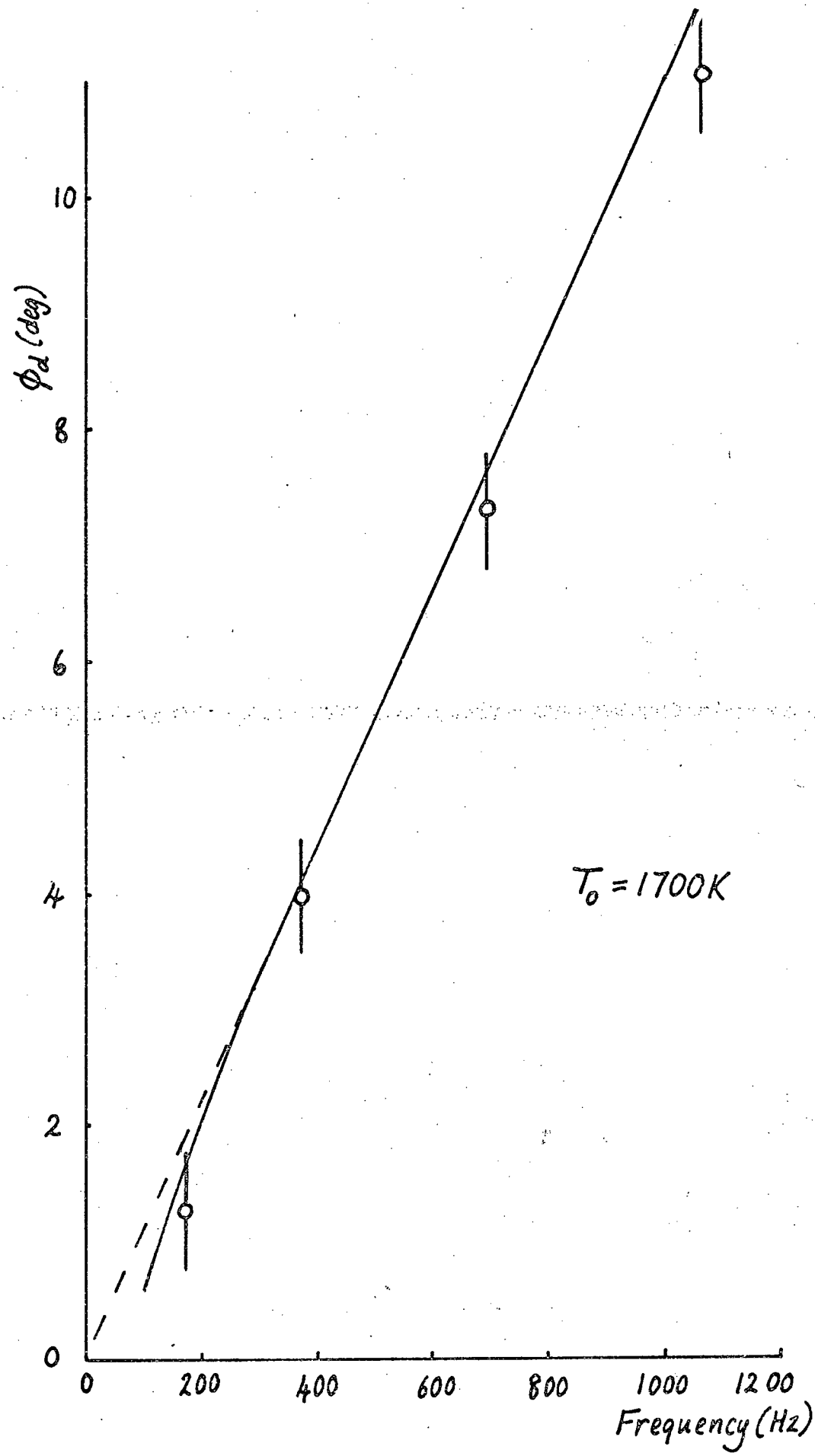

Sec.4.5.4. Fig.1b - Excess phase lag between current and radiation detector waveforms

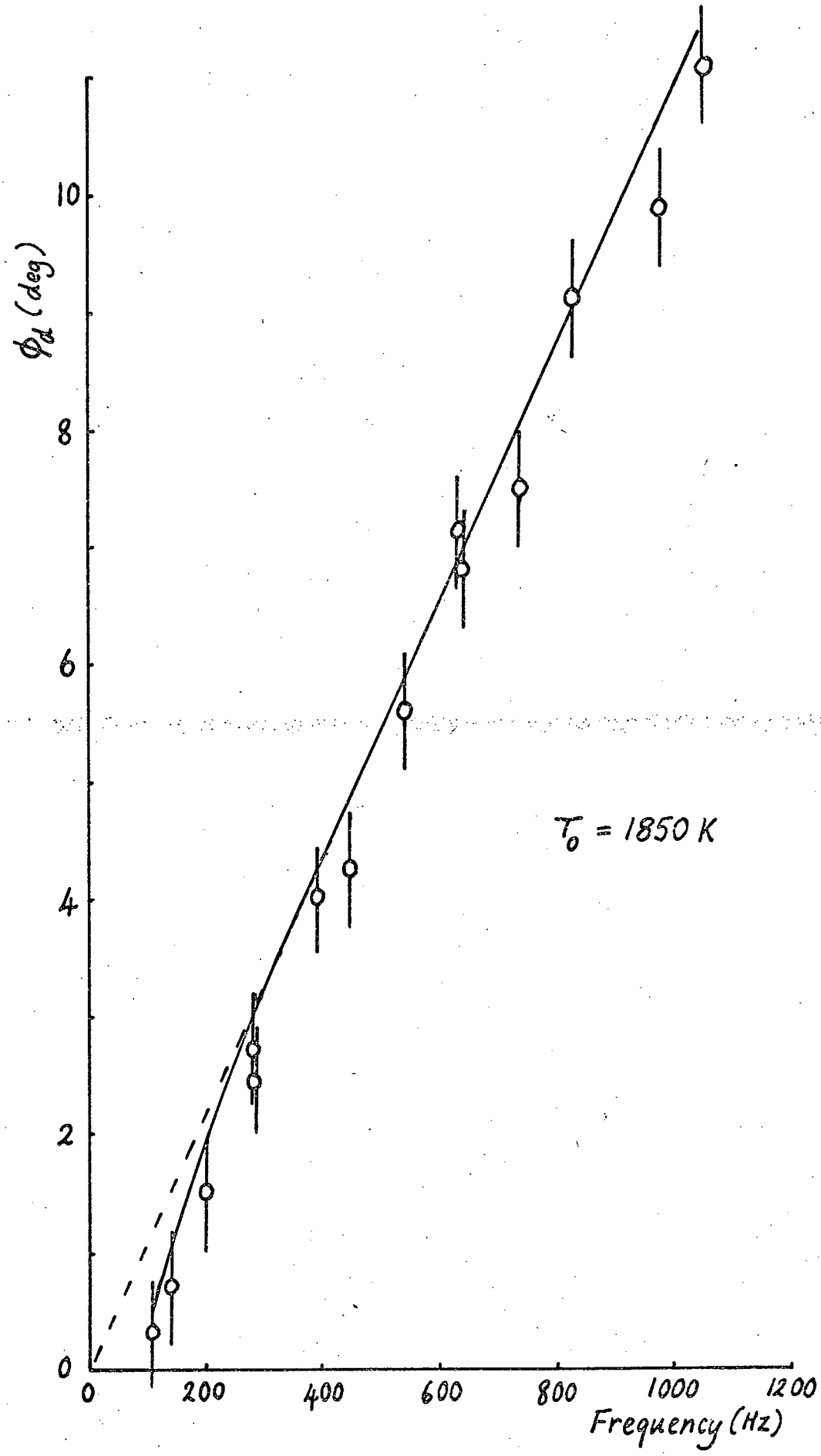

Sec.4.5.4. Fig.1c - Excess phase lag between current and radiation detector waveforms

measurements. These corrections have been incorporated in Fig. 1 by modifying the curves indicating the low-temperature behaviour of the phase, producing the slight curvature evident at the low-frequency end. These modified curves then represent the expected behaviour of the phase angle in the absence of vacancy relaxation effects.

Again, null results are apparent. The general conclusions are as indicated in the previous section, except that we can now infer that any vacancy relaxation peak of significant size must now lie outside rather wider limits; this is because the method is more sensitive to small vacancy phase angles than is the amplitude method.

If we consider the results for 1850 K, at which temperature a 10% vacancy contribution to the low-frequency specific heat is suggested, the peak phase angle at $\omega = \omega_{max}$ say is ~ 0.04 radian ($= 2.3^{o}$), using the curve* for exact kinetics. It does not however fall to 1^{o} as the frequency is increased until the frequency is some $9\omega_{max}$, nor does it reach 1^{o} until the frequency is decreased to about $0.25\omega_{max}$. The corresponding band of frequencies from which ω_{max} is excluded by the null results in the 100 Hz - 1 kHz range is therefore $\sim$ 10 Hz - 4 kHz. Again, there are alternative interpretations of the results, to be discussed later.

The results of this and the preceding section could in principle be complicated by any effect on the radiation detector system's frequency response arising from the change in light intensity and spectral distribution as

* Page 33

the specimen mean temperature is increased. Experiments were made using masks and filters to vary these quantities, but no effect on the phase shift across the detector system was observed; most of this phase shift in any case arose from the amplifier, which was not subject to such possible effects.

4.5.5 Comparison of a transient method with the modulation method

The lower end of the available frequency range in the preceding experiments is determined by the onset of serious mechanical vibration effects. Attempts were made to extend this range to study longer times by using a transient method, instead of the modulation method.

The simplest available method is to switch off the heating current, and simply observe the resulting rate of temperature fall using the calibrated radiation detector and a measuring oscilloscope. The available temperature range is however very small ($\sim$ 20 K), because of curvature effects due to the detector characteristic, and is crossed in times of only a few ms. It is therefore necessary, if a useful time extension is to be achieved, to reduce the rate of cooling by switching off only a part of the current.

The modifications made to the basic modulation experiment circuit were simple. The D.C. heating current power supply was switched to its constant voltage mode, and a known series resistance (Sullivan decade box .01% grade) included in the arm of the circuit containing specimen and dummy. This resistance was in the range

0-10 Ω and could be varied in steps of 0.1 Ω. Initially, it was shorted out by a switch, and the switch was then opened to produce the desired fall in temperature.

It was found that the current switching was rapid, within < 0.1 ms, and that the current then varied only because of the changing resistance of specimen and dummy. For the calculations, it was necessary to know the instantaneous current through the specimen at the mean temperature corresponding to the centre of the oscilloscope trace from which the rate of fall of temperature was determined. This was found subsequently by using the resistance box to reset the D.C. output of the radiation detector to the level corresponding to the centre of the oscilloscope trace. The required currents were measured using D.C. potentiometry.

An A.C. modulation measurement was then made at this same temperature so that, by comparing the results of the transient and modulation methods, detector calibration could be avoided.

If i is the current required to maintain this temperature and i' is the instantaneous current flowing at this temperature during the transient, then the rate of loss of heat is

$$mC_p(dT/dt) = R_o(i^2 - i'^2), \qquad \ldots (4.3)$$

while in the modulation experiment at the same temperature T_o

$$mC_p|\theta_1|\omega = 2i_o i_1 R_o \qquad \ldots (4.4)$$

in the high-frequency approximation of section 2.2.2. If c_p is the same for both methods, and the detector sensitivity is the same,

$$(dV_{od}/dt)/V_{1d} = (i^2 - i'^2)/2i_o i_1 \quad \ldots (4.5)$$

This relationship was verified over the temperature range 1500 K - 1800 K within an accuracy of $\sim$ 4%, using times of $\sim$ 30 ms from the start to the finish of the oscilloscope trace. The relatively poor accuracy arises, of course, largely because the quantity (dV_{od}/dt) is determined directly from the gradient of the oscilloscope trace, involving a $\sim$ 2% uncertainty.

These experiments were not continued because of this relatively large uncertainty.

4.5.6 Absolute measurements of the specific heat

In contrast to the comparative studies of the specific heat described in the preceding sections, an absolute measurement was of particular interest since it was expected to show, by comparison with the Kraftmakher and Lanina results, whether the vacancy relaxation phenomena occured at very high frequencies (when the results should agree) or at very low frequencies. In the latter case, differences were to be expected at temperatures sufficient to give measurable vacancy effects.

Such absolute measurements required calibration of the radiation detector to an accuracy near the stability limit for the system set by drifts in specimen temperature. The

method adopted was to calibrate the detector immediately before the modulation measurements, and to repeat the calibrations immediately after; a mean was taken of the two calibrations, and a large difference (> 1%) between them provided a criterion for rejecting measurements. Frequently the modulation measurements were themselves repeated after the second calibration, as a further check on drift.

The detector calibration procedure was as has been described in section 4.4.5, the change in D.C. output for a known change of specimen temperature (determined via the resistance) giving the sensitivity. Individual determinations of this quantity were made using a parabolic fit to the output/specimen temperature characteristic, and the determinations differed from the mean by not more than $\sim \frac{1}{2}\%$. A minimum of four such determinations was used for each measured point, and it is estimated that the overall accuracy of this calibration process was itself $\sim \frac{1}{2}\%$.

The specific heat measurements were made by the modulation method, determining the amplitude of the temperature modulation from the output of the detector amplifier, using the phase-sensitive detector as measuring instrument. For most measurements, the calibrated 30 dB setting of the associated low-noise amplifier was used, though the 40 dB setting was used at the lowest temperatures (< 1300 K). The use of at least 30 dB of extra amplification was required here so that the phase-

sensitive detector could be used sufficiently near full scale to give good linearity. At temperatures above 1600 K, it was necessary to mask down the radiation detector to reduce its sensitivity to avoid overloading the radiation detector amplifier during calibration using the usual temperature interval; the size of this interval ($\sim \pm 20$ K) could not, of course, be reduced significantly without destroying the accuracy of its potentiometric determination. In consequence, 30 dB of amplification was used right up to the maximum temperatures.

The modulation frequencies used lay in the range $\sim$ 200-400 Hz, giving the best overall accuracy. For each measurement of specific heat, several frequencies were used (at least four); the calculated values of $(\omega V_{1d}/i_1)$ did not deviate from their mean by more than 1%.

The modulation amplitudes used correspond to $i_1/i_o \sim$ 0.1 - 0.3, and were in the range 0.2 K - 1 K. The results appeared to be independent of the modulation amplitude used.

Specific heats were calculated from the relationship

$$C_p(\bar{\omega}) = 2i_o i_1 R_o/\omega m|\ \theta_1\ |,$$

assuming the high-frequency approximation. No corrections were required for deviation from this at the frequencies used. The values of $|\theta_1|$ in this expression were calculated from the measured detector output V_{1d} using the detector sensitivity dV_{od}/dT obtained by the D.C. calibration; this calibration itself gave dV_{od}/dr_e directly, and was converted using the values of the temperature coefficient

of resistivity $\alpha(0) = dr_e/dT$ used by Kraftmakher and Lanina (see section 4.3.2). The effective specimen mass m in this expression was estimated as explained in section 4.3.5. The quantity $\bar{\omega}$ represents a mean frequency (equivalent to $\sim$ 300 Hz) for the measurements. The difference in D.C. voltages across specimen and dummy gave $i_o R_o$, and i_1, the modulating current, was measured using the Dynamco A.C. digital voltmeter across the 1 Ω standard resistance carrying the heating current.

The values of $C_p(\bar{\omega})$ obtained in this way for various temperatures are shown in Fig. 1.* The uncertainty shown derives mainly from three sources: the measurement of $(V_{1d}\omega/i_1)$, the detector calibration (dV_{od}/dr_e) and the estimation of m. The first two together contribute an uncertainty of 1%, while a further 1% uncertainty arises from m. For the purposes of the figure, the uncertainty in $\alpha(0)$, $\sim$ 2%, has been omitted so that a direct comparison of Kraftmakher and Lanina's results, which used the same values of $\alpha(0)$, may be made. As will be discussed in section 5, the validity of such a direct comparison rests on the assumption that vacancy relaxation effects are negligible.

The order in which the experimental measurements were taken is shown by the alphabetical sequence of the letters

* Page 159

associated with the points. This sequence was adopted to reveal any effects due to changes in the specimen with time, and particularly any effects due to high temperature ageing. None were observed, consistent with the fact that during the measurements shown the resistances at $0^{o}C$ of specimen and dummy remained constant within 2 parts in 10^{3}.

In the temperature region around 1500 K, it was possible to check on a possible systematic effect due to masking down the radiation detector; in fact, as exemplified by points g and h , measurements made at the same temperature with and without masking agreed closely.

It is evident from the figure that the agreement of the present results (curve 1) with the reported results of Kraftmakher and Lanina (curve 2) is reasonably good. Below about 1550 K, the present results lie above curve 2, but the discrepancy is only $\sim$ 1%, and could easily be explained by the uncertainty in the determination of specimen mass. Above 1550 K however, the present results lie below curve 2, again by amounts $\sim$ 1%; if then curves 1 and 2 are brought into agreement at the lower temperatures, a discrepancy of some 2% arises at the higher temperatures. This is very near, and may well be within, the limits of experimental uncertainty. It is also evident from the figure that by comparison with the extrapolated values (curve 3) the present results show an enhancement comparable with that reported by Kraftmakher. Curve 4 represents the drop-calorimeter work of Jaeger and Rosenbohm (1939); the relevance of this curve will be

discussed in section 5.3.3, but it is appropriate to point out here that it is a fitted curve rather than a representation of their original results, which they do not give. The present results for high temperatures lie above this fitted curve also.

4.5.7 Summary of results relating to the behaviour of vacancies

The significant results obtained in this work on platinum fall into two categories. Firstly, null results were obtained in the investigations into the possible frequency dependence of specific heat. The conclusion is that if the vacancy contribution to the specifc heat is as large as suggested by Kraftmakher, then the vacancy relaxation peak must, at $\sim$ 1850 K, lie outside the range 10 hz - 4 kHz. Alternatively, if the peak is within that range, the vacancy contribution must be smaller than Kraftmakher suggests.

Secondly, there is reasonable agreement between the absolute values of specific heat obtained by the present method, relying on the emitted radiation, and those obtained by Kraftmakher's resistance bridge method. A small ($\sim$ 2%) discrepancy is evident at the higher temperatures, where the present results tend to lie below the others, though this is of doubtful significance in view of the experimental uncertainties. In effect, then, both methods show an enhancement of specific heat at high temperatures, so that the enhancements reported by Kraftmakher cannot be attributed to the peculiarities of the resistance bridge method.

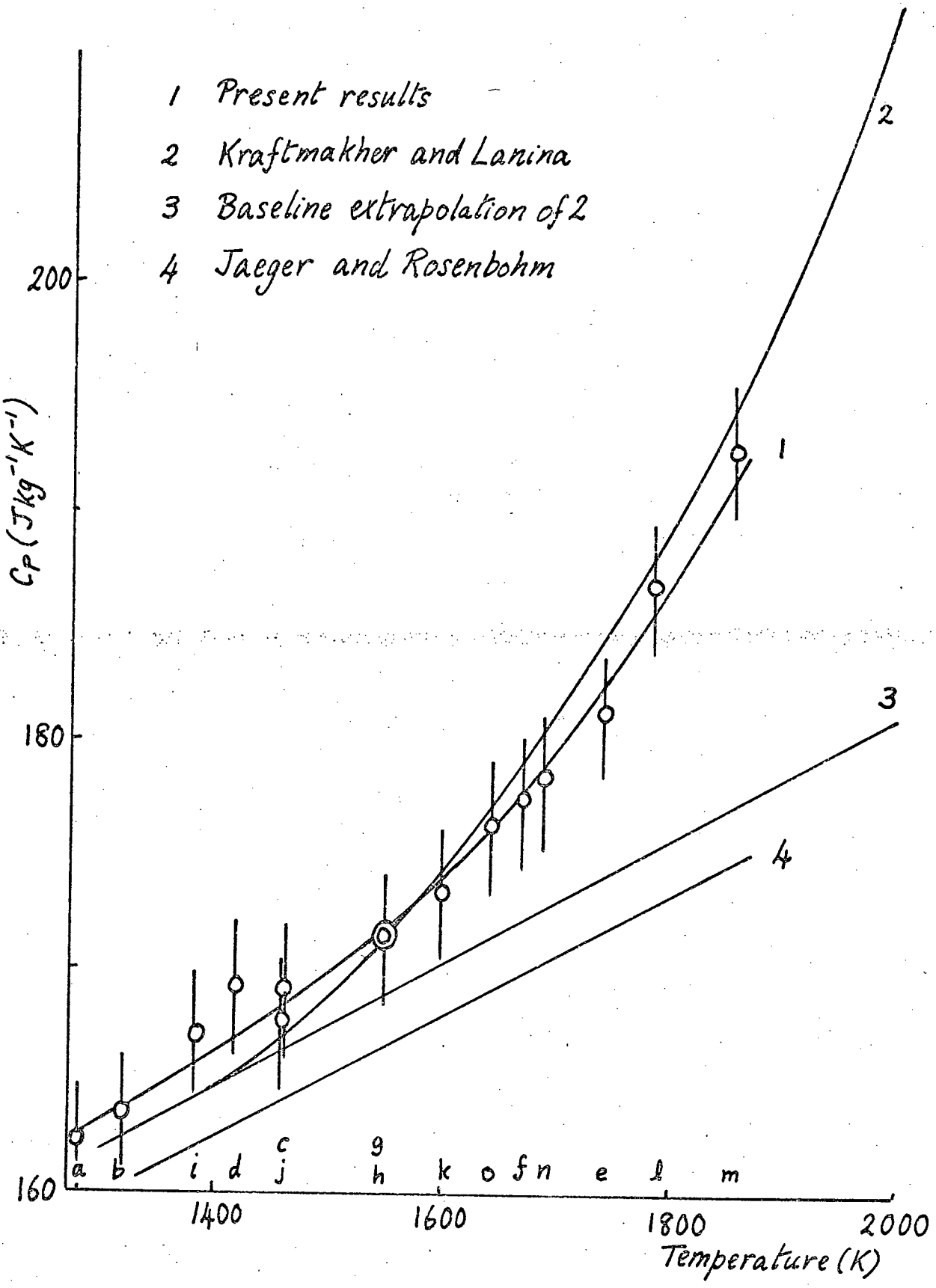

Sec.4.5.6. Fig.1 - High temperature specific heat of platinum

The discussion of these results, and their relationship to other work in the field, forms the subject of section 5.

Table of values for Fig.1, section 4.5.6.

Run	T_o(K)	$10^{-3}c_p/\alpha$(Jkg^{-1})	$10^3\alpha$(K^{-1})	c_p(Jkg^{-1}K^{-1})
a	1285	57.9	2.802	162.2
b	1463	65.1	2.594	168.9
c	1323	59.5	2.750	163.6
d	1423	64.1	2.638	169.0
e*	1743	71.0	2.550	181.1
f*	1673	70.4	2.520	177.4
g*	1553	67.6	2.534	171.3
h	1553	67.6	2.534	171.3
i	1383	62.2	2.684	166.9
j	1463	64.6	2.594	167.6
k*	1608	68.8	2.518	173.3
l*	1788	72.5	2.572	186.5
m*	1858	73.4	2.626	192.8
n*	1693	70.5	2.528	178.2
o*	1643	70.5	2.516	177.3

The runs appear in chronological order.

The symbol * denotes that a mask was used to reduce detector sensitivity.

5. Discussion

In this section, we shall consider various models that have been put forward to account for the enhancement of specific heat at high temperatures, a phenomenon confirmed by the present results for platinum which were summarised in the preceding section (4.5.7). These results afford the possibility of distinguishing between the proposed models, and, with the help of other evidence concerning vacancy effects, enable an interpretation of the enhancement to be given for platinum; finally, the extent to which similar interpretations hold for other metals of interest is examined.

5.1 Proposed explanations of the specific heat enhancement

5.1.1 Model I - Large vacancy concentrations and short relaxation times

In the preceding sections, the only explanation advanced for the large "extra" specific heat in metals at high temperatures measured by modulation methods (Kraftmakher and Strelkov 1966)[b] has been the view put forward by these authors that the observed enhancements are due to the energy associated with creation and destruction of vacancies. They took the view that the background specific heat could be satisfactorily estimated by a linear extrapolation of the data for temperatures immediately below the region in which enhancement effects became important. This view has also been taken by Hoch (1965), by Kirillin et al. (1968) and by Chekhovsky and Petrov (1968), among others.

The "extra" specific heat Δc_p was plotted against 1/T, giving both an activation energy, interpreted as a formation energy E^F, and the equilibrium vacancy concentration (section 2.3.1). These concentrations were, however large, typically $\sim$ 1% at T_M, and an order of magnitude larger than those reported by the X-ray parameter/length measurements in metals where a comparison was possible. For gold, Kraftmakher and Strelkov (1966) give $C_{eq}(T_M)$ = 0.4% by the modulation method, while Simmons and Balluffi (1962) obtained 0.07% by the other method. Stored

energy methods on quenched specimens have given results which are somewhat contradictory for this quantity - 0.045% (de Sorbo, 1960) and 0.21% (Pervakov and Chotkevic, 1960). For copper, Kraftmakher (1967) obtained 0.5%, compared with 0.02% by the method of Simmons and Balluffi (1963).

The X-ray parameter/length experiment has not yet been performed for platinum. Edwards, Speiser and Johnston (1951) measured the X-ray parameter as a function of temperature, and Kraftmakher (1967[a]) measured the thermal expansion using a modulation technique; these results are subject to the problems of interpretation discussed below. The results of the modulation measurements of the specific heat of platinum using the resistance bridge method (Kraftmakher and Lanina 1965; see also section 2.3.1) are shown in Fig. 1 in direct and semilogarithmic plots. For comparison, the values of the temperature coefficient of resistance obtained by these authors using D.C. measurements (section 4.3.2) are similarly shown. They interpret the specific heat results as giving

$$C_{eq}(T) = \exp(4.5)\,\exp(-1.6\ eV/kT),\quad C_{eq}(T_m) = 1\% \quad \ldots (5.1)$$

and, using linear extrapolation for α as indicated,

$$C_{eq}\rho_v = (2.1 \times 10^{-4}\ \Omega m)\,\exp(-1.6\ eV/kT) \quad \ldots (5.2)$$

so that at the melting point $(C_{eq}\rho_v)_m = 2.4 \times 10^{-8}\ \Omega m$, contributing about 4% of the resistivity. Thus

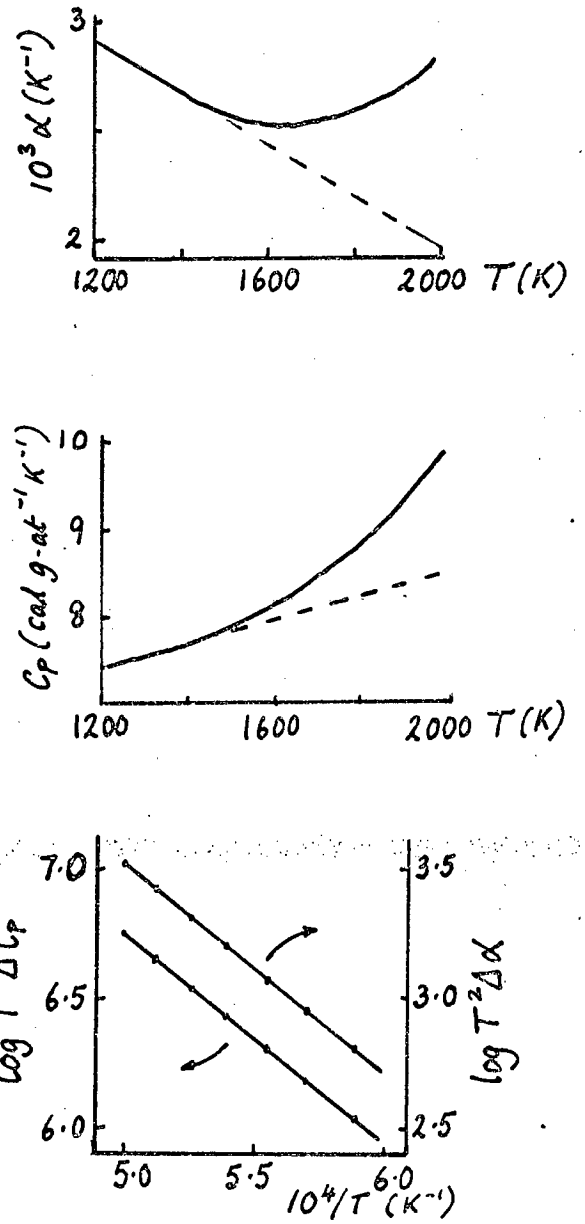

Sec.5.1.1. Fig.1 - Interpretation of resistance and specific heat measurements for platinum according to Kraftmakher and Lanina

$\rho_v = 2.4 \times 10^{-8}$ Ωm/at.%.

The value 1.6 ± 0.15 eV is in good agreement with that reported by Jackson (1965), who gave 1.51 ± 0.04 eV for platinum quenched from low temperatures, and it is also roughly half the activation energy for self diffusion, for which values of ∿ 2.9 eV are reported (see section 5.3.2).

A review by Kraftmakher and Strelkov (1970) adhered to the view that the large vacancy concentrations were correct, and that the low concentrations obtained by the X-ray method were attributable to vacancy formation without an increase in volume equal to the volume associated with one lattice site. They postulated that this could occur for vacancies associated with an internal imperfection, or, for vacancies in the bulk material, by mechanical relaxation of the neighbouring atoms.

To account for the specific heat enhancements observed in the modulation experiments, they took the view that the vacancy concentration was maintained at or near a value corresponding to the equilibrium concentration at the instantaneous temperature by an efficient network of internal sources, so that the vacancy relaxation time was negligibly short compared with the modulation period at all temperatures at which a measurable enhancement was observed.

These views are by no means universally accepted, and two other explanations have currency; these are described below.

5.1.2 Model II - anharmonic contributions to the specific heat

An alternative model for the enhancement of the specific heat is reviewed by Hoch (1970), and lies in the possible extra specific heat contributed by the lattice at high temperatures. In a lattice made up of atoms bound by linear restoring forces (i.e. in the harmonic approximation to a real lattice) the specific heat above the Debye temperature is constant; for the anharmonic forces present in a real lattice, the next approximation to the specific heat is a linear increase with T, i.e.

$$c_p = a + bT. \qquad \ldots (5.3)$$

Hoch points out that this approximation is based on the Grüneisen-Mie equation of state (Mott and Jones 1958)

$$c_p = c_v(1 + 3\lambda\gamma T) + c_{el}T \qquad \ldots (5.4)$$

where λ is the linear thermal expansion coefficient, γ is the Grüneisen constant and c_{el} is the electronic specific heat, so that if λ, γ and c_{el} are constant the lattice plus electronic specific heat at constant pressure is a linear function of T. He argues that this equation fails to represent the anharmonic contributions correctly at high temperatures, and that the expression

$$c_p = 3RF(\theta_D/T) + cT + dT^3 \qquad \ldots (5.5)$$

should be employed, following the calculations of Liebfried (1955). Here $F(\theta_D/T)$ is the Debye function from

$T = \theta_D$ to the melting point. This equation fitted the results for refractory metals (Cr, Mo, W, Nb, Re) and also the results of Brooks and Bingham (1968) for aluminium without requiring a vacancy term.

He concludes that within the $\sim$ 1% experimental accuracy of specific heat measurements, observed effects can be accounted for by the assumption of anharmonic contributions to the specific heat and that, for vacancy effects to show up, an accuracy of $\sim$ 0.1% would be required.

This explanation thus denies the existence of large vacancy concentrations. It is thus essentially independent of the vacancy relaxation time; the relaxation time associated with the anharmonic effects would of course be negligibly short. We shall from now on consider with these anharmonic effects any deviation from the linear rise of specific heat with temperature *not* due in some way to vacancy effects, i.e. we shall include any such effects due to electronic specific heat since for our purposes they are experimentally indistinguishable.

5.13 Model III - that the enhancements are spurious, and result from a neglect of the effect of vacancy relaxation on the resistance temperature coefficient

Van den Sype (1970)[a] put forward an alternative interpretationof the high-temperature specific heat based upon the importance of allowing for vacancy relaxation effects. He pointed out that in the work of Kraftmakher and Strelkov on tungsten (1962) (which used the resistance bridge method outlined in section 2.3.1) the resistance fluctuations were used to determine the temperature

modulation. If the modulation period is short compared with τ_v, the measurement is effectively at high frequency, and the directly-measured quantity is $c_p(\infty)/\alpha(\infty)$; this is then converted to "specific heat" by use of the values of resistance temperature coefficient measured under static conditions, i.e. $\alpha(0)$. The quantity thus derived is what Van den Sype calls c_k:

$$c_k = \frac{\alpha(0)}{\alpha(\infty)} c_p(\infty). \qquad \ldots (5.6)$$

Clearly, if $\alpha(0)/\alpha(\infty) > c_p(0)/c_p(\infty)$, an apparent enhancement compared with the values of $c_p(0)$ measured quasi-statically will result if c_k is plotted as a function of temperature.

Van den Sype cites the drop-calorimeter measurements of Leibowitz et al. (1969) on the enthalpy of tungsten, in which no enhancement was found. He accounts for the 50% difference at 3600 K between these results and those of Kraftmakher and Strelkov by assuming that $\tau_v > 5$ ms (to be long compared to the modulation periods resulting from frequencies 40 Hz - 150 Hz), and that $E^F = 3$ eV, $C = 0.1\%$ and $\rho_v = 0.4$ μΩm/at.%. That this value of ρ_v is several times larger than the value obtained by quenching he attributes to a variation in ρ_v with temperature.

The essential features of this model are, then, that the vacancy relaxation time is long, and that the ratio $\alpha(0)/\alpha(\infty)$ is large enough to account for the enhancements.

5.1.4 Combinations of the above models

It is perhaps worth remarking that the above models are not entirely incompatible. In particular models II and III can be combined to give a model in which both anharmonic and vacancy relaxation effects occur. Model II can also be combined with I to give a model in which the extra specific heat arises partly from anharmonic effects and partly from vacancies following the temperature modulation with a short relaxation time.

In what follows, we shall attempt to decide between all these possibilities.

5.2 The relevance of the present work to the problem of interpreting specific heat enhancements in platinum

5.2.1 General considerations

In principle, the measurements described in section 4* are of a kind which should, at least for platinum, enable a choice to be made from simple models I-III above. The relevant points are (1) that measurements up to high modulation frequencies have been carried out, and (2) that absolute measurements of specific heat have been made using a method of determining the temperature modulation which does not depend on the resistance modulation. We may summarise the results expected from such measurements according to each model as follows:

* Summarised in section 4.5.7.

		Model I	Model II	Model III
1.	Effect on measured values of c_p of increasing the modulation frequency to a 'high' value	decrease	none	none
2.	Comparison of measured c_p with values of c_k at 'similar' frequencies	$c_p = c_k$	$c_p = c_k$	$c_p < c_k$

In this table, it has been assumed that the upper frequencies of modulation are sufficiently high to guarantee that the vacancy concentration cannot follow them. It has also been assumed that the use of the light emitted by the specimen as a way of determining the temperature modulation is free from the objection that D.C. calibration is inappropriate.

The first assumption depends on the minimum credible value for τ_v in a well-annealed specimen; it appears to be valid, as will be discussed below in relation to the high frequency results. The second relies on the fact that the effects of temperature change on the light emitted appear to be much greater than any possible effect attributable to the vacancies created or destroyed by the change. For example, a change of 1 K near the melting point of platinum gives a fractional change in detector output of $\sim 6 \times 10^{-3}$, but gives a change in vacancy concentration of only $\sim 5 \times 10^{-5}$ even assuming a concentration of 1%; the effect of these vacancies on the light output would presumably be only via the associated change in specimen dimensions, giving a fractional change in detector output $\sim 3 \times 10^{-5}$, negligibly

small compared with 6×10^{-3}. By contrast, the fractional change in resistivity near the melting point is $\sim 0.45 \times 10^{-3}\ K^{-1}$ of which, on Kraftmakher's interpretation no less than 30%, or $0.15 \times 10^{-3}\ K^{-1}$, is due to vacancies. Even assuming a more normal vacancy concentration leading to a vacancy resistivity of say only 1%, the contribution is still $\sim 8\%$ ($0.04 \times 10^{3}\ K^{-1}$). The question of whether or not vacancies are contributing to α is therefore crucial if the resistance modulation is used to measure temperature modulation, as Van den Sype realised.

Given these assumptions, the results can be interpreted as set out below.

5.2.2 Deductions from the high-frequency measurements

In sections 4.5.3 and 4.5.4, an account was given of the null results of experiments designed to look for a variation of apparent specific heat with frequency. The accuracy of these measurements was such that, assuming vacancy concentrations according to model I, an effect would have been observed had the vacancy relaxation peak at 1850 K been at a frequency below 4 kHz. On this model, the peak must of course lie well above the modulation frequency of Kraftmakher and Lanina's experiments, $\sim$ 30 Hz, so that agreement with model I can be obtained only if the peak lies above 4 kHz. This corresponds to $\tau_v < 40\ \mu s$.

Lifetimes as short as this can only occur if defects within the bulk of the material are active as sources and sinks. This is the condition that operates during the annealing of quenched in defects, and the lifetimes there

observed can be extrapolated to give an estimate of the high-temperature vacancy lifetime (see section 1.4)*. In the earlier quenching work, significant plastic strains were often introduced, increasing the dislocation density and reducing τ_v. Thus Gertsriken and Novikov (1959), using the thermoelectric power to study the vacancies, obtained a figure of 10^6-10^7 for the number n_o of jumps made by the average vacancy to destruction, corresponding to $\tau_v \sim 4$ μs at 1850 K. In his experiments on platinum, Jackson (1965) observed that this plastic strain effect could be eliminated by quenching rapidly from fairly low temperatures, below ∿ 1300 K, and obtained $n_o \sim 5 \times 10^8$, which would correspond to $\tau_v \sim 400$ μs at 1850 K. This value of τ_v as a lower limit assuming active internal sources and sinks appears more appropriate to the high-temperature specific heat measurements, where the dislocation density is expected to be that of the well-annealed metal.

This conclusion would be invalidated if the diffusion rate for vacancies at the high temperatures were significantly different from that extrapolated from annealing temperatures; such a difference might arise if annealing occurred by a monovacancy mechanism, while divacancies predominated at high temperatures. Polák (1967) has studied the kinetics of quenched-in vacancies in platinum, and concludes that the results are consistent with thermal equilibrium between monovacancies and divavancies, the divacancy binding energy being 0.18 eV, and migration energies $E^M_{IV} = 1.45$ eV, $E^M_{IIV} = 1.11$ eV, all

* Page 6

±.05 eV. Similar values were obtained by Jackson (1965). The assumption of thermal equilibrium between the two species leads to estimates of the relative fluxes for monovacancies and divacancies respectively as at least 40 : 1, even near the melting point, indicating that divacancy migration is not likely to be sufficient to provide the large concentration changes necessary to follow a high-frequency temperature modulation.

The results of the high-frequency measurement are, for these reasons, considered to be significant, and lead us to reject Model I.

In consideration of model II, although the dominant effects are assumed to be anharmonic, a small contribution to the high-temperature specific heat from vacancies must exist at suitably low frequencies. The resolution of the high frequency measurements would not be good enough to detect a frequency variation of specific heat arising from relaxation of such a contribution if it were less than $\sim$ 3 %, as would be the case if the vacancy concentration corresponded to the typical values $\sim$ 0.1% obtained by the X-ray parameter/length measurements near the melting point of other metals. We may conclude that for model II the null results add no significant information, though they are, of course, consistent with the model.

For model III, null results are to be expected, as even the 30 Hz measurements of Kraftmakher and Lanina are supposed to be at high frequency, and, *a fortiori*, no relaxation effects will be seen in the 100 Hz - 1 kHz region.

Finally, then, the results of the high-frequency measurements appear to exclude model I, but are consistent with the other two models. If the dominant effects are anharmonic, there is no reason to exclude a small vacancy contribution, whatever the relaxation behaviour; similarly, even if the dominant effect is due to low-frequency vacancy relaxation, an anharmonic contribution is not excluded.

5.2.3 Deductions from the absolute measurements of specific heat

The question of the agreement between the absolute measurements of specific heat described in section 4.5.6 and the results of Kraftmakher and Lanina is of particular importance in deciding whether the effects of model II or those of model III dominate the specific heat enhancement. In Fig. 1, the former results are shown as measured values of $c_p/\alpha = X_A$ say. This ratio corresponds to the directly-measured quantity, the resistance/temperature results from the questionable procedure of Kraftmakher and Lanina (see section 4.3.2)* entering only in determining the mean temperature used as abscissa in the plot. The plot is therefore not much affected by any errors in these results. Also shown are Kraftmakher and Lanina's own values for $c_p/\alpha = X_K$ say, again not much affected by any errors in the resistance/temperature results. The agreement at temperature below 1600 K is good; there is a tendency however for the curves to diverge slightly above this temperature, though the difference is only of the order of the experimental errors ($\sim$ 1%).

* Page 98

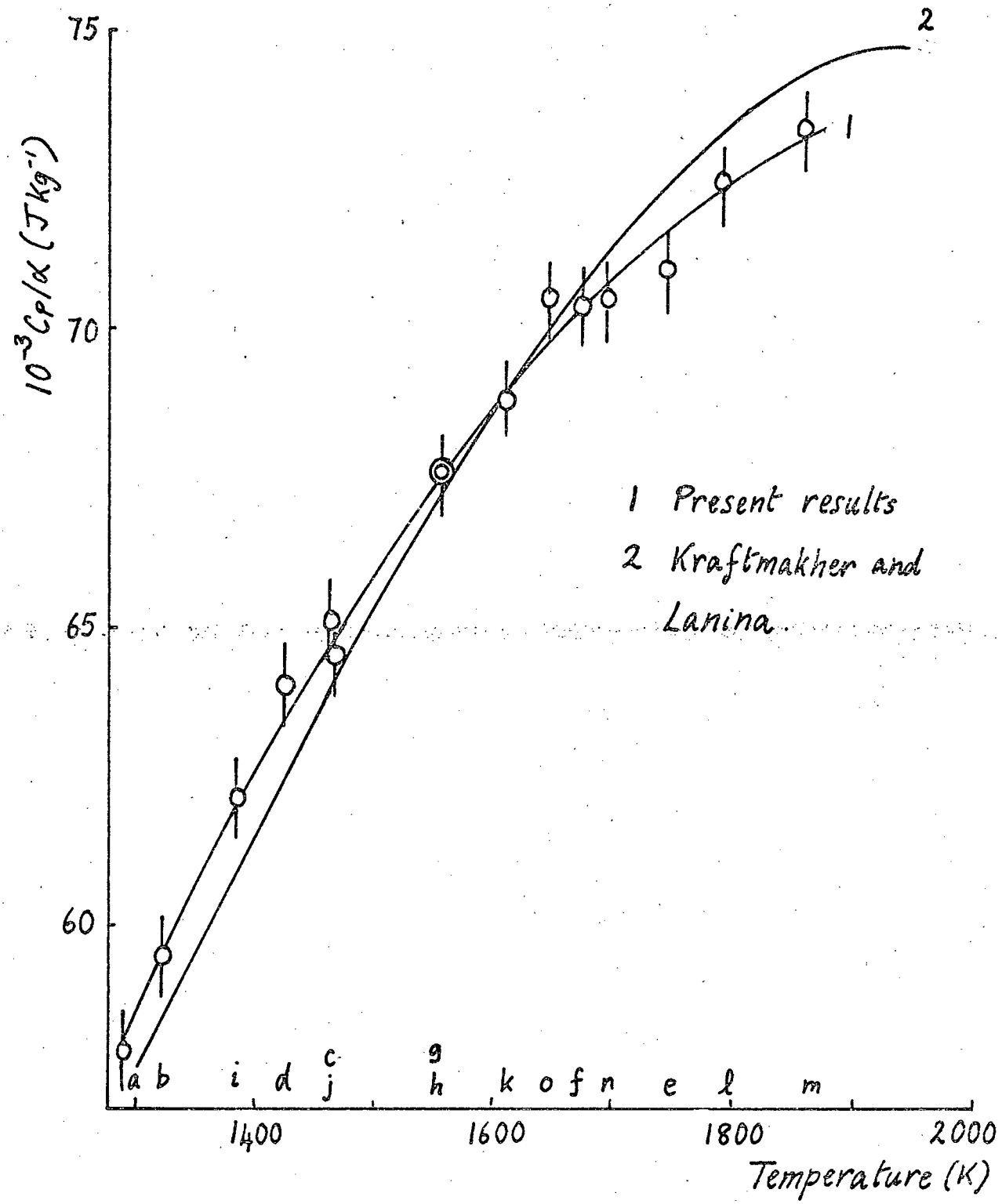

Sec.5.2.3. Fig.1 - c_p/α for platinum as a function of temperature - experimental results

In Fig. 2, these experimental results are again compared, but the present results X_A are shown as a curve (curve 2) fitted to the Kraftmakher and Lanina results X_K (curve 1) below 1450 K, assuming that any disagreement below that temperature is due to errors in the determination of specimen mass. The disagreement between the curves is at most 2½%. Now, according to model II, X_A and X_K should agree. On model III, however, X_K represents $c_p(\infty)/\alpha(\infty)$, whereas X_A is $c_p(\infty)/\alpha(0)$; in particular, if the temperature variation of $c_p(\infty)$ were to be taken as linear, i.e. if $c_p(\infty)$ were to be correctly represented by Kraftmakher's extrapolation, then curve 4 would result for the values measured by the radiation detector method. This curve is significantly different from the X_A values (curve 2), showing that we cannot account for all the specific heat enhancement on the basis of low-frequency vacancy relaxation, and it is clear that anharmonic (or electronic) effects are dominant in the enhancement of specific heat at high temperatures.

The remaining curve (3) in Fig. 2 shows the values of c_p/α obtained by extrapolating the low-temperature value of c_p and α according to Kraftmakher and Lanina's procedures. It is included to make the point that, even at 1850 K, the deviation of the curves of measured c_p/α from this curve is large, and does not arise simply from possible errors in the resistance/temperature results.

If we accept that anharmonic effects dominate the high-temperature specific heat, we are left with the

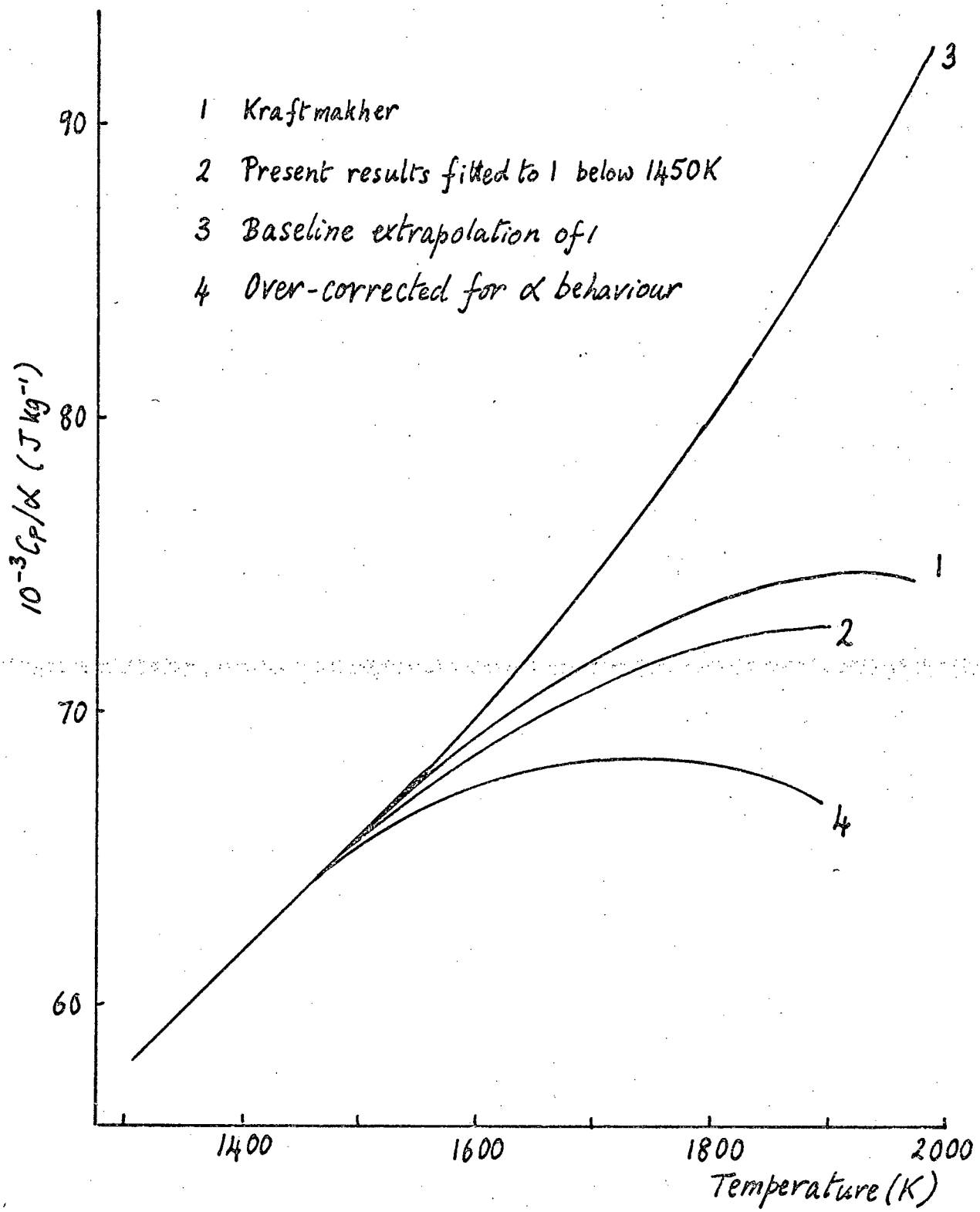

Sec.5.2.3. Fig.2 - c_p/α for platinum - extrapolated and experimental curves

problem of the extent to which vacancy effects contribute. This would be easy if we were certain as to the origin of the small discrepancy between the X_A and X_K curves at high temperatures, not much outside experimental error. If it is a genuine effect, we have evidence of low-frequency vacancy relaxation; if not, then we cannot exclude vacancy effects, except to remark that they must be fairly small, contributing not more than $\sim$ 3% to α if τ_v is long, or, if τ_v is short, not more than about 3% to c_p by the argument of the preceding section.

To make further progress, we must examine other evidence, relating particularly to the expected values of c_p, α and τ_v in platinum.

5.3 Other evidence relating to the interpretation for platinum

As we have seen, the interpretation of the specific heat results involves not only the quasi-static values of c_p and α, but also their high frequency values, and the vacancy lifetime τ_v. These are quantities which may be studied in other ways, and the purpose of this section is firstly to use this other evidence to check the conclusions reached above, and secondly to investigate whether these conclusions can be made more definite.

5.3.1 The vacancy relaxation time in platinum

The results of quenching and annealing experiments were used in section 5.2.2 to obtain an estimated lower limit of $\sim$ 400 μs for τ_v at 1850 K, on the assumption of efficient internal source/sinks such as dislocations in the well-annealed metal. An upper limit can correspondingly

be set for diffusion-limited relaxation on the assumption that the surface of the specimen is the dominant source/sink; for the $\sim$ 50 μm diameter specimens used, this gives $n_o \sim 3 \times 10^{10}$ and $\tau_v \sim 40$ ms. Of course, if this relaxation process is production-limited by the low efficiency of the surface as a source, this estimate fails, and τ_v would be even longer. Intermediate estimates correspond to grain boundaries as predominating sources, or to dislocations in the bulk acting at low efficiency. We cannot therefore exclude the possibility that τ_v may be long enough ($> \sim 10$ ms) to give low-frequency relaxation effects below 30 Hz unless we can show that the internal dislocations are effective sources under the conditions of the modulation experiment.

The generally accepted picture of vacancy production at a dislocation is that of vacancy-induced climb, the jogs on the dislocation providing sites where the vacancies may easily be created or destroyed. In this process, a critical parameter is the 'driving force' for climb deriving from the subsaturation or supersaturation of vacancies relative to the equilibrium concentration. This may be seen by a simple argument: the free energy change on creating a vacancy is

$$\Delta G = E^F - TS^F; \qquad \ldots (5.7)$$

now for a vacancy concentration C, the configurational entropy per vacancy is

$$S^F_{con} = kC \ln(1/C), \qquad \ldots (5.8)$$

so that in equilibrium, of course,

$$\Delta G = E^F - TS^F_{th} + kT \ln C_{eq} = 0. \quad \ldots (5.9)$$

Suppose now the crystal is subjected to an external stress σ inducing climb of unit length of a dislocation. The force F per unit length of dislocation line is σb, where b is the Bürgers vector; it will perform work σb if the dislocation climbs unit distance, producing $1/b^2$ vacancies. The work done per vacancy created is Fb^2 so that ΔG becomes

$$\Delta G = E^F - TS^F - kT \ln(1/C) - Fb^2$$

$$= kT \ln(C/C_{eq}) - Fb^2. \quad \ldots (5.10)$$

A supersaturation C/C_{eq} thus provides a driving force per unit length of dislocation μ/b^2, where $\mu = kT \ln(C/C_{eq})$ is the chemical potential.

Lomer (1958) considered this in relation to an edge dislocation pinned at both ends a distance $2l$ apart. The driving force must now be sufficient to overcome the line tension, leading to the approximate condition for climb

$$\ln(C/C_{eq}) > G_s b^4/kTl \quad \ldots (5.11)$$

where G_s is the shear elastic modulus. At diffusion temperatures, $kT \sim 0.1$ eV and $G_s b^3 \sim 4$ eV so that

$$\ln(C/C_{eq}) > 40b/l; \quad \ldots (5.12)$$

a dislocation source of length 1 μ thus requires a supersaturation of only ∿ 1%, and values of μ of only ∿ 10^{-3} eV.

This discussion however ignores the question of production of the necessary jogs to maintain climb. This can in principle occur by homogeneous nucleation of a pair of jogs in a piece of smooth dislocation line, or by heterogeneous nucleation at special sites. Thomson and Balluffi (1962 a, b) considered the former case in a detailed kinetic model for climb, showing that for an unconstrained dislocation the climb rate is diffusion limited if the jog-formation energy is sufficiently low. Unfortunately, knowledge of the parameters entering their expressions is poor, in particular because of lack of detailed knowledge of dislocation-core configurations; quantitative estimates are unreliable.

Balluffi and Seidman (1965) reviewed the subject of dislocation climb in metals, classifying situations by the size of the driving force as measured by μ. 'Large' values of μ (> 0.1 eV) are typically encountered in annealing experiments following quenching and dislocations are effective sinks under these conditions. They show also that, contrary to the random-walk treatments (e.g. Kuhlmann-Wilsdorf 1965), dislocations are probably active during the down-quench itself. In their own experiments on pulsed heating of gold to elevated temperatures, the values of μ started at -0.3 eV and fell to -5 x 10^{-3} eV; the dislocation source efficiency (related to the diffusion-limited rate) was ∿ 0.1, but the generation rate fell off somewhat as the

vacancy concentration neared equilibrium. In the work of Koehler and Lund (1965) on gold/0.1 at.% silver alloy on the other hand, pulsed heating experiments showed no evidence of dislocation source activity. 'Moderate' values of μ (0.1 eV $> \mu > 10^{-3}$ eV) are encountered during mechanical stresses, and also due to the line tension of small dislocation loops. It appears that in the growth and shrinkage of small dislocation loops, as observed by electron microscope techniques, efficient climb occurs under values of μ as low as 0.04 eV (in aluminium). Conversely, 'low' values of μ ($< 10^{-3}$ eV) as encountered in the sintering of voids do not appear to result in dislocation climb.

We may estimate maximum values of μ for the modulation amplitudes used in our experiments on platinum as ~ 0.005 eV, assuming a modulation amplitude of 1 K and that the vacancy concentration remains at its mean value. These are certainly much less than encountered in quenching and annealing experiments. Kraftmakher and Lanina do not give the modulation amplitude, but it cannot exceed this by more than one order of magnitude. Under these circumstances, we cannot guarantee that internal dislocations will operate efficiently, and τ_v may therefore be long.

Because of this, the work of Heigl and Sizmann (1972) on the pulse-heating of platinum is of particular relevance; this followed on the initial experiments of Sizmann and Wenzl (1963). Heigl and

Sizmann developed electronic apparatus capable of pulsing wires to elevated temperatures for times as short as 1 ms, observing the vacancies so generated by their effect on the resistance at liquid nitrogen or liquid helium temperatures. Rapid quenching rates were obtained by blowing cool helium over the specimen. With this apparatus, they were able to investigate the kinetics of vacancy generation in detail. The results were consistent with diffusion-limited supply of vacancies from a network of planar sources $\sim$ 5 μm apart, interpreted as dislocations arranged in small-angle sub-grain boundaries. This simple model held until up to $\sim$ 30% of the equilibrium vacancy concentration had been generated. For the interpretation, they take the mono-vacancy diffusion coefficient to be

$$D_{IV} = 4.9 \times 10^{-6} \exp(-1.38 \text{ eV}/kT) \text{ m}^2 \text{ s}^{-1} \quad \ldots (5.12)$$

following the analysis of quenching and self-diffusion results by Schumacher, Seeger and Harlin (1968). This corresponds to lifetimes $\sim$ 100 ms at the temperatures of generation used in the pulse experiments ($\sim$ 1200 K).

From these results, we may determine the vacancy lifetimes shown in Fig. 1; the lines refer to the three specimens used by Heigl and Sizmann. The difference between samples 1 and 2 is attributed to a difference in heat treatment, 2 having received a 2 h anneal at 1500°C, 1 having received only annealing at 1200°c. The high-temperature anneal coarsens the sub-grain structure (McLean 1957), giving longer relaxation times; the order of magnitude of the sub-grain size is reasonable

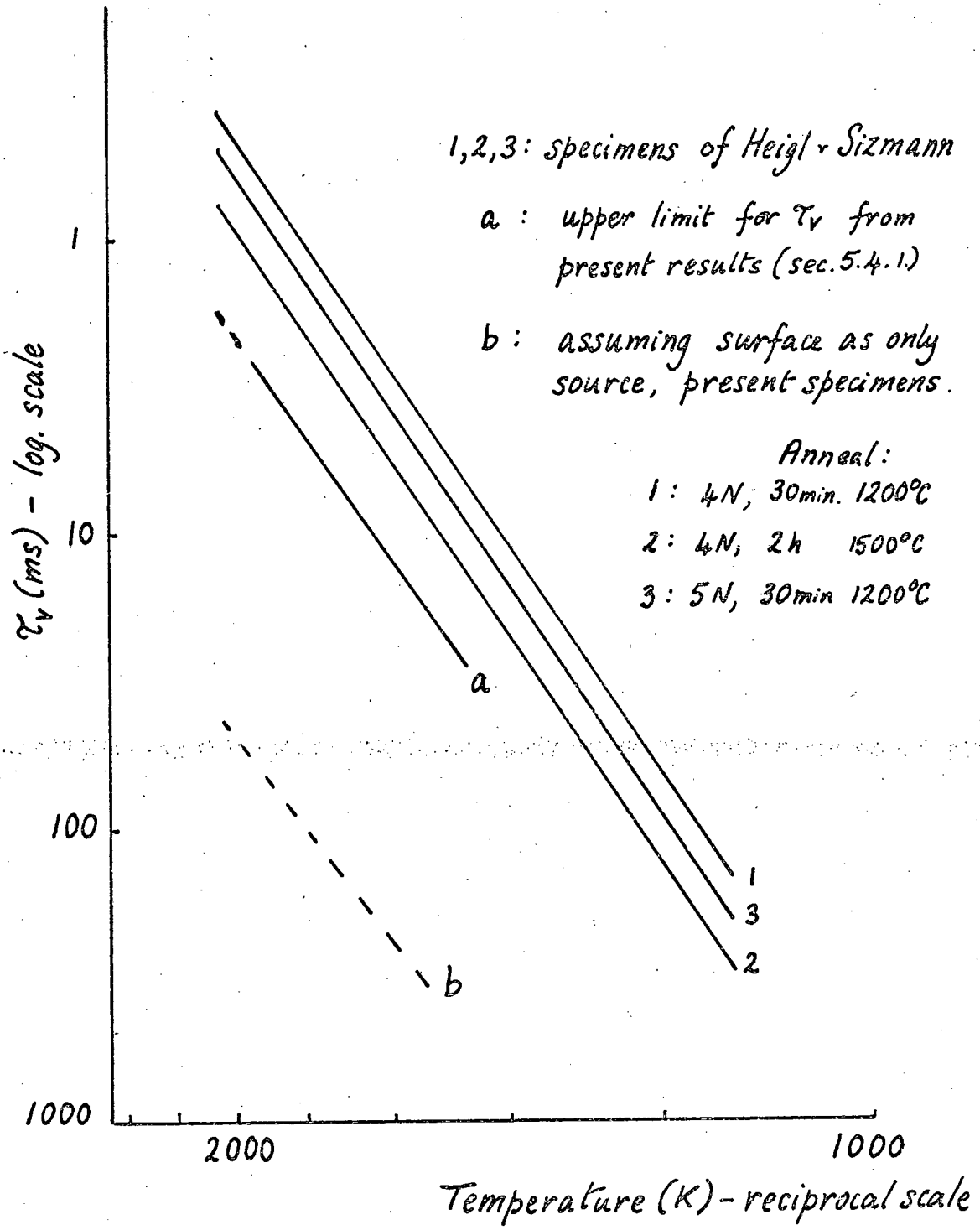

Sec.5.3.1. Fig.1 - Vacancy lifetimes in platinum

(Guinier and Dexter 1963). These samples were of 4N purity; sample 3 was of 5N purity, and received only the low-temperature anneal. The relaxation times are $\sim$ 0.5 ms at T_m, or $\sim$ 1.5 ms at 1850 K.

Such values of τ_v give small, but not negligible, relaxation effects even at the low modulation frequencies of Kraftmakher's experiments. As will appear later, good agreement between the present results and those of the resistance bridge method can be secured on the basis of these relaxation times (see section 5.4.1), or the somewhat longer times corresponding to a rather coarser subgrain structure following high-temperature annealing. We therefore adopt these as a working hypothesis, while noting the possibility that, as the driving force of the modulation experiments is perhaps 100 times smaller than in the pulse experiments, the lifetimes may not be comparable.

Very long values of τ_v have been reported in pulse-heating experiments on aluminium by Bokshtein et al. (1968) using specimens 0.3-0.6 mm in thickness. Vacancies were observed to contribute substantially to the specific heat only if the pulse duration was > 1 second, giving relaxation times $\sim$ 4 s at $\sim$ 640°C (913 K) which correspond to the surface of the specimen as the dominant source. (The grain size in these experiments exceeded the thickness of the specimen.) For an alloy Al/1.7 at.% Cu, similar effects were observed except that τ_v was even longer, calculated to be two orders of magnitude greater at

comparable temperatures; this difference was attributed to a decrease in vacancy mobility due to interaction with the copper atoms.

In Bokshtein's experiments, the temperature pulses were 1-13 K, the larger figure corresponding to a subsaturation of 15%, μ = .01 eV, and exceeding Lomer's estimate by an order of magnitude. Even according to Thomson and Balluffi's theory one would expect efficient dislocation climb in aluminium because of its high stacking fault energy, and hence its probable low jog energy (Seidman and Balluffi 1965). Bokshtein attributes the discrepancy to impurity effects, pointing out that a binding energy for an impurity-dislocation interaction as low as 1/10 of the vacancy formation energy will prevent climb with supersaturations of 3o% if the concentration of impurities is as high as 10^{-4}; the argument is similar to that of Lomer given below. Confidence in Bokshtein's results is increased by the fact that they agree in all respects with those obtained by quenching, except that, in the non-equilibrium (quenching) studies, the vacancy diffusion distance corresponds to the quantity estimated from the dislocation density. The comparative results for τ_v at T_m are shown in Fig. 2, plotted against the path length to the sink. Use of this curve for our specimens gives $\tau_v \sim$ 20 ms at T_m, if the specimen radius is used, agreeing reasonably well with our previous estimate, while if 5 μm is used we obtain $\sim$ 1 ms.

It is not clear how far the proposed impurity argument

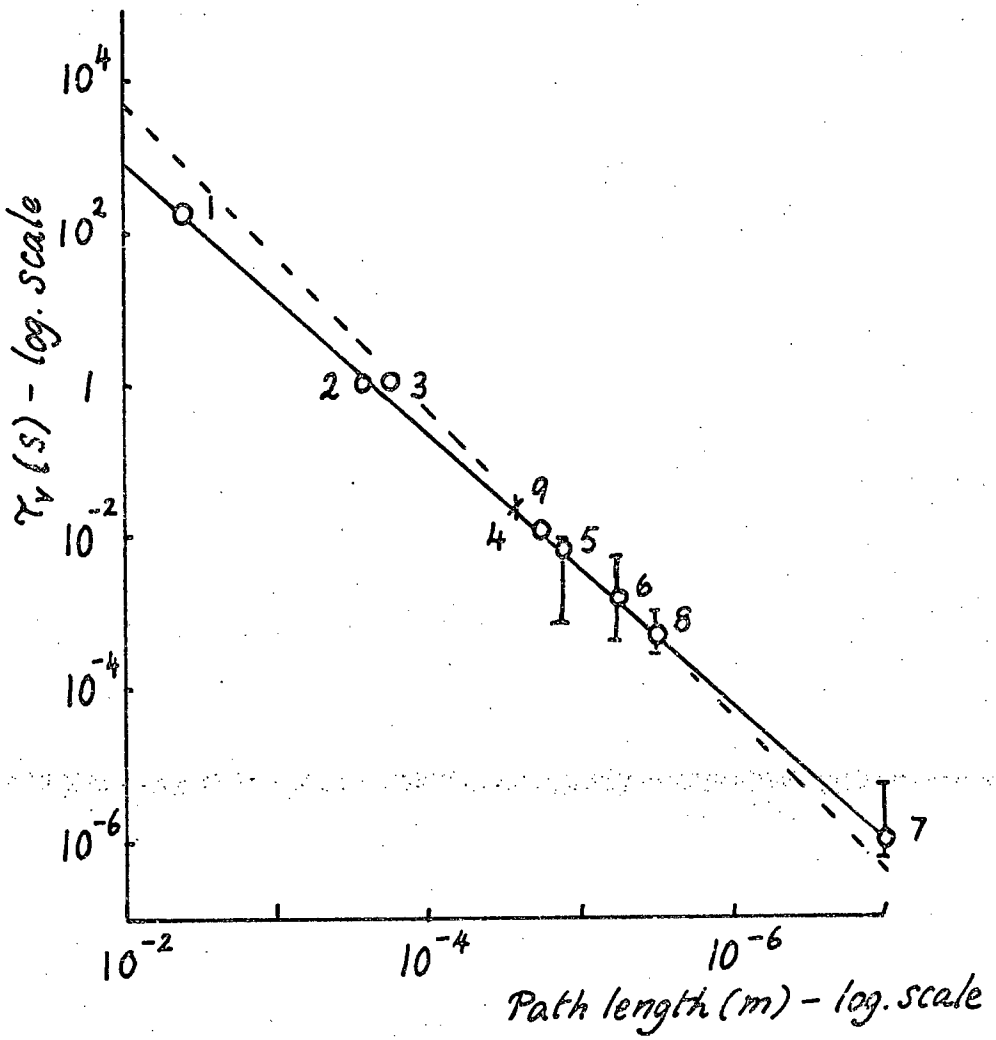

Sec.5.3.1. Fig.2 - Melting-point values of τ_v for various metals (see over for legend)

Legend for Fig.2, section 5.3.1.

Points 1-7 after Bokshtein et al. (1968)

Point	Metal	Reference
1	Al	Guarini and Schiavini (1966)
2	Al	Bokshtein et al. (1968)
3	Pb	"
4	Al	Nechaev (1968)
5	Au	Seidman and Balluffi (1965)
6	Cu	Nechaev (1968)
7	Al	Nechaev (1968)
8	Pt	Heigl and Sizmann (1972)
9	Pt	(assuming surface to be only source)

Solid line after Bokshtein et al. (1968)

Dashed line : theoretical, gradient 2.

applies to platinum; the impurities found are often of the platinum group of metals, and might impede climb but little. We shall indeed see (section 5.4.1) that lifetimes corresponding to surface generation are too long to fit both the present results and those of Kraftmakher and Lanina.

5.3.2 The vacancy contribution to the high-temperature resistivity of platinum

Kraftmakher and Lanina's extrapolation procedure for determining the vacancy contribution to $\alpha(0)$ has already been mentioned (section 5.1.1); it led to large contributions being assigned to vacancies ($\sim$ 20% at 1850 K).

This extrapolation procedure was first used in this way by MacDonald (1953 a,b) for the alkali metals; subsequently it was applied by others (e.g. to Cu and Au by Meechan and Eggleston (1954), and to Al by Simmons and Balluffi (1960a)). The 'extra' resistance obtained in this way generally gives good straight lines when used for an activation-energy plot, but the 'formation energies' so derived do not always agree with those obtained by other methods, nor do the magnitudes of these supposed vacancy contributions to the resistivity always agree with quenching studies. The theoretical basis of the procedure is based on a result of Mott and Jones (1936), valid for temperatures not too high:

$$\frac{d}{dT}\left(\ln \frac{R}{T}\right) = 2(3\lambda)\gamma, \qquad \ldots (5.14)$$

where 3λ is written for the volume coefficient of expansion and γ is the Grüneisen constant. If the term on the right

is independent of temperature, this can be integrated to give

$$R \simeq T \exp 6\lambda\gamma T \simeq T(1 + 6\lambda\gamma T), \quad \ldots (5.15)$$

the last form applying when $6\lambda\gamma T << 1$. Nicholas (1955) has seriously questioned the validity of the approximations involved in the application of this to Meechan and Eggleston's results, pointing out that at least a cubic, and possibly a quartic, term is required. He proposes that $\ln(R_{\text{measured}}/T)$ be plotted as a function of T, and obtains good fits to their results without requiring any vacancy term. It is of interest that the parabolic extrapolation had given values for the vacancy resistivity in gold an order of magnitude larger than those obtained by quenching (Bauerle and Koeher, 1957). Improved extrapolation techniques were used for gold by Mišek and Polák (1963) who attempted to solve empirically the difficulty resulting from the temperature variation of $\lambda\gamma$, but these authors concluded that the problem had not been overcome. For aluminium, the discrepancy between results of Simmons and Balluffi and quenching studies was only a factor of two, indicating perhaps that anharmonic effects play a less important part in aluminium than in metals of higher melting point. Even for these results, however, Wilders (1968), in a project under the joint supervision of A. F. Brown and the author, was able to show that the formation energies were critically dependent on details of the fit. More recently, Ascoli, Guarini and Queirolo

(1970) have given an extrapolation method (for Au, Ag, Cu) based on an observed linearity of $\ln(R_{measured}/T)$ when plotted as a function of T; this has no particular theoretical justification, but is used as an empirical justification for the expression

$$\ln(\rho_o/T) = A_1 T + A_2 + \ln|1 + \bar{\lambda}(T - T')| \qquad \ldots (5.16)$$

A_1 and A_2 being constants and $\bar{\lambda}$ a mean coefficient of linear expansion for the temperature range T' to T. This gives formation energies in satisfactory agreement with other types of measurement, but the values of extra resistivity again exceed by factors of 4-10 those of quenching experiments.

These authors observe that such factors might be due to a failure of Mattheissen's rule for vacancies, as argued by Van den Sype in proposing large contributions from vacancies to the temperature coefficient of resistance (section 5.1.3). There appears to be no confirmation of such a hypothesis for temperatures approaching the melting point. Failures of the rule have on the other hand, been observed for vacancies quenched into gold; between the temperatures 4.2 K and 300 K, a fourfold increase of vacancy resistance was noted (Conte and Dural, 1968).

For platinum, the situation is particularly complicated. The band structure of platinum (Mott and Jones 1936) is interpreted in terms of a Fermi level located towards the middle of the s-band, and just below

the upper edge of the d-band. The current is largely carried by the s-electrons, the d-electrons having low mobility, and the large lattice resistivity is ascribed to the high probability of s-d transitions associated with the high density of states in the d-band. This structure is thought to be responsible for the nature of the temperature variation of resistivity in platinum, involving a negative T^2 term. This argument would not however apply to the vacancy resistivity; the resistance of a vacancy arises largely from s-s transitions because of the small amplitude of d-wavefunctions in the region of the perturbing potential associated with the vacancy, these wavefunctions being highly localised. One might not therefore expect the vacancy resistivity behaviour to be very different from that of a more 'ordinary' metal.

Under these circumstances, the extrapolation procedure of Kraftmakher and Lanina is not trustworthy. Alternative extrapolation procedures in fact yield markedly different results; for example, a plot of $\ln(R/T)$ against T for their data (Fig. 1) gives an adequate straight line, but only about half the 'extra' resistance given by their method.

In view of the uncertainties of extrapolation methods, we are led to consider the evidence of quenching experiments.

The work of Jackson (1965) has already been mentioned (section 5.3.1) in connection with the vacancy lifetime in quenched platinum. Jackson's results are shown in Fig. 2, in which the resistivity increase in specimens quenched rapidly (6×10^4 K s^{-1}) is shown logarithmically as a

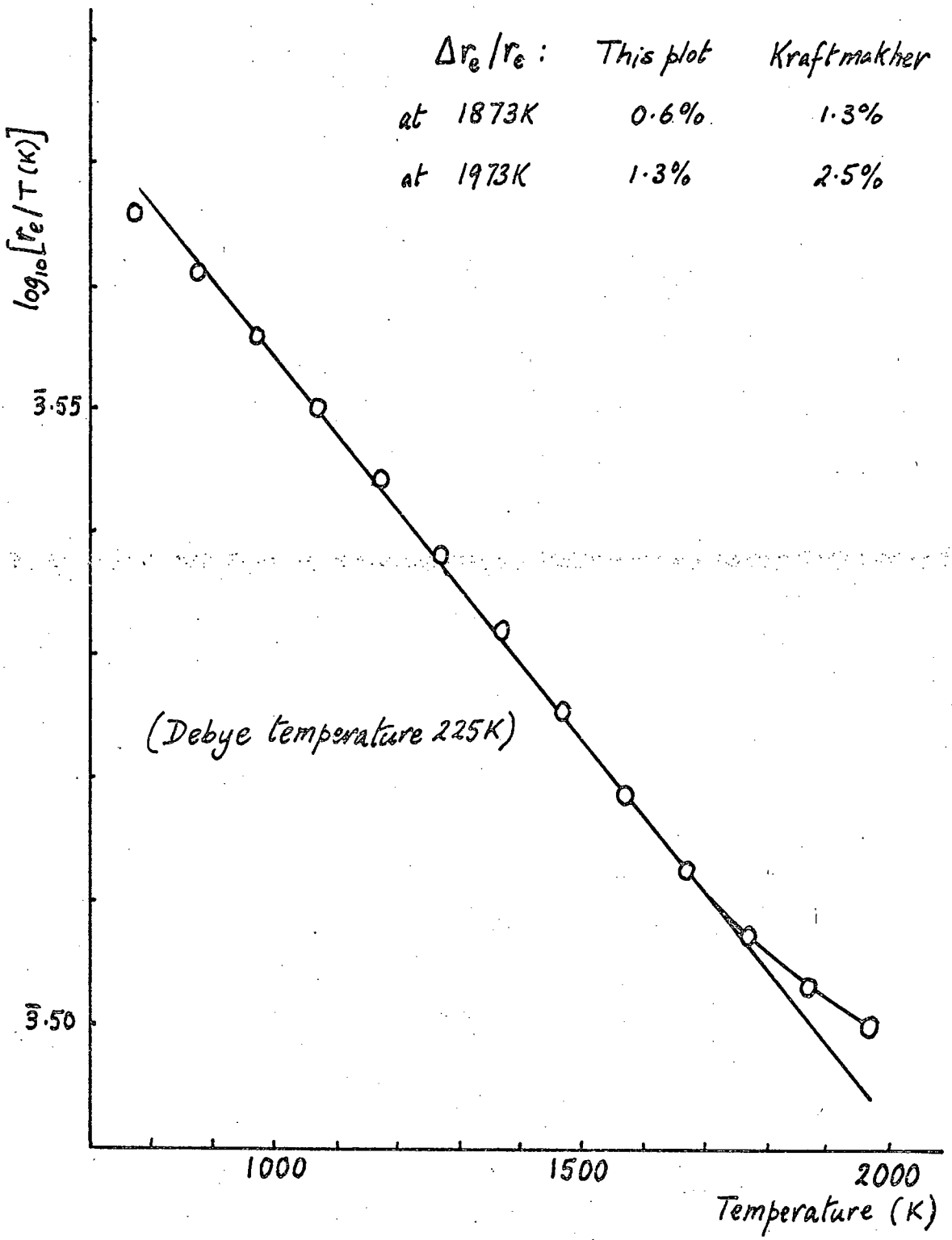

Sec.5.3.2. Fig.1 - Alternative extrapolation procedure, showing $\log(r_e/T)$ vs T for platinum

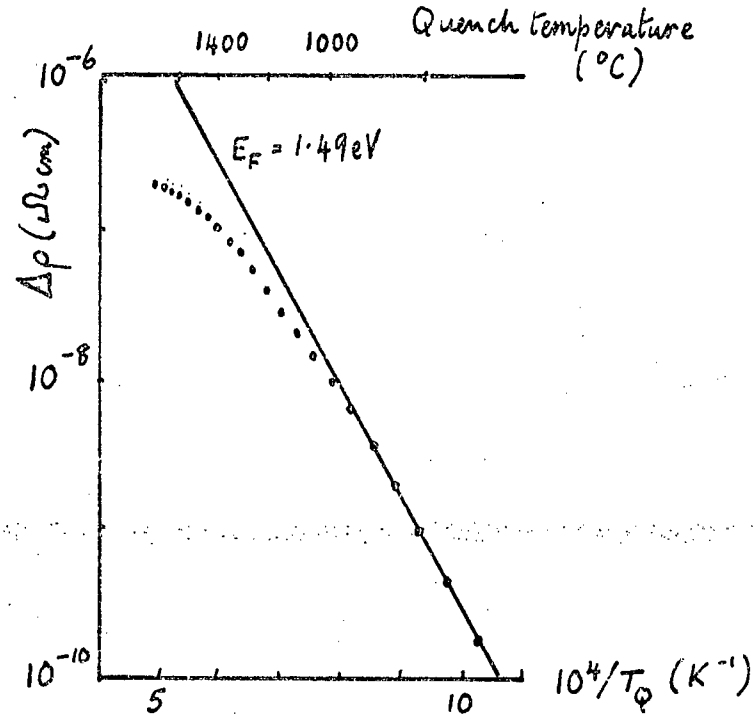

Sec.5.3.2. Fig.2 - Quenched-in resistivity for platinum (results of Jackson, 1965)

function of reciprocal quench temperature. He interprets the lowered slope at high temperatures as evidence of vacancy loss, so that only the low-temperature results should be used, as indicated by the solid line. This line gives the reasonable value of E^F of 1.49 eV, and Jackson's final result from such low-temperature quenches is 1.51 ±.04 eV. Taking this value of E^M = 1.38 ±.05 eV gives Q = 2.89 ±.07 eV good agreement with the self-diffusion values of 2.96 ±.06 eV and 2.89 ±.04 eV measured respectively by Kidson and Ross (1957) and by Cattaneo Germagnoli and Grasso (1962). However, the absolute values of the vacancy resistivity obtained using these low-temperature results are large, corresponding to a vacancy contribution to the melting-point resistivity of some 3%. This agrees well with the contribution obtained by Kraftmakher and Lanina's extrapolation method. Their value of E^F = 1.6 eV was also in adequate agreement with that of Jackson. Kraftmakher and Strelkov (1970) noted this in their review, commenting that this was "apparently the only case where agreement has been obtained between quenching and thermal equilibrium experiments". Accepting Jackson's interpretation, we obtain for the vacancy contribution to α at 1850 K a value of $\sim$ 20%, corresponding of course to Kraftmakher and Lanina's value.

However, this quantity is very sensitive to the details of the extrapolation of Jackson's low-temperature results, a range of $\sim$ 10% - 40% corresponding to Jackson's quoted experimental uncertainties on E^F; the probability that

Jackson's values are high is noted by Schumacher, Seeger and Harlin (1968) in their analysis of helium-II quenches, and quenching and self diffusion results generally, for platinum. They prefer $E^F = 1.49$ eV, with a corresponding reduction in the vacancy contribution to the resistivity.

A lowered values of resistivity is consistent with the results for "infinite" pulse time obtained by Heigl and Sizmann by the method described above (section 5.3.1). They obtain

$$C\rho_v = (6.9 \pm 0.1) \times 10^{-5} \exp\left(-(1.51 \pm 0.02)\text{eV}/kT\right) \Omega\text{m} \quad ..(5.17)$$

giving a contribution to $\alpha(0)$ of only 13% at 1850 K. It is interesting to note that this is in good agreement with the value deduced from the extrapolation shown in Fig. 1.

Both Heigl and Sizmann and Schumacher et al. consider the question of relating the resistivity to vacancy concentration via the resistance of Frenkel pairs produced in electron irradiation; the comparison is not straightforward, but leads to the values:

	ρ_v (Ωm/at.%)	S^F/k	$C(T_m)$
Schumacher ...	6×10^{-6}	1.3	0.84×10^{-3}
Heigl ...	15×10^{-6}	1.45	0.81×10^{-3}

All these appear reasonable.

In what follows, we shall use Heigl and Sizmann's values for $C\rho_v$, though this is not critical to the interpretation. The agreement between Kraftmakher and

Lanina's extrapolation and the work of Jackson is not regarded as significant.

5.3.3 The vacancy contribution to the high-temperature specific heat of platinum

Accepting the values of $E^F \sim 1.5$ eV from the quenching experiments, we may calculate the equilibrium vacancy concentration at the melting point of platinum using simply a theoretical value $S^F = k$ indicated by the studies of Schmid, Schottky and Seeger (1964) suggesting a range $0.5k - 1.2k$ for noble metals. The result is $\sim 5 \times 10^{-4}$, close to the corresponding value for gold, and contributing some 2 J kg^{-1} to the total specific heat ($\sim$ 200 J kg^{-1}). The large enhancements reported by Kraftmakher and Lanina correspond to $S^F = 4.5k$.

There seems little justification for their extrapolation procedure since c_p is not generally thought to be a linear function of temperature even in the absence of vacancy effects. An important source of non-linearity arises from thermal expansion as can be seen from the thermodynamic relation

$$c_p = c_v + \{(3\lambda)^2 V/k_T\}T, \qquad \ldots (5.18)$$

where k_T is the isothermal compressibility, λ the coefficient of linear expansion and V is the volume. We may express this alternatively by use of the Grüneisen relation

$$\lambda = \gamma c_v/3k_T V \qquad \ldots (5.19)$$

in the form

$$c_p = c_v(1 + 3\lambda\gamma T), \qquad \ldots (5.20)$$

which is just the Grüneisen-Mie equation of section 5.1.2 omitting the electronic specific heat. Now, even if c_v is constant, λ is not, but increases approximately linearly with T. Values of k_T for high temperature are not available, but a commonly-used approximation (e.g. Loewenthal, 1962) takes V/k_T as temperature-independent; c_p then increases according to a T^3 term. Kirby and Rothrock (1968) give values for the thermal expansion obtained by an optical comparison method, and the values of λ derived from them (see also section 5.3.4) may be used to extrapolate low-temperature specific heat measurements into the vacancy range: we take the values for specific heat in the 300 K - 1000 K range (Kendall, Orr and Hultgren, 1962) and, using a linear extrapolation for c_v, calculate curve 4 (Fig. 1), assuming that V/k_T remains at its room-temperature value (Smithells, 1962). Curves 1 and 2 show the results of this work and of Kraftmakher and Lanina respectively; it is clear that the variation of λ can account for a substantial part of the observed curvature of c_p vs. T plots.

Unfortunately, more sophisticated analyses of the anharmonic contributions to specific heat, while not excluding the possibility of non-linear behaviour sufficient to account for most of the 'enhancement', are not as yet capable of giving reliable quantitative

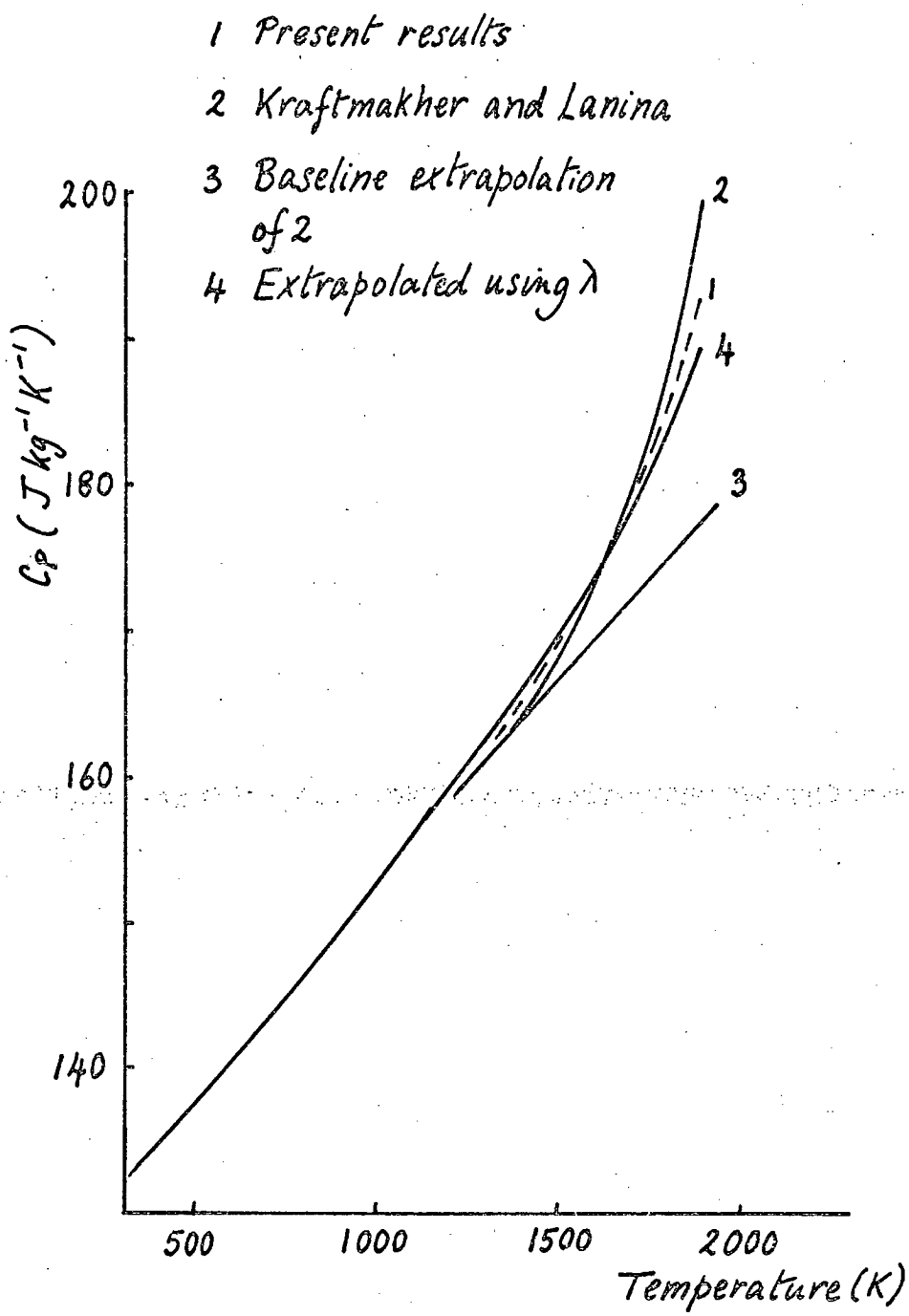

Sec.5.3.3. Fig.1 - Comparison of specific heat results with those extrapolated using the thermal expansion coefficient

estimates for such effects. A simple model of atoms oscillating in an anharmonic potential well is of course adequate to show a linear variation with T. Earlier theoretical analyses (e.g. Keller and Wallace (1962)) appear to stop at a term linear in T. More recently, Stedman, Almquist and Nilsson (1967) used the measured temperature-shifts of phonon frequencies in aluminium and lead to calculate the linear term, but high temperatures were not covered ($\nmid$ 500 K for Al) and again higher-order terms were excluded. Leadbetter (1968) found fair agreement between these results and those of simple models (see Liebfried and Ludwig, 1961) of close-packed crystals giving a negative anharmonic contribution to c_v proportional to T; he also discusses the separation of measured thermodynamic quantities into quasi-harmonic and explicitly anharmonic contributions, and finds good agreement with the other approaches. For lead, he finds explicit higher-order anharmonic contributions, as well as a contribution due to vacancies. A theory of lattice instability leading to large positive anharmonic contributions near the melting point has recently been put forward by Ida (1970); again, quantitative comparison is difficult.

In this situation, comparison of the modulation method results with those of conventional quasi-static calorimetry would be especially interesting. The results c_k of Kraftmakher and Lanina, according to the long vacancy lifetime hypothesis, should lie above these values by an amount corresponding to the difference between $\alpha(0)$ and $\alpha(\infty)$; the present results, corresponding to $c_p(\infty)$ should

nearly agree, assuming in both cases that the direct $c_p(0) - c_p(\infty)$ vacancy contribution is small. Unfortunately this comparison is difficult for platinum. Touloukian (1970) tabulates the results of various workers, showing values up to 2043 K (Kendall, Orr and Hultgren, 1962); in fact these values represent an extrapolation of measurements below 1435 K, and are of no immediate interest. The only other results for high temperatures are those* of Jaeger and Rosenbohm (1939) by the drop method, in which, as Oriani (1955) has observed, serious systematic errors arose at high temperatures because the heat loss during the drop was not taken properly into account. In fact, at the maximum temperature given for these results (1873 K) c_k exceeds the value obtained on Jaeger and Rosenbohm's fitted curve by some 8%, and even our value of c_p exceeds it by 5%; Kraftmakher and Lanina (1965) did not regard even the larger figure as significant. An additional complication in the comparison is that the values both of c_p and c_k involve the suspect $\alpha(0)$ values directly, and their precision is therefore at best $\sim \pm 3\%$, even assuming the correctness of the procedure for obtaining $\alpha(0)$ (section 4.3.2). We are therefore unable to regard the results of this comparison as meaningful.

The conclusion of this section is thus somewhat negative: there is no reason to deny the possibility that the observed enhancements are due wholly or partly to anharmonic contributions.

* See Fig.1 of section 4.5.6, page 159

As has been mentioned, the electronic contribution to the specific heat is, for our purposes, experimentally indistinguishable from anharmonic effects since both have negligible relaxation times. The specific heat of the electrons in a metal is usually regarded as contributing a term proportional to T to the total specific heat at temperatures below the Fermi temperature T_F.

To first order in T (Kittel 1966) we then have $C_{el} = (\pi^2/3)Z_F k^2 T$, where Z_F is the density of states in energy at the Fermi level. For metals in which the free-electron approximation is a reasonable one, this leads to small effects $\sim$ 1% of the total specific heat at the melting point. For metals such as platinum however the band structure is not such that this is a good approximation, as explained in the previous section; the density of states in the neighbourhood of the Fermi level is high, and the electronic contribution to the specific heat for such metals is correspondingly increased (Mott and Jones 1936) by perhaps an order of magnitude.

This linear contribution ($\propto T$) of course does not result in an 'enhancement' of the kind that Kraftmakher observes, since he uses a linear baseline extrapolation. The interest in the electronic specific heat lies in the possibility that there may be strong higher-order effects, as suggested by Friedel in a comment on Hoch's paper (1970), in situations where the density of states curve is a rapidly-varying function of temperature.

Loewenthal (1962) compared values of c_v (calculated from c_p measurements by allowing for thermal expansion) with those calculated on the basis of measurements of electronic specific heat at liquid helium temperatures. For molybdenum and tungsten, a linear rise of c_v with temperature was obtained in good agreement with the low-temperature measurements. The maximum temperatures (2100 K for Mo, 2400 K for W) were such that considerable curvature in the c_p vs. T curves was apparent.

This suggests that even in these metals higher-order terms in the electronic specific heat are not the dominant cause of specific heat enhancement; in any case, it would be surprising if the higher-order terms in platinum contributed as much as say 10% of the total specific heat when the total electronic contribution is itself only of this order.

We shall, therefore, assume that the dominant cause of any enhancement <u>not</u> due to vacancy effects is to be found in the anharmonic lattice behaviour, while not excluding a smaller electronic contribution. The relative importance of these effects does not in any case affect our earlier conclusion, that non-vacancy effects appear fully adequate to explain observed enhancements.

5.3.4 The vacancy contribution to the coefficient of linear thermal expansion for platinum

The remaining quantity of interest is λ, the coefficient of linear thermal expansion. We expect this to be influenced by vacancy creation; in fact, assuming no mechanical relaxation round a vacancy, the vacancy contribution to λ is just

$$\Delta\lambda_v = d(C/3)/dT = E_F C_{eq}/3kT^2, \qquad \ldots (5.21)$$

so that a concentration of 10^{-3} near the melting point gives $\Delta\lambda \sim 1.5 \times 10^{-6}\ K^{-1}$, compared with measured values of $\lambda \sim 15 \times 10^{-6}\ K^{-1}$.

The quantity is of particular interest because Kraftmakher and Cheremisina (1965) have measured values of λ directly using a modulation method (section 2.4.3) in which the length changes of the specimen were registered by shining a light beam past the end of the specimen on to a photodetector; the length changes thus modulated the light falling on the photodetector at the modulation frequency of 20 Hz. The results for platinum (Kraftmakher, 1967[a]) are shown in Fig. 1, together with the results of Kirby and Rothrock (1968) by a quasi-static method. Also shown are the X-ray parameter results of Edwards, Speiser and Johnston (1951). From the deviation of his results from an extrapolated line, Kraftmakher obtained a formation energy for vacancies of 1.7 eV and a melting-point concentration of 0.8% on the assumption that the deviation was due to vacancies whose volume was half the

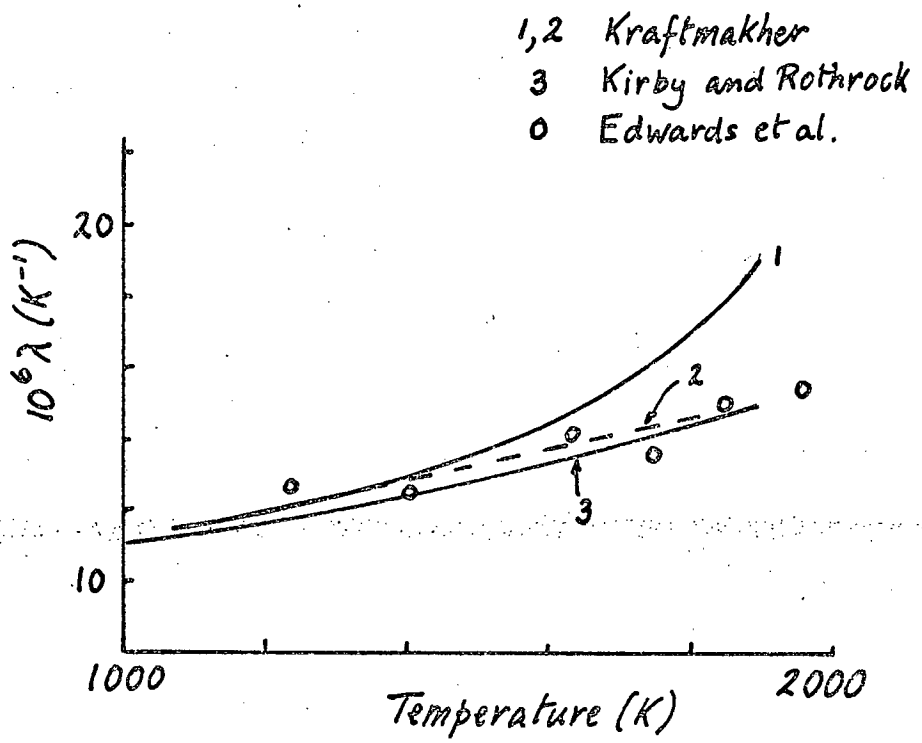

Sec.5.3.4. Fig.1 - Thermal expansion coefficient of platinum

atomic volume. This was to be compared with values of 1.6 eV and 1% from the specific heat work (Kraftmakher and Lanina, 1965).

This interpretation was criticised by Van den Sype (1970)[b] on the same basis as his criticism of the specific heat results (section 5.1.3), in that, as the temperature modulation was calculated via the specific heat results, it was determined via the resistance modulation, and should have been corrected for the difference between $\alpha(0)$ and $\alpha(\infty)$; this assumed that the vacancy lifetime was long, > 10 ms. He accounted for the observed enhancement of λ by taking at 1900 K the values $\rho_v = 6 \times 10^{-6}$ Ωm/atom fraction, $E^F \sim 1.35$ eV, $C_{eq} = 0.3\%$, and by taking the vacancy volume to be half the atomic volume.

At 1850 K, Kraftmakher's value of $\Delta\lambda$ is about 13%, which would require a value of $|\alpha(0) - \alpha(\infty)|/\alpha(0)$ of at least this magnitude if Van den Sype's explanation is to be accepted. Such values would 'correct' the c_k values to values of $c_p(\infty)$ which showed a decreasing slope with increase of temperature, an unlikely behaviour. It appears therefore as if the correction proposed by Van den Sype is too drastic; in fact, since the enhancement of the specific heat at 1850 K found by Kraftmakher and Lanina is only 6%, no one correction factor will produce straight lines for both $c_p(\infty)$ and $\lambda(\infty)$ when plotted as a function of temperature. The correction factor obtained by taking the difference between the present results for c_p and the results c_k is as we have seen $\sim 2\frac{1}{2}\%$, though a value as high as $\sim 5\%$ would be

possible. The remaining enhancement of λ is thus $\sim$ 10%; this could be a spurious effect arising from the procedure (section 4.3.2) adopted by Kraftmakher and Lanina for determining $\alpha(0)$, on which the values of λ directly depend.

Alternatively, we may try the hypothesis that Kraftmakher is correct in ascribing the effects to vacancies following the modulation: here the comparison with the quasi-static values of Kirby and Rothrock is surely decisive evidence against it, because the discrepancy is very large at high temperatures. There is also the suggestion of a significant discrepancy even below 1500 K, which could arise through errors in $\alpha(0)$ or by other systematic error.

Accepting, though, the increase in λ as genuine, we have to explain a $\sim$ 10% enhancement; it will be argued in the next section that a possible explanation of this is that the correction factor to be applied in the thermal expansion experiment is not necessarily the same as in the resistivity-bridge experiment since Kraftmakher's samples were not identical in these experiments; a comparatively small increase in τ_v would account for the larger correction factors needed in the latter experiment.

5.4 The interpretation of specific heat enhancements in metals

5.4.1 Platinum (T_m = 2042 K)

In the preceding sections, we have examined the evidence relating to platinum; previously, we concluded that the observed specific heat enhancements in the

present experiments are predominantly due to anharmonic or electronic effects. We note that the evidence is consistent with this. Additionally, the hypothesis of such long relaxation times that even a modulation frequency of 30 Hz is infinite appears to be excluded because it would lead to a difference of $\sim$ 13% between the measured values of $c_p(\infty)$ and c_k.

A small discrepancy is to be expected if we take the values of τ_v corresponding to the results of Heigl and Sizmann together with their values of $\rho_v C$. Using the value for the specimen annealed at high temperature, the discrepancy (arising from the effect of vacancy relaxation on α) is readily calculated using the relaxation curves of section 2.3.3 to obtain values of f, taking 30 Hz as the modulation frequency for the c_k measurements:

T(K)	τ_v(ms)	x	$(1-f)$	$\left(\alpha(0)-\alpha(\infty)\right)/\alpha(0)$	Correction to c_k (%)
1850	1.6	1.3	0.06	0.13	1.0
1750	2.7	1.7	0.14	0.08	1.1
1650	4.8	2.3	0.35	0.045	1.6
1550	7.9	3.0	0.50	0.028	1.4
1450	13	3.8	0.65	0.017	1.1
<1400					<1.0

Although these corrections are too small to explain the discrepancy, we can explain it if we make the not implausible assumption that the vacancy lifetime is a factor ~ 2.5 times longer, corresponding to a sub-grain size $(2.5)^{\frac{1}{2}}$ times larger; such a coarsening could be due to the high temperatures used in the Kraftmakher-Lanina experiment. We then obtain similarly:

T(K)	τ_v(ms)	x	$(1-f)$	$\left(\alpha(0)-\alpha(\infty)\right)/\alpha(0)$	Correction to c_k (%)
1850	4.0	2.1	0.25	0.13	3.3
1750	6.8	2.7	0.43	0.08	3.4
1650	12	3.7	0.60	0.045	2.7
1550	20	4.8	0.70	0.028	2.0
1450	32	6.0	0.76	0.017	1.3

This correction to c_k would thus account for some 2% of the discrepancy between the high temperature and low temperature comparisons of the results. Obviously τ_v cannot be significantly longer. Alternatively, we may ascribe the discrepancy to experimental errors and take the vacancy lifetime as somewhat shorter, though it is difficult to believe that it will be shorter than that calculated from the results of Heigl and Sizmann. In any event therefore, we have a good estimate of τ_v in platinum in a modulation experiment, equivalent to ~ 1 ms at the melting point.

Given this value of τ_v, we can assign an upper limit to the vacancy concentration based upon the null result of the frequency-dependence experiments (section 4.5.4): at 1850 K, the relaxation peak is at $\sim$ 250 Hz, and would certainly have been detectable given a vacancy concentration in excess of $\sim 10^{-3}$; $C(T_m)$ is therefore $< \sim 4 \times 10^{-3}$, in agreement with the estimates made above.

The thermal expansion coefficient experiment of Kraftmakher and Chereminina can now be explained if we postulate that in this experiment τ_v was somewhat longer, so that a larger correction to α corresponding to almost the full value of $\alpha(0) - \alpha(\infty)$ is required. Even for this, τ_v at 1850 K must exceed only $\sim$ 10 ms. It is stressed, however, that such an explanation is speculative, and that confirmatory experiments in which c_p and λ are measured on the same specimen are needed.

Our conclusion on the vacancy generation problem in platinum is that, even in a modulation experiment, the generation mechanism proposed by Heigl and Sizmann appears to account for the relaxation behaviour; the low driving forces for climb encountered in the experiment do not appear to preclude this mechanism.

In what follows, we shall examine results for certain other metals of interest, with a view to discovering how widely an interpretation similar to the above may be applied.

5.4.2 Tungsten (T_m = 3653 K)

Tungsten is of interest as the metal first investigated by Kraftmakher (1962) using the resistance-bridge modulation technique; large vacancy concentrations were reported (3.4% at T_m). Van den Sype (1970) criticized these results not only because relaxation effects were ignored (section 5.1.3) but also because they differed from the drop-calorimeter measurements of Leibowitz et al. (1969) which showed no enhancement. Kraftmakher (1971), replying to these criticisms, observed that the resistance rise in tungsten is quite small, so that, to explain the observed 50% enhancements of c_p, α would have to show a marked change in behaviour and begin to decrease with temperature. He also examined the results of the drop-method cited, and claimed that the large disagreement was a result of the use of an approximating function inadequate for the high-temperature range. In fact, though the uncertainties in the drop measurements are such that Kraftmakher's results can almost be reconciled with them, a better fit is obtained if the enhancements are somewhat reduced corresponding to a small correction for vacancy relaxation. Against this, Kraftmakher (1966) has also measured the specific heat using the light emitted from the specimen as a method of determining the temperature modulation, much as in the present experiments, and reports agreement between the two modulation methods, though as comparative results are not given it is difficult to assess the significance of this. From quenching experiments (Schultz 1964), however, it is known that the vacancy contribution

to the resistivity of tungsten is small ($\sim 10^{-10}$ Ωm at 3300 K when the resistivity is $\sim 10^{-6}$ Ωm) which makes the contribution to α negligible (< 1%).

These results for tungsten tend to confirm our general model: the enhancements cannot be explained on Van den Sype's hypothesis. Also, the low values of vacancy resistivity by quenching are difficult to reconcile with large vacancy concentrations, and suggest anharmonic or electronic effects as responsible for the enhancements.

5.4.3 Molybdenum (T_m = 2873 K)

Results for c_p have been compared by Hoch (1970) in his review, to show that the results obtained by the modulation method agreed with those obtained otherwise. In particular, he compares results of a drop method (Hoch 1965), a rapid pulse-heating method (Taylor and Finch, 1964), a quasi-static slow pulse method (Rasor and McClelland, 1960) the resistance-modulation method of Kraftmakher (1964) and the sample-brightness modulation method (Kirillin et al., 1968). At 2000 K, the agreement is within 5%, and within 10% at 2800 K. Again, vacancy resistance effects appear to be relatively unimportant, the accuracy of the comparison being such that any small effects would not be revealed. All measurements show however a specific heat enhancement of $\sim$ 25% - 35% at the higher temperature. Taylor and Finch varied heating rates between 10^3 and 6×10^4 K s^{-1} without finding any change in the results. This last rate is so high that it compares with rapid quench rates, and an effect would be expected if vacancies were causing the enhancements that we

attribute to anharmonic effects.

5.4.4 Copper (T_m = 1356 K)

Copper is important here because very low modulation frequencies have been used (Kraftmakher 1967)[b]. In these experiments, a thermocouple was employed to determine the temperature modulation, which was of amplitude < 5 K and period 13 s. Large specific heat enhancements were observed under circumstances where Van den Sype's objection did not apply. The measured values of specific heat agreed closely with those obtained by Brooks et al. (1968) using an adiabatic calorimeter. The enhancements, interpreted as vacancy effects, corresponded to a concentration of 0.5% at the melting point. As mentioned in section 5.1.1, this is 25 times that obtained by the X-ray parameter/length measurement. Their comments noted there, that the latter measurements are unreliable because of vacancy formation without a corresponding increase in volume, are difficult to uphold. The elastic relaxation around point defects in a crystal affects the macroscopic volume and the volume of the unit cell equally, provided the defects are distributed statistically; for a cubic metal (such as copper or gold) complications due to departures from this would not arise unless some preferred orientation existed because of sample preparation. It does not appear likely either that by creation of vacancies at internal sources of low packing density the displaced atoms could all be accommodated with an expansion per atom of only $\sim$ 1/25 atomic volume. This experiment is therefore a powerful argument for anharmonic effects as an explanation of enhancements.

5.4.5 Gold (T_m = 1336 K)

For gold, Kraftmakher's modulation experiments (1966)[a] used a potentiometric compensation circuit in place of the resistance bridge; otherwise the technique was unaltered, and the results obtained are still subject to the possible errors resulting from neglect of vacancy relaxation. In section 2.3.3 we estimated $\left(\alpha(0) - \alpha(\infty)\right)/\alpha(0)$ to be $\sim$ 10% at T_m on the basis of quenching experiments, and this would account for most of the observed enhancement ($\sim$ 12%), suggesting that the behaviour of c_p with T should be fairly linear. Unfortunately, suitable comparison data appear to be lacking; however, one might expect the lower melting point metals to show less drastic anharmonic effects than those such as tungsten. The values for vacancy concentration derived by Kraftmakher were six times higher than the X-ray/length parameter values, and the remarks of the previous section apply here too.

5.4.6 Aluminium (T_m = 933 K)

Aluminium is an interesting metal because of the rather large vacancy effects found in it. The X-ray parameter/length measurements (e.g. Simmons and Balluffi, 1960)[b] give melting-point vacancy concentrations of $\sim 9 \times 10^{-4}$, with activation energies $\sim$ 0.7 eV. This leads to a calculated contribution to the specific heat of $\sim$ 30 J kg^{-1} K^{-1}, the total being $\sim$ 1200 J kg^{-1} K^{-1} so that there is a genuine $\sim$ 3% vacancy effect.

The definitive experiments are those of Bokshtein et al. (1968) already mentioned in connection with vacancy

lifetime (section 5.3.1). They observed a vacancy contribution to c_p as measured by a slow pulse method, and were able to identify it unequivocally by the fact that no such contribution was effective for pulses shorter than about 1 s. Fig. 1 shows their results. The difference in specific heats corresponds to some 5% at the melting point, somewhat larger than our estimate. Also of interest is the form of the $c_p(\infty)$ curve, which shows no detectable anharmonic effect.

This appears to be in contradiction to the interpretation of Brooks and Bingham (1968) who measured c_p by dynamic adiabatic calorimetry; they used an extrapolation procedure to estimate a 10% excess specific heat at the melting point, too large to be ascribed to vacancies alone. They attributed most of this to anharmonic effects. However, the precision of Bokshtein's results is not such as to exclude anharmonic effects entirely.

Guarini and Schiavini (1966) used a high precision microcalorimeter which was capable of detecting thermal reactions in the specimen (e.g. vacancy annealing) by the departure of the cooling-curve from exponential form. They obtained a melting-point concentration of $(6 \pm 0.8) \times 10^{-4}$, with a formation energy of 0.70 ± 0.03 eV.

The experiments of Bokshtein and of Guarini and Schiavini show definitely that vacancy contributions to the specific heat are detectable, and indicate that for a low-melting point material they may be large enough to compete seriously with anharmonic effects. In view of this,

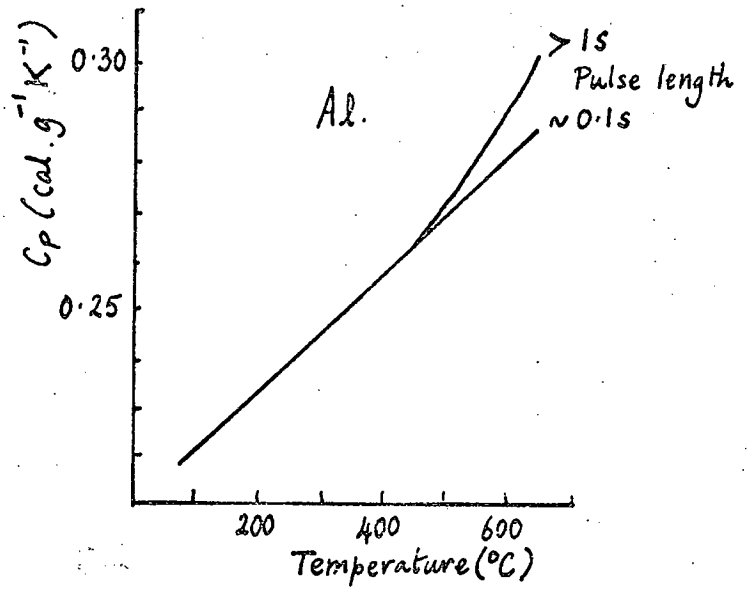

Sec.5.4.6. Fig.1 - Results of Bokshtein et al. for aluminium

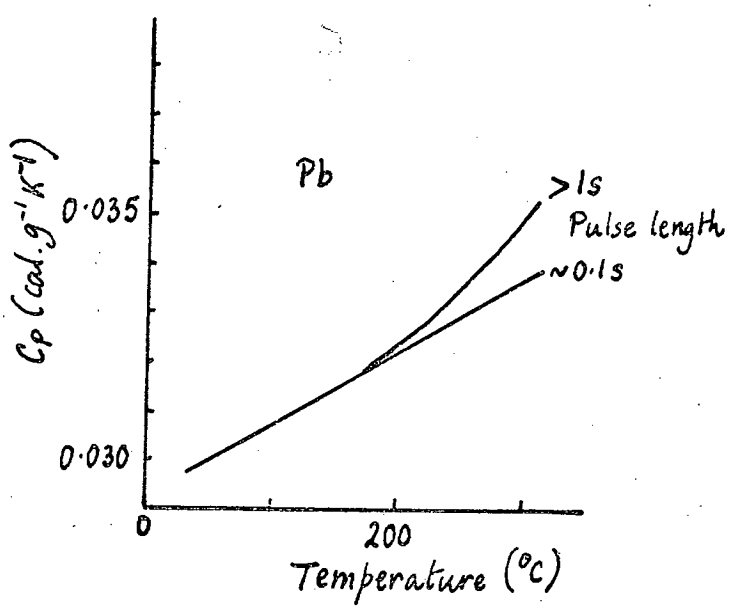

Sec.5.4.7. Fig.1 - Results of Bokshtein et al. for lead

modulation experiments in aluminium would be of particular interest. No such experiment seems to have been performed. In Pochapsky's early pulse work (1953) enhancements were observed, though the high value of E^F = 1.17 eV and the disagreement of his α values with those of Simmons and Balluffi (1960) do not lend confidence. The α values in any case would require correction for vacancy relaxation effects.

5.4.7 Lead (T_m = 600 K)

The results of Bokshtein et al. (1968) shown in Fig. 1 allow a similar conclusion to the one for aluminium. Anharmonic effects appear to be small compared with the vacancy effect.

5.5 Conclusion

From the preceding discussion we may conclude as follows:-

1. In high melting-point metals, the observed enhancements of the specific heat are largely caused by effects other than vacancy effects; they appear to be due predominantly to anharmonic behaviour of the lattice, but a possible electronic contribution is not excluded.

2. In low melting-point metals, it appears that the vacancy contribution to the specific heat is more important, and may be a significant source of enhancement.

3. There is no reason to suppose that equilibrium vacancy concentrations are not correctly given by the

results of X-ray parameter/length comparison experiments. The large values given by some extrapolation procedures are erroneous.

4. In specific heat experiments generally, long vacancy lifetimes may be encountered; the effects of these upon the determination should be taken into account unless the experiment is quasi-static. Such effects however do not account for the whole of the observed enhancement of specific heat.

5. Though the general behaviour of the thermal expansion coefficient in a modulation experiment appears consistent with these conclusions, detailed confirmation of this is still required.

These conclusions suggest several experiments:

1. Comparison of the resistance-modulation and sample-brightness modulation methods directly on the same specimen for a material known from quenching experiments to have a large vacancy contribution to the resistivity. This would give $\left(\alpha(0) - \alpha(\infty)\right)/\alpha(0)$; a comparison with the quenching results then gives information on the behaviour of ρ_v with temperature.

2. Comparison of very low frequency and high frequency modulation methods on a material (e.g. Al) with a large vacancy contribution to the specific heat.

3. A similar investigation of the thermal expansion coefficient, and further investigation of this coefficient generally, using modulation methods.

It is ironic to reflect that although proposed ten years ago as a method of studying vacancies near equilibrium, the modulation method has not yet been used successfully for a study of the detailed kinetics of the processes of vacancy creation and destruction in metals. In view of its undoubted advantages over pulse-heating methods in terms of accuracy and convenience, it is to be hoped that this study will soon be achieved.

Appendix A

Note on the exact vacancy kinetics for a cylindrical surface source

The diffusion equation becomes, following Van den Sype (1965)

$$\frac{\partial^2 c}{\partial r^2} + \frac{1}{r}\frac{\partial c}{\partial r} = \frac{\partial c}{\partial t} \qquad \ldots \text{A1}$$

where the units are chosen to make $D_v = 1$, and c represents the vacancy concentration as a fraction of the equilibrium value. The boundary condition is, at $r = a$,

$$c(a,t) = \sin \omega t. \qquad \ldots \text{A2}$$

If $F(r,p)$ is the Laplace transform of $c(r,t)$, equation A1 becomes

$$\frac{d^2F}{dr^2} + \frac{1}{r}\frac{dF}{dr} - pF = 0 \qquad \ldots \text{A3}$$

and the boundary condition is

$$F(a,p) = \omega/(p^2 + \omega^2). \qquad \ldots \text{A4}$$

The solution is

$$F(r,p) = \frac{\omega}{p^2 + \omega^2}\frac{J_o(jp^{\frac{1}{2}}r)}{J_o(jp^{\frac{1}{2}}a)} \qquad \ldots \text{A5}$$

which may be inverted and averaged over r to give, in the limit as $t \to \infty$, the steady-state response

$$\langle c(r,t) \rangle_r = X \sin \omega t + Y \cos \omega t$$

where

$$X = \frac{1}{\alpha^+}\frac{J_1(\alpha^+)}{J_0(\alpha^+)} + \frac{1}{\alpha^-}\frac{J_1(\alpha^-)}{J_0(\alpha^+)}$$

and

$$Y = \frac{-j}{\alpha^+}\frac{J_1(\alpha^+)}{J_0(\alpha^+)} + \frac{j}{\alpha^-}\frac{J_1(\alpha^-)}{J_0(\alpha^+)}, \qquad \ldots \text{A6}$$

the symbols $\alpha^{\pm}$ denoting $j\alpha(\pm j\omega)^{\frac{1}{2}}$.

For computation, it is convenient to use the polar representations M, θ of the Kelvin functions and write

$$X = \frac{-\sqrt{2}\, M_1(x)}{x\, M_0(x)} (\cos\beta - \sin\beta)$$

$$Y = \frac{-\sqrt{2}\, M_1(x)}{x\, M_0(x)} (\cos\beta + \sin\beta) \qquad \ldots \text{A7}$$

where $\beta = \theta_1(x) - \theta_0(x)$ and x is, in ordinary units, $\alpha(\omega/D_v)^{\frac{1}{2}}$. Van den Sype gives a similar form for Y but does not deal with X, the quantity plotted as f in Fig.1 of section 2.3.3. Y is just the $\phi_v/\phi_{v\ max}$ of Fig.2 of that section.

The values of M_0, θ_0 and M_1, θ_1 required for the computation were taken from the Royal Society Mathematical Tables Vol.10, pages 36-43 (Young and Kirk, 1964).

Journal of Scientific Instruments (Journal of Physics E) 1968 Series 2 Volume 1

A technique for measuring small, fast changes in resistance

D Anderson,† J M Anderson‡ and A H Seville§
Solid State Physics Laboratory, Department of Natural Philosophy, University of Edinburgh

MS *received 21 August 1967, in revised form 25 October 1967*

Abstract A carrier-frequency bridge method is described whereby rapid changes in electrical resistance can be studied with a time resolution of the order of $\frac{1}{3}$ms and typical sensitivity of the order of 10 nΩ in a specimen of resistance of the order of 1 mΩ.

1 Introduction

The study of small time-varying changes in electrical resistance is generally difficult unless the variation is sufficiently slow to permit the use of quasi-static techniques such as are possible with the potentiometer. This paper describes a means of extending this study to changes occurring in times of a few milliseconds.

Particular applications exist in the investigation of defects in metals. Although a wide range of thermally activated defect processes can be examined by using resistance measuring instruments with a slow response, the temperature must be kept low so that the process is sufficiently slow. The present method allows some extension to higher temperatures, and, perhaps more important, may enable measurements to be made when the processes cannot be slowed down to allow a quasi-static measurement.

One such process occurs in the pastic deformation of zinc, where deformation 'jumps' may be observed, each associated with a sharp change in electrical resistance; it was for the study of this that the present apparatus was designed. The resistance changes are complete in times varying from about 1 ms at 100°C to about 100 ms at 0°C and, since the process can not be further slowed by cooling below 0°C due to the onset of a quite different deformation mechanism, the apparatus was designed to cover this time scale. For this work, long term stability and absolute calibration were not required, and this allowed some simplifications in the design.

The results of the work on zinc have been published elsewhere (Anderson and Brown 1965). In a specimen of resistance of the order of 1 mΩ, changes as small as the order of 10 nΩ could be detected, with a time resolution of the order of $\frac{1}{3}$ms. The apparatus is now being used to investigate resistance changes during yielding in iron and in copper alloys, and to study the equilibration of vacancy concentration in noble metals near the melting point. It is proposed to use it to look for rapidly decaying components of radiation damage in metal specimens produced, for example, by a pulsed beam of protons at energies of a few mega electron volts.

† Now at the Department of Electrical Engineering, Heriot Watt University, Edinburgh.
‡ Now at the Carnegie Laboratory of Physics, University of Dundee.
§ Now at the Department of Physics, The City University, London.

2 Apparatus

The resistance measuring circuit is shown schematically in figure 1. The specimen and a dummy of the same size and

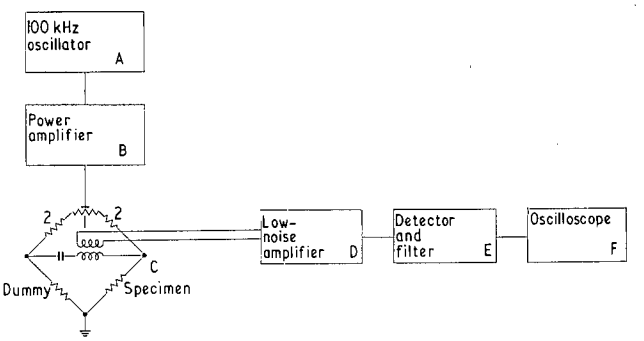

Figure 1 Resistance measuring circuit

material are made adjacent arms of a Wheatstone bridge C fed by a 100 kHz oscillator A and power amplifier B giving a sinusoidal waveform and capable of passing a current of several amps at 100 kHz through the specimen. Since changes in specimen resistance are small compared with the resistance of the upper ratio-arms of the bridge, the current through the specimen is essentially constant and the output from the bridge is an out-of-balance signal at 100 kHz whose amplitude depends linearly on the resistance of the specimen. Changes in specimen resistance thus appear as amplitude modulation of this signal. The signal is fed via a step-up transformer to the low-noise amplifier D, following which the carrier frequency is removed by the detector E leaving only the modulating signal to be displayed on the oscilloscope F.

A carrier-frequency system is preferred to a d.c. system largely because it enables use of a step-up transformer to link the bridge to the amplifier without the introduction of excessive distortion of the signal. Also, design of the amplifier is somewhat simplified. Skin effects have been avoided for the 2 mm diameter specimen used by the choice of carrier frequency. These effects could be put to advantage if it were desired to investigate changes occurring near the surface of a specimen.

2.1 *Oscillator and power amplifier*

The 100 kHz oscillator uses a crystal-controlled multi-

vibrator and is coupled to the power amplifier by a tuned transformer, thus freeing the waveform of harmonics which would appear at the bridge output and might overload the low-noise amplifier. Power from the push–pull output stage is adjustable up to 25 w and is fed to the bridge through a second tuned transformer.

2.2 *Bridge circuit*

Several designs of bridge circuit have been used, all based on the Wheatstone principle; for the work on zinc, the bridge was as in figure 1. If the relationship between specimen resistance and output voltage magnitude is to be approximately linear, the resistive component of that voltage must be several times larger than any reactive component due to unbalanced stray capacitance and inductance. A small constant reactive component can be tolerated, since the bridge can be unbalanced slightly to give a large enough resistive component. A limit is set by the onset of saturation effects in the low-noise amplifier when the bridge voltage exceeds about 10 mv. For the present study, a sufficiently small reactive component ($<0 \cdot 1$mv) was obtained simply by keeping to a symmetrical physical layout; the changes in this component were negligible compared with the changes in the resistive component, so that it could be taken as constant. If accurate absolute measurements were required, a more sophisticated bridge, with control of reactive unbalance, would be needed.

2.3 *The low-noise amplifier*

The circuit is shown in figure 2. The first stage consists of two low-noise, low-distortion triode valves used in a cascode circuit to minimize the effect of anode-grid capacitances. Noise is further reduced by restricting the bandwidth, and a pass-band of $\pm 1 \cdot 5$ kHz about the carrier frequency of 100 kHz was selected since the expected time scale of the transients was a few milliseconds. The bandwidth could be changed, of course, to suit other applications. Shaping of the passband is carried out according to the design procedure of Belrose (1956) and the measured response curve is shown in figure 3.

2.4 *The detector*

The detector circuit is shown in figure 4. The cut-off voltage can be adjusted by varying the voltage on the grid of the third valve. The filter allows through only the modulation signals up to 3 kHz.

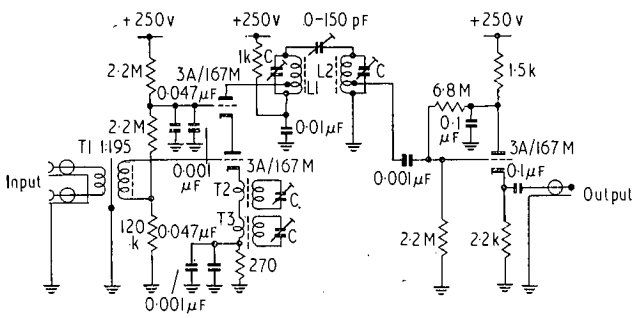

Figure 2 Low-noise amplifier
Approximate frequencies (kHz) : T_2C 103; T_3C97; L_1C 101·5; L_2C 98·5

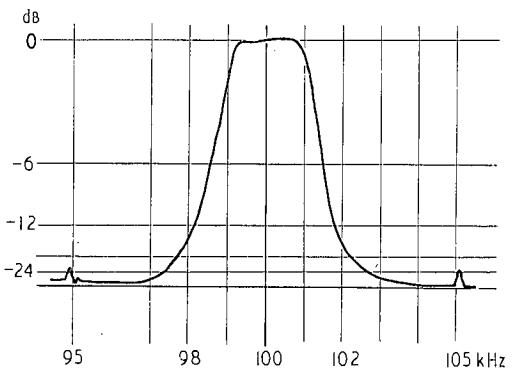

Figure 3 Sweep-frequency oscillator trace of low-noise amplifier pass-band (the peaks at 95 kHz and 105 kHz are frequency markers)

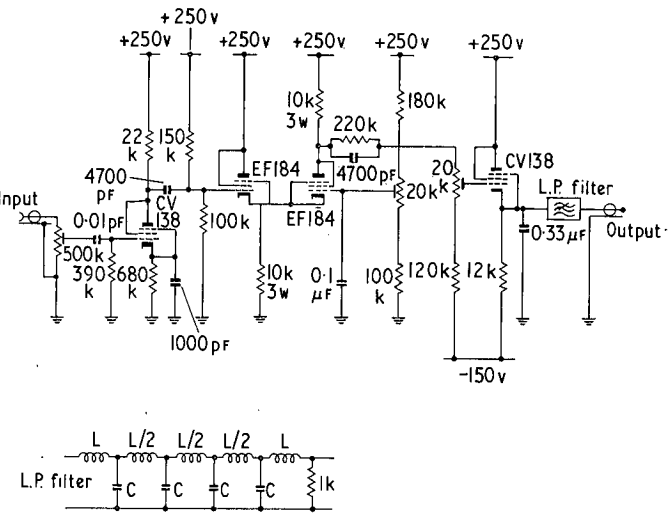

Figure 4 Demodulator and low-pass filter

3 Instrument performance

The amplifier and detector systems was tested by using pulses of known decay time to modulate a carrier waveform which was then amplified and passed through the detector. The decay time of the test pulses is shown plotted against that of the outgoing pulses in figure 5, showing that changes occurring in times down to about $\frac{1}{3}$ ms were followed by the system. The smallest resistance changes which could be resolved in a specimen of resistance of the order of 1 mΩ were of the order of 10 nΩ, this limit being set by the amplifier noise, which was equivalent to approximately 30 nv at the input, measured with the input short-circuited.

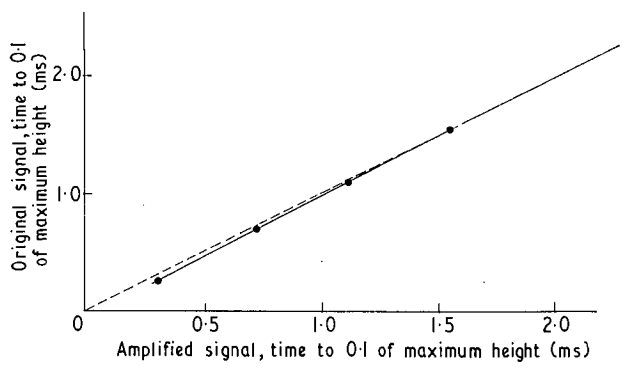

Figure 5 Response of amplifier and detector system to test pulses

Acknowledgments

We gratefully acknowledge the generous financial support received from the Dounreay Experimental Reactor Establishment of the United Kingdom Atomic Energy Authority.

References

Anderson J M and Brown A F 1965 *Phys. Stat. Sol.* **12** 309–20

Belrose J S 1956 *Wireless World* **62** 435–8

Appendix B

Published work:

"A technique for measuring small, fast changes in resistance" by D. Anderson, J. M. Anderson and A. H. Seville.

(Journal of Physics E, 1968, series 2, 1, 423-425)

References

Akimov A I and Kraftmakher Ya A 1970 phys.stat.sol. 42 K41

Anderson D Anderson J M and Seville A H 1968 J. Phys. E Ser 2 1 423-25

Anderson J M and Brown A F 1965 phys.stat.sol. 12 309-20

Ascoli A Germagnoli E and Guarini G 1966 Acta Met. 14 1002

Ascoli A Guarini G and Queirolo G T 1970 Cryst. Lattice Defects 1 159-163 (For Ag see Ascoli et al 1966)

Balluffi R W and Seidman D 1965 Phys. Rev. 139 1824

Bauerle J E Klabunde C E and Koehler J S 1956 Phys. Rev. 102 1182

Bauerle J E Koehler J S 1957 Phys. Rev. 107 1493

Belrose J S 1956 Wireless World 62 435-8

Blackburn D A 1962 private communication

Bokshtein B S Bokshtein S Z Zhukovitskii A A Kishkin S I Kornelyuk L G and Nechaev Yu S 1968[a] Diffuzia v Metallikh i Splavakh, Russian Collection Tul'sk Politekhn Inst. Tula 65-74

Bokshtein B S Bokshtein S Z Zhukovitskii A A Kishkin S I Kornelyuk L G Nechaev Yu S 1968[b] Dokl. Acad. Nauk SSSR 183 1280-82

Bokstahler L I 1925 Phys. Rev. 25 677

Brooks C R Norem W E Hendrix D E Wright J W and Northcutt W G 1968 J. Phys. Chem. Solids 29 565

Brooks C R and Bingham R E 1968 J. Phys. Chem. Solids 29 1553-60

Brown A F 1966 App. Materials Research 67-75

Brown A F 1971 "Diffusion under mechanical stress", in "Diffusion Processes" ed. Sherwood J N et al, Gordon and Breach London 1971, p219-29

Carslaw H S and Jaeger J C 1959 "Conduction of Heat in Solids" 2nd Ed Clarendon Press Oxford p105-9 327-34

Cattaneo F Germagnoli E and Grasso F 1962 Phil. Mag. 7 1373

Chekhovsky V Ya and Petrov V A 1968 "Formation energy of heat vacancies in molybdenum and their concentration" contributed paper, International Conference on Vacancies and Interstitials in Metals, Kernforschungsanlage Jülich, W. Germany; in Jül-Conf-2 (Vol 1) KFA p6-18

Conte R R and Dural J 1968 Phys. Letters 27A 368-9

Corbino O M 1910 Phys. Z 11 413-7

Davisson C and Weekes J R Jr 1924 J. Opt. Soc. Am. 8 581-605

De Sorbo W 1960 Phys. Rev. 117 444

Edwards J W Speiser R and Johnston H L 1951 J. Appl. Phys. 22 424

Faulkner E A and Stannett R H O 1964 Electronic Engineering 36 159-61

Foote P D 1915 Bull. Nat. Bur. Stand. 11 607

Frenkel J I 1926 35 652

Fryburg G C 1967 J Chem Phys 24 175-80

Gerlich D Abeles B and Miller R E 1965 J. App. Phys. 36 76

Gertsriken S D and Novikov N N 1960 Fiz. Metal. Metalloved 9 224-235

Guarini G and Schiavini G M 1966 Phil. Mag. 14 47

Guarini G and Schiavini G M 1967 Phil. Mag. 15 805

Guinier A and Dexter D 1963 "X-ray studies of materials", Interscience Publ, N.Y., p104

Heigl F and Sizmann R 1972 Crystal Lattice Defects 3 13-27

Hoch M 1965 "The energy and entropy of vacancy formation in bcc refractory metals" GE-TM 65-12-2

Hoch M 1970 "Equilibrium measurements in high-melting point materials" in "Vacancies and Interstitials in Metals" ed Seeger et al, North Holland p81-90

Holland L R 1963 J. Appl. Phys. 34 2350

Holland L R and Smith R C 1966 J. Appl. Phys. 37 4528-36

Ida Y 1970 Phys. Rev. B1 2488

Jackson J J 1965 "Point defects in quenched platinum" in "Lattice Defects in Quenched Metals" ed Cotterill et al, Academic Press p467-78

Jaeger F M and Rosenbohm E 1939 Physica 6 1123-5

Jain S C and Krishnan K S 1954[a] Proc. Roy. Soc. (London) A222 167

Jain S C and Krishnan K S 1954[b] Proc. Roy. Soc. (London) A225 1,7,19

Jain S C and Krishnan K S 1955 Proc. Roy. Soc. (London) A227 141

Jain S C Goel T C and Narayan V 1969 J. Phys. D. 2 109-13

Johnson Matthey and Co Limited 1952 "Platinum for Resistance Thermometry" J. M. Co Ltd London

Jost W 1952 "Diffusion in Solids, Liquids and Gases" Academic Press p45-6

Kanel O M and Kraftmakher Ya A 1966 Fiz. Tverd. Tela 8 291

Keller J M and Wallace D C 1962 Phys. Rev. 126 1275

Kendall W B Orr R L and Hultgren R 1962 J. Chem. Eng. Data 7 516-8

Kidson C V and Ross R 1957 Proc. Int. Conf. Radioisotopes Sci. Res. Paris 1 185

Kirby R E and Rothrock B D 1968 European Conf. on Thermophysical Properties of Solid Materials at High Temperatures

Kirillin V A Scheindlin A E Chekovskoy V Ya and Petrov V A 1968 Proc. 4th Symp. on Thermophysical Properties ASME p54

Kittel C 1966 "Introduction to Solid State Physics" 3rd edn Wiley and Sons, N.Y. p.211

Koehler J S and Lund C 1965 "Non-equilibrium situations involving vacancies in gold" in "Lattice Defects in Quenched Metals" ed. Cotterill et al, Academic Press p1-14

Korostoff E 1962 J. Appl. Phys 33 2078-9

Kraev O A 1967 Teplo fizika Vysokikh Temperatur 5 817-20

Kraftmakher Ya A 1962 Zh. Prikl. Mekh. Tekh. Fiz. 176-80 (see also Kraev 1967 for a development of the method)

Kraftmakher Ya A and Strelkov P G 1962 Fiz. Tverd. Tela 4 2271-2274

Kraftmakher Ya A 1963 Zh. Prikl. Mekh. Tekh. Fiz. 2 158

Kraftmakher Ya A 1964 Fiz. Tverd. Tela 6 503

Kraftmakher Ya A and Cheremisina I M 1965 Zh. Prikl. Mekh. Tekh. Fiz. 2 114-115

Kraftmakher Ya A and Lanina E B 1965 Fiz. Tverd. Tela 7 123-6

Kraftmakher Ya A and Strelkov P G 1966[a] Fiz. Tverd. Tela 8 580

Kraftmakher Ya A 1966 in "Issledovaniya pri vysokikh temperaturakh" Nauka, Novosibirsk p5-54

Kraftmakher Ya A and Strelkov P G 1966[b] Fiz. Tverd. Tela 8 1049-52

Kraftmakher Ya A 1967[a] Fiz. Tverd. Tela 9 1528-9

Kraftmakher Y A 1967[b] Fiz. Tverd. Tela 9 1850

Kraftmakher Ya A and Strelkov P G 1970 "Equilirbium concentration of vacancies in metals" in "Vacancies and Interstitials in Metals" ed. A. Seeger et al, North Holland p.59-80

Kraftmakher Ya A 1971 Phys. Stat. Sol. (b) 48 K39

Kuhlmann-Wilsdorf D 1965 "Vacancies and vacancy complexes in quenched f.c.c. metals" in "Lattice Defects in Quenched Metals" ed. Cotterill et al, Academic Press p.269-318

Leadbetter A J 1968 J. Phys. C. Ser. 2 1 1481-1504

Leibowitz L Chasnov M G and Mishler L W 1969 Trans. MS AIME 245 981

Liebfired G 1955 "Gittertheorie der mechanischen und thermischen Eigenschaften der Kristalle" in "Handbuch der Physik Vol.VII part 1" Springer-Verlag Berlin p104

Liebfried G and Ludwig W 1961 "Theory of anharmonic effects in crystals" in "Solid State Physics Vol.12" ed Seitz and Turnbull Academic Press p276-444

Loewenthal G C 1963 Australian J. Phys. 16 47

Lomer W M 1958 "Vacancies and other point defects in metals and alloys", Institute of Physics monograph and report series No.23 p94

Lovejoy D R 1964 Canad. J. Phys. 42 2264-85

Ludeke C A 1942 J. Appl. Phys. 13 418-23

MacDonald D K C 1953[a] J. Chem. Phys. 21 177

MacDonald D K C 1953[b] J. Chem. Phys. 21 2097

MacLean D 1957 in "Grain Boundaries in Metals", Clarendon Press, Oxford p200

Meechan C J and Eggleston R R 1954 Acta Met. 2 680

Misek K and Polak J 1963 J. Phys. Soc. Japan 18 Suppt.II 179

Mott N F and Jones H 1936 "The Theory of the Properties of Metals and Alloys" Clarendon Press Oxford, p192-4 and 268-9

Nechaev Yu S 1968 Candidate's dissertation Moscow

Nicholas J F 1955 Acta Met. 3 411

Oriani R A 1955 Acta Met. 3 232

Pervakov V A and Chotkevic V I 1960 Dokl. Akad. Nauk. 134 1328

Polak J 1967 Phys. Stat. Sol. 21 581

Rasor N S and McClelland J D 1960 J. Phys. Chem. Solids 15 17

Roeser W F and Wensel H T 1941 in "Temperature, its Measurement and Control in Science and Industry, Vol.I" American Institute of Physics, Reinhold N.Y. p1312, 1314

Schmid G Schottky G and Seeger A 1964 Phys. Stat. Sol. 4 439

Schultz H 1964 Acta Met. 12 761

Schultz H 1965 "Quenching of vacancies in tungsten" in "Lattice Defects in Quenched Metals" ed. Cotterill et al, Academic Press p761-5

Schumacher D Seeger A and Harlin O 1968 Phys. Stat. Sol. 25 359

Seeger A and Mehrer H 1970 "Analysis of self-diffusion and equilibrium measurements" in "Vacancies and Interstitials in Metals" ed. Seeger et al. North Holland 1970 p1-58

Seidman D and Balluffi R W 1965 Phys. Rev. 139 1824

Shestopal V O 1965 Fiz. Tverd. Tela 7 3461

Simmons R O and Balluffi R W 1960[a] Phys. Rev. 117 62

Simmons R O and Balluffi R W 1960[b] Phys. Rev. 119 600

Simmons R O and Balluffi R W 1962 Phys. Rev. 125 862

Simmons R O and Balluffi R W 1963 Phys. Rev. 129 1533

Sizmann R and Wenzl H 1963 Z. Naturforshg 18 a 673-4

Smith K K and Bigler P W 1922 Phys. Rev. 19 268

Smith R C and Holland L 1966 J. Appl. Phys. 37 4866

Smithells C J 1962 "Metals Reference Book Vols.I and II" Butterworths

Stedman R Almqvist L and Nilsson G 1967 Phys. Rev. 162 549

Stoker J J 1950 "Nonlinear Vibrations in Mechanical and Electrical Systems" Interscience, N.Y. p103-9

Taylor R E and Finch R A 1964 J. Less-common Metals 6 283

Thomson R M and Balluffi R W 1962[a] J. Appl. Phys. 33 803

Thomson R M and Balluffi R W 1962[b] J. Appl. Phys. 33 817

Touloukian Y S 1970 "Thermophysical Properties of Matter, Vol.4 - specific heats of metallic elements and alloys; Vol.7 - thermal radiative properties of metallic elements" Plenum N.Y.

Van den Sype J 1965 Ph.D. Thesis, University of Pennsylvania

Van den Sype J 1970[a] Phys. Stat. Sol. 39 659

Van den Sype J 1970[b] Scripta Metall. 4 251-4

Wilders D J 1968 "An investigation of vacancies in metals" Project report for the Degree in Applied Physics, The City University, London

Worthing A G 1941 "Temperature radiation emissivities and emittances in "Temperature, its Measurement and Control in Science and Industry" American Institute of Physics, Reinhold N.Y. p1164-87

Young A and Kirk A 1964 "Royal Society Mathematical Tables Vol.10", Cambridge University Press, p36-43

Zwicker C 1928 Z. Physik 52 668

ACKNOWLEDGEMENTS

The help and advice of Professor A. F. Brown throughout this work is most gratefully acknolwedged.

Thanks are due to the Science Research Council and to the Dounreay Experimental Reactor Establishment of the United Kingdom Atomic Energy Authority for their generous financial support.

The valuable technical assistance of Mr. D. Anderson and Mr. J. P. Weight is acknowledged with thanks, as is that rendered generally by the technical and workshop staff of both the Department of Natural Philosophy of the University of Edinburgh and the Department of Applied Physics of the City University.

The work of Mrs. B. Patel in preparing the typescript is much appreciated.

ABSTRACT OF THESIS

Name of Candidate Adrian Heywood Seville

Address 4 Coppelia Road, Blackheath, London SE3.

Degree Ph.D. *Date* 1972

Title of Thesis Studies of vacancies in metals by modulation methods

The investigation of vacancies in metals is discussed with particular reference to methods using sinusoidal temperature modulation about an elevated mean temperature; the theory of these methods is given for the case of thermal vacancies near equilibrium.

A first experiment is described briefly, in which the phase of the temperature modulation of a specimen is compared with that of the associated resistance modulation. The temperature modulation of a gold wire (diameter $\sim$ 50 μm) was observed using the variation in the light emitted; a carrier-frequency bridge was used to observe the resistance modulation. The modulation frequency was $\sim$ 20 Hz, and the mean temperature 1000 K - 1200 K. The phase comparison accuracy ($\pm$ about 5°) was not adequate to reveal any vacancy relaxation effects, and null results were obtained.

A second modulation experiment is described in which the specific heat of a platinum wire specimen (diameter $\sim$ 50 μm) was measured. The amplitude of temperature modulation was determined from the variation in light emitted from the specimen. Results are given for modulation frequencies in the range 100 Hz - 1 kHz and mean temperatures 1200 K - 1900 K. Above 1500 K, the measured specific heat exceeds the values extrapolated from the low-temperature results. Such effects have been commonly interpreted in terms of large vacancy concentrations ($\sim$ 1% at the melting point). Reasons are given for preferring an explanation based on lower vacancy concentrations, and taking into account anharmonic and vacancy relaxation effects.

Use other side if necessary.